9-2012

Chemistry at Silicone - Inorganic Oxide Interfaces

Joseph W. Krumpfer
University of Massachusetts Amherst, joseph.krumpfer@gmail.com

CHEMISTRY AT SILICONE - INORGANIC OXIDE INTERFACES

A Dissertation Presented

by

JOSEPH W. KRUMPFER

Submitted to the Graduate School of the
University of Massachusetts in partial fulfillment
of the degree requirements for the degree of

DOCTOR OF PHILOSOPHY

September 2012

Polymer Science and Engineering

CHEMISTRY AT SILICONE - INORGANIC OXIDE INTERFACES

A Dissertation Presented

by

JOSEPH W. KRUMPFER

Approved as to style and content by:

_____
Thomas J. McCarthy, Chair

_____
E. Bryan Coughlin, Member

_____
Sankaran Thayumanavan, Member

_____
David A. Hoagland, Head, PS&E

To my parents

ACKNOWLEDGMENTS

First and foremost, I would like to thank my advisor, Tom McCarthy, for all the help and advice he has given me throughout these last few years. Tom is a great advisor, an excellent teacher, and just someone I am glad to know. Tom gave me the freedom and opportunities to pursue many different areas of research but always managed to keep me from going too far astray. His genuine curiosity and passion for learning has been an inspiration to me and has driven me to be a much better scientist and person. It is easy to look back and see how much I have grown and learned over the past few years, and I owe most of this to Tom. There are not enough words of gratitude in the English language to express my appreciation for all of the hard work and time Tom has put into my education and growth. So, I will simply say 'Thank you.'

I would also like to thank the remainder of my thesis committee, Dr. Bryan Coughlin and Dr. Sankaran Thayumanavan, for pushing me to excel in every aspect of my work. Their input and advice was invaluable not just in achieving doctoral objectives, but also for pursuing my future goals. I would also like to thank Dr. Michael Knapp for his help through the defense process.

Next, I would like to thank all past and current members of the McCarthy group, Lichao, Scott, Joonsung, Dalton, Bokyung, Peiwen, Maria, Pei, Yan, Minchao, Liming and Jack. I would particularly like to thank Peiwen Zheng, my classmate, who went through all the steps with me, and whose advice and help were always greatly appreciated. I would also like to thank Pei Bian for his help and many clever ideas. Finally, I would like to thank Jack Hirsch for his help and the many engaging conversations and advice both on research, sports, and life. I could not imagine this thesis being as successful without each and every one of you.

I would like to thank CHM, MRSEC, CUMIRP, Shocking Technologies, Henkel and 3M for their financial support of my research and study. I must also thank all of the faculty and staff of the Polymer Science and Engineering Department for creating an excellent learning environment. I would like to acknowledge Lisa and Maria for a lot of unseen work in keeping things running smoothly. I would like to thank Wei Chen, Maria Lerum, and my lab students at

Mount Holyoke College for a wonderful and enjoyable first teaching experience. I would also like to thank Dr. Alex Fadeev, who taught me many fundamental research skills and made silicon (Si) my favorite element.

I would also like to thank the class of 2007 and all of the friends I've made in and around Amherst. Especially, Brent Hammer for many shared adventures and always being a good friend, and Kathleen McEnnis whose time, conversation over coffee, and friendship were integral to my happiness throughout these years. Many people inside and outside of the Amherst area have also been a big part of my life over the last few years, and I would like to thank Cathy, Travis, Mai, Itza, Zak, Sam, Kate, Melissa and most certainly Sean, who has been and always will be a brother to me. Finally, I would like to thank Anna-Katharina Hesse for traveling the world with me, providing unlimited support and understanding, and always being there when I needed her.

Finally, I would like my to thank my family for their love and support throughout the years. They have seen me through every obstacle and milestone in my life, and I could not have made it this far without them.

ABSTRACT

CHEMISTRY AT SILICONE - INORGANIC OXIDE INTERFACES

SEPTEMBER 2012

JOSEPH W. KRUMPFER, B.S., SETON HALL UNIVERSITY

M.S., UNIVERSITY OF MASSACHUSETTS - AMHERST

Ph.D., UNIVERSITY OF MASSACHUSETTS - AMHERST

Directed by: Professor Thomas J. McCarthy

This dissertation describes research performed using siloxane polymers. This includes the reactions of siloxane polymers with inorganic oxide surfaces to form covalently attached monolayers, and the electrical properties of crosslinked silicone composite films fabricated by compounding with nickel particles. In addition to these topics, the use of contact line pinning as a practical and controllable method for the deposition of materials on superhydrophobic and chemically patterned surfaces is also described.

The first chapter provides a general review of siloxane polymer chemistry, focusing in particular on the relationship between molecular structure and physical properties. The use and fabrication of silicone composite materials is also discussed, including typical methods for crosslinking siloxane polymers and the effects of filler materials. Finally, contact angle hysteresis and contact line pinning phenomena are presented.

Following this introduction, four separate but interrelated projects are presented. First, the surface modification of titania via hydridomethylsiloxanes is discussed. This work represents an extension of the reaction of hydridosilanes and provides an environmentally clean method for the hydrophobization of titania. Linear and cyclic hydridomethylsiloxanes, as well as hydridomethylsiloxane-*co*-dimethylsiloxane polymers, are used as reagents and the resulting surfaces are discussed. Unpredicted results from this method lead to the consideration of poly(dimethylsiloxane) as a previously unconsidered reagent presented in the next project.

The second project discusses the covalent attachment of siloxane polymers, particularly poly(dimethylsiloxane), to a range of inorganic oxide surfaces, including titania, nickel oxide,

alumina, and silica. This reaction is presented as a thermally activated equilibrium process, and offers insight into certain aging processes found in silicone materials. Particular focus is made on the development of a highly reproducible method for the fabrication of low contact angle hysteresis surfaces. Furthermore, this reaction is shown to be general for the siloxane bond through the reaction of functional and cyclic siloxanes.

The third project describes the preparation of electrically conductive silicone coatings, containing nickel and titania particles. The effect of nickel concentration and geometry on the electrical properties of these coatings is examined and the effects on the percolation threshold are presented. In addition to this, the addition of titania nanoparticles to diminish electrical conductance is also investigated.

The fourth project discusses the contact line pinning of liquids on hydrophobic surfaces. In this chapter, the use of ionic liquids exhibiting no vapor pressure is used to experimentally determine the de-wetting process of liquids from pillared, superhydrophobic surfaces through micro-capillary bridge rupture. Furthermore, this technique is used as a preparative technique for the fabrication of individual salt crystals supported on pillared surfaces.

TABLE OF CONTENTS

LIST OF TABLES

LIST OF FIGURES

FIGURE PAGE

CHAPTER 1

INTRODUCTION

1.1 History and Development of Siloxane Polymers

It is nearly impossible to remove the discovery and development of siloxane polymers from the world and history surrounding them.[1-4] For this reason, it is important to examine these two aspects in addition to the chemistry of siloxane polymers to have a full understanding of the material. Silicon (Si) is the second most abundant element on the earth's crust (25.7% by mass) and is predicted to be the eighth most common element by mass in the universe. However, silicon rarely occurs as a pure element but almost exclusively occurs as silica and silicate minerals by bonding with the most common element in the earth's crust, oxygen. Throughout the history of mankind, silica and silicate minerals have been used as essential components in architectural materials, jewelry, and art.

It was not until 1824 that elemental silicon was isolated by Jöns Jakob Berzelius. He reduced potassium fluorosilicate with potassium by holding the materials over the flame of a spirit lamp.[5] As an aside, it should be noted that electric ovens did not exist until near end of the 19th century, so all of these early experiments were performed using open flames and coal beds. In his experiments, Berzelius isolated the dull, brown powder of amorphous silicon. He named the element "silicium" (from the Latin silex, silicis for "flint") due to its few similarities to other metals, particularly in electrical conductivity, which caused much debate on the true nature of this element. It was not until 1831 that silicon got its current name from Thomas Thomson[6] due to its similarities in reactivity to the nonmetals boron and and carbon, and it was nearly three decades later in 1854 that the crystalline form of the element was isolated by Henri Deville.[7] Since then, elemental silicon become an industry standard for semi-conductors and solar-cell fabrication.

Elemental silicon has many interesting properties. In appearance, it is a hard, brittle, shiny, blue-grey, metallic-looking material with a diamond-lattice crystal structure. In its crystal form it has a density of 2.33 g/cm^3 and a melting point of 1414 °C. Unlike other non-metals,

silicon is an excellent semi-conductor, with a resistivity of 10^3 Ω·m. Modern commercial production of elemental silicon requires the heating of silica (sand) with carbon above 2000 °C. In terms of chemical behavior, silicon is commonly tetracovalent, although being a second period element, it can also be hexacovalent. It is a common misconception to assume silicon reacts similarly to carbon, but in reality the larger atomic size and electropositive nature of silicon, gives it many similarities to boron, germanium, and tin, as well.[8]

With the isolation of elemental silicon, the development of reactive organosilanes became possible. Berzelius isolated (1824) the first reactive chlorosilane, $SiCl_4$, and the collaboration of Charles Friedel and James Mason Craft produced (1863) the first organosilane, $Si(C_2H_5)_4$, through the reaction of diethylzinc and silicon tetrachloride. Friedel continued work on organosilicon chemistry with Albert Ladenburg for several years afterward. It was Ladenburg[9] who produced the first organosiloxane, through the synthesis of diethyldichlorosilane, $(C_2H_5)_2SiCl_2$, and subsequent reaction with water in 1874, to form a syrupy, odorless liquid which he called "silicon diethyl oxide". Ladenburg continued to make many further developments in organosilicon chemistry, but it was not until Frederick S. Kipping began work in the field that siloxane polymers really came into being.

Often referred to as the "grandfather of silicone chemistry", Kipping became the preeminent researcher in organosilicon chemistry between 1899-1936, during which period he published 50 papers,[10] and opened up many avenues in organosilicon chemistry through the use of Grignard reagents. In fact, much of the basic information on siloxane polymers derives from Kipping's work. Furthermore, although a misnomer, "silicone" was first coined by Kipping in 1901 as an analogue to the carbon-based ketone when he believed he had isolated diphenylsiliconoxide, Ph_2SiO.[11] However, it soon became clear that silicon does not form a double bond with oxygen, but rather reacts to form linear and cyclic oligomers with silicon-oxygen single bonds. Despite this, the name "silicone" became prevalent, and this continues to be a common name for the class of polymer featuring a backbone with alternating silicon and oxygen atoms (also called siloxane polymers).

There were many significant global events that occurred during the early 20th century. War engulfed all of Europe, the stock market crashed, automobiles replaced horses, and tensions continued to grow between nations. Perhaps it was the volatility of the time in which he lived, that in 1936 after 36 years in the field, Kipping[12] declared, "[Given that] the few [organosilicon compounds] which are known are very limited in their reactions, the prospect of any immediate and important advances in this section of organic chemistry does not seem to be very hopeful." Kipping would have been correct in this assessment, as the polymerization of siloxanes using Gringard reagent-prepared starting materials wasn't entirely practical, if not for the growing industrial interest in silicone polymers.

It was around this point that academic interest in siloxane polymers became almost completely overshadowed by the work conducted in industry, particularly by J. Franklin Hyde (Corning Glass Works), and Eugene Rochow (General Electric). Kipping, and the later work of Stock[13] on PDMS, had shown that siloxane polymers had many useful properties, including excellent electrical insulation properties, and it was these properties in which these companies were most interested in the early 1940s. Siloxane polymers quickly became a serious business causing the unification of Corning Glass Works and Dow Chemical Co. to form Dow Corning in 1943. This is due to the fact that Dow Chemical Co. could provide the magnesium necessary for the formation of Grignard reagents which Corning Glass Works could use to produce dimethyldichlorosilane (Eq. 1-1), the monomer required for the condensation reaction of poly(dimethylsiloxane) (PDMS) (Eq. 1-2). In fact, the Dow Corning #4 Compound, a simple silicone grease, was the new company's first commercial product. This compound proved invaluable in preventing corona discharges from aircraft electrical systems caused by the moisture at high altitudes. It is from Dow Corning that much of the information on the condensation polymerization of dichlorosilanes is derived.

$$CH_3MgBr + SiCl_4 \longrightarrow (CH_3)_4Si + (CH_3)_3SiCl + (CH_3)_2SiCl_2 + (CH_3)SiCl_3 + MgBrCl \quad \text{(Eq. 1-1)}$$

$$n\ (CH_3)_2SiCl_2 + H_2O \longrightarrow \text{┼}(CH_3)_2SiO\text{╫}_n + 2nHCl \quad \text{(Eq. 1-2)}$$

However, several factors limited the potential of silicones through the Grignard method. First, the separation of the resulting chlorosilanes proved very difficult, as the difference in boiling points of these compounds is a few degrees. Second, Grignard synthesis is not practical on a large, plant-size scale. Third, this process was not economically desirable. It is this point that focus shifts to Eugene Rochow at General Electric. In what is known as "the most important single experiment and the best single day's work in the history of the silicones industry",[3] Rochow developed an efficient and cost-effective way to form chlorosilanes on a large scale, through catalysis with copper on May 9, 1940 (Eq. 1-3). This method, known as the Direct Process, is still in use today. It should be noted that this method was independently developed by the German chemist Richard Müller a few weeks after Rochow's discovery, and for this reason, this process is also known as the Rochow-Müller Process.

$$2\ CH_3Cl + Si \xrightarrow{Cu} (CH_3)_2SiCl_2 \qquad \text{(Eq. 1-3)}$$

Shortly after this discovery, the United States was drawn into the Second World War at the end of 1941. Silicones became invaluable materials for military aircraft and submarine engines. In fact, silicone coatings were a major factor in giving the Allied Forces air superiority during the conflict, as they could fly higher than their German counterparts. For this reason, information regarding the synthesis and production of siloxane polymers became well-guarded secrets for national security. This had several profound impacts on the future of silicone chemistry. First, work in this field was not published during this time, and even Rochow's breakthrough Direct Process did not appear in publication until 1945.[14] Second, General Electric and Dow Corning, otherwise competitors in the silicones market, were mandated to work together to support the war effort. This meant that patents submitted by each company were held until after the war had ended, and this resulted in a series of patent lawsuits which further delayed the release of information on silicone production. For these reasons, much of the information concerning silicone polymers and resins did not appear in publication until the late 1940s and early 1950s. As it turned out, the courts finally ruled that each company could freely use the

other's patents, i.e., Dow Corning had access to Rochow's Direct Process, and GE had access to Hyde's condensation reactions.

After the war, as military orders for silicones were cancelled, the two companies were forced to develop new applications for these materials in order to maintain their businesses. It is because of this, that many of the modern commercial uses for silicones now exist, including adhesives, lubricants, surfactants, anti-foaming agents, and hydrophobic coatings. Today, the silicone and silane industry is a multi-billion dollar field which still utilizes the same chemistries developed by Hyde and Rochow.

1.2 Structure and Properties of Siloxane Polymers

Siloxane polymers have many properties which greatly separate them from carbon-based polymers. These properties derive from the vast differences in chemical nature between these types of polymers. The atomic radius of silicon (117.6 pm) is much larger than carbon (70 pm). Silicon is also much more electropositive than carbon, with Pauling electronegativities of 1.9 and 2.5, respectively. Table 1.1 shows a list of Pauling electronegativities of several atoms.[15] Because of this lower electronegativity, many silicon compounds are more reactive than their carbon-based analogues. For example, the silicon-chlorine (Si-Cl) bond is much more reactive than the carbon-chlorine (C-Cl) bond, and in fact, it readily undergoes hydrolysis in the presence of water.

Table 1.1. Electronegativity of common elements

Element	B	Si	H	P	S	C	I	Br	N	Cl	O	F
Electronegativity	2.0	1.9	2.2	2.2	2.6	2.5	2.7	3.0	3.0	3.2	3.4	4.0

The importance in electronegativity and the most pronounced difference with carbon is perhaps seen in the silicon-hydrogen (Si-H) bond, commonly called hydrosilane. Here, the polarity of the bond is such that the hydrogen atom has a partial negative charge, $Si^{\delta+}$-$H^{\delta-}$. This is the exact opposite for the carbon-hydrogen (C-H) bond, $C^{\delta-}$-$H^{\delta+}$. Due the partial negative charge,

silicon hydride is more appropriately named "hydridosilane," and this is the name which is used in subsequent chapters. Furthermore, the Si-H bond readily undergoes hydrolysis in basic aqueous media and has a slow reaction with water. It is also a reducing agent, and in that respect is again similar to boron hydride and aluminum hydride. Reactions of this functionality with titania surfaces are discussed in Chapter 2.

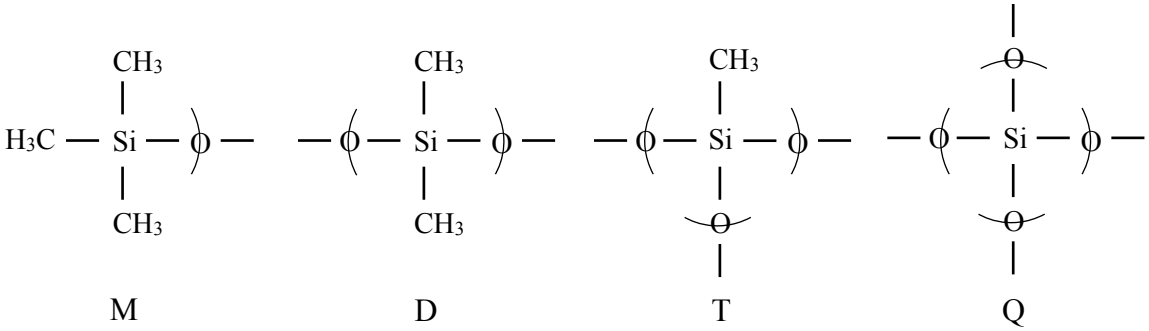

Figure 1.1. Common nomenclature of molecular units in silicone chemistry

As previously discussed, silicon is most commonly bonded to oxygen atoms. Early silicone chemists adopted a unique nomenclature to designate the number of oxygen atoms bonded to silicon in which silicon bonded to 1, 2, 3, or 4 oxygen atoms is denoted as M, D, Q, and T, respectively. Figure 1.1 gives a depiction of these different structures for reference. Another unique and common method of notation used by silicone chemists is to divide oxygen atoms in half when writing repeat units in these structures. This is solely to identify silicon as bonded to its correct number of oxygen atoms and does not mean to suggest that silicon is bonded to only half an oxygen atom. Using this nomenclature, siloxane structures can be easily written as MM (hexamethyldisiloxane), MD_2M (decamethyltetrasiloxane), or D_4 (octamethylcyclotetrasiloxane).

The chemical structure of the most common silicone polymer, poly(dimethylsiloxane) (PDMS), is shown in Figure 1.2a. Siloxane, or silicone, polymers are defined as polymers with backbones of alternating silicon and oxygen atoms. It is this siloxane bond which contributes to the unique structure and properties of siloxane polymers and makes them so different than other polymers. The large difference in electronegativity between silicon (1.9) and oxygen (3.5) results

in a backbone that is approximately 51% ionic in nature.[16] The larger atomic radius of silicon contributes to larger bond lengths for Si-O and Si-C (1.63 and 1.90Å) when compared to C-O and C-C bonds (1.43 and 1.53Å). These larger bond lengths and the ionic nature of the Si-O bond also contribute to the much larger bond angles of Si-O-Si (143°) than C-C-C (109.5°). These differences in bond lengths and bond angles found in siloxane polymers allow pendent groups to be spaced much further apart for greater rotational freedom than found in their carbon-carbon polymer analogues, as seen in the structure of poly(isobutylene) (PIB) in Figure 1.2b. Furthermore, the ionic nature of the siloxane bond does not have the same limitations on directionality. Rochow describes structure and flexibility of poly(dimethylsiloxane) such that "the silicon atom and its associated pair of methyl groups swing as a unit, as though the silicon-oxygen bond were a ball and socket joint." Mark later commented[17] on the siloxane backbone, "The bond angle is so flexible that it can readily pass through the 180° state." For these reasons, its not altogether accurate to attribute a finite bond angle in siloxane polymers as it is to carbon-based polymers, since this backbone is capable of incredible flexibility.

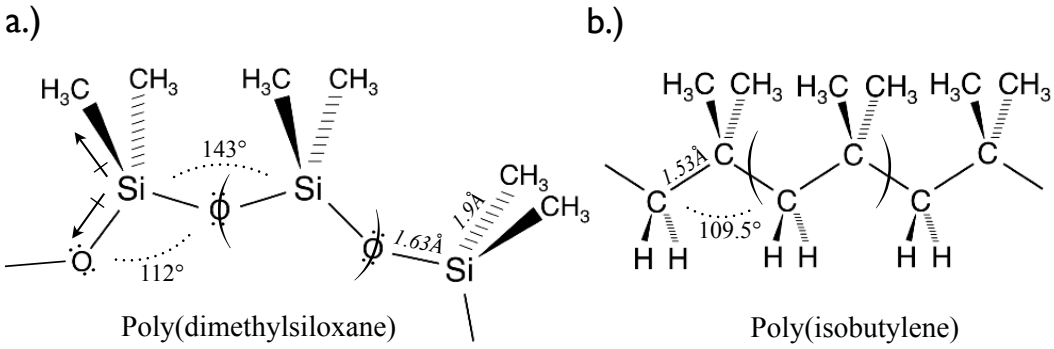

Figure 1.2. A comparison of molecular structures drawn with correct bond angles and proportional bond lengths of a.) poly(dimethylsiloxane) and b.) poly(isobutylene) to highlight the differences between siloxane and carbon-carbon backbone polymers.

The ionic nature of the siloxane backbone also contributes to the high thermal stability of these polymers. The disassociation energy of the Si-O bond is 444 kJ/mol, making them thermodynamically stronger than C-C bonds (346 kJ/mol). In fact, for many years, many scientists believed the siloxane bond to be nearly unbreakable, largely due to its similarities to

silica (SiO_2). However, this ionic nature also makes siloxane polymers much more reactive to Lewis acids and bases.[18] This was poignantly demonstrated by Speier when he demonstrated that siloxane polymers reacted with acids, alcohols, and even water. Although these results were never formally published, they appear in a more recent monograph.[3] In this respect, the chemical reactivity of the siloxane bond is akin to the O-H bond, which is thermodynamically more stable than C-H bonds, but also more reactive to ionic species.

The ionic nature and high degree of rotational and torsional freedom of the chemical bonds in poly(dimethylsiloxane) result in unusually low intermolecular forces and a low cohesive energy. This low cohesive energy was greatly debated in the early 1940s, as the strength of silicone rubbers was unpredictably low with a tofu-like quality. PDMS differs from other polar polymers which typically have higher cohesive energies, because nearly every bond in PDMS is polar. This includes the Si-C bonds (~12% ionic) which may aid in the "repulsion" of other siloxane chains. This gives volatile siloxanes much lower boiling points than their alkane analogues. It also causes only very slight changes (i.e. remains almost constant) in viscosity with respect to temperature. Furthermore, the low intermolecular forces impart very low surface tensions to silicone fluids ($\gamma_{LV} \sim 20$ dyn/cm). Finally, these low intermolecular interactions give silicones an extremely high free volume which can be seen in the low glass transition temperature of PDMS ($T_g \sim -120$ °C). This means PDMS is a liquid at room temperature.

These molecular attributes of poly(dimethylsiloxane) translate to the following physical characteristics:[7,19]

1. low chemical reactivity (except with acids/bases)
2. high thermal stability
3. wide service temperature range
4. low flammability
5. high dielectric strength
6. negligible temperature dependence on viscosity
7. high compressibility

8. high shear strength

9. high gas permeability

10. low surface tension (hydrophobicity)

The chemical reactivity of siloxane polymers was previously discussed, and much of the thermal characteristics are due to the ionic nature of the siloxane backbone. Table 1.2[20] provides an easy reference for the thermal properties of poly(dimethylsiloxane). PDMS is stable in the absence of oxygen up to 350 °C, and decomposes almost entirely into cyclic oligomers with D_3, D_4, and D_5 being the primary decomposition products. In the presence of oxygen, PDMS is stable up to 250 °C yielding a solid oxidation product of SiO_2 (along with water and CO_2), yet another difference between carbon-based materials which yield the gaseous oxidation product of CO_2. The fact that silicones yield a solid oxidation product contributes to their low flammability. The high free volume and low intermolecular interactions prevent liquid PDMS from undergoing crystallization upon cooling.[21] Rather, crystallization of PDMS occurs after heating from the glass transition temperature and is referred to as "cold crystallization".

Table 1.2. Thermal Properties of Poly(dimethylsiloxane)

T_g	T_c^*	T_m	T_d (O_2)	T_d (N_2)	k (kW/m·K)	C_P (kJ/kg·°C)	α (ppm/°C)
-120°C	-80°C	-40°C	250°C	350°C	0.15	1.5	30-300

The high free volume and low intermolecular interactions of silicones contribute to the remaining physical properties previously listed (6-10). One particularly interesting property of poly(dimethylsiloxane) which is not directly addressed in this list is the polymer's interactions with water. Silicones are highly water repellent (water contact angles[22] are θ_A / θ_R = ~106° / ~105°) making it suitable for hydrophobic coatings. However, liquid silicones are known to spread across the surface of water to form a monomolecularly thick film.[23] This is due to ionic interactions between the water surface and the siloxane backbone. In addition to this, the permeability of water vapor through silicone membranes[20] is significantly higher than other

gases, nearly 12 times greater than CO_2 and 60 times greater than O_2. This unique relationship with water makes classifying PDMS as "hydrophobic" difficult and means that PDMS liquids should, and do have, high amounts of molecular water within them.

Other important properties of silicones are their high biocompatibility and non-toxicity. Although a purely synthetic and man-made polymer, silicones are environmentally-safe materials that degrade readily in soil to form its major oxidation products, silica, carbon dioxide, and water, which are all naturally occurring materials.[24] Since nearly all organisms evolved on the surface of this planet, silica is not a toxic material and most life-forms respond in the same manner to silicone polymers. For these many unique properties, silicone materials have been used in a wide range of applications, from astronaut boots to nuclear reactor coatings. They are also biocompatible and used in many cosmetics and pharmaceutical products. Silicone surfactants are important materials in anti-foaming agents. The high temperature usage range of silicone polymers makes them particularly suitable for a large number of applications.

1.3 Synthesis and Preparation of Siloxane Polymers

The polycondensation reaction of difunctional silanes, particularly dimethydichlorosilane is the oldest method for the preparation of poly(dimethylsiloxane)[9,25] (Eq. 1-2). However, this polymerization technique is not the favored method, as it results in a by-product (HCl) which is corrosive to silicone polymers and it is also difficult to achieve high molecular weights. This is due to the well-known equilibration of siloxanes to form a mixture of linear and cyclic species. Rather, the ring-opening polymerization (ROP) of cyclic siloxanes via acid or base initiators is the preferred method for achieving high molecular weight polymers.

Traditional ring-opening of cyclic siloxanes is achieved using an anionic initiator, such as KOH or silanolate species (Figure 1.3a), although the use of cationic initiators is also well-known.[25] Thermodynamically speaking, the ring-opening polymerization (ROP) of D_4 is drastically different than other ring-opening polymerization methods (Figure 1.3b).[26] This cyclic siloxane has neglible ring strain, and there is no enthalpic driving force ($\Delta H_p^{298K} \sim 6.4$ kJ/mol) for

this polymerization to proceed as there is in typical ROP syntheses. Rather, this is an entropically driven reaction ($\Delta S_p^{298K} \sim 194.4$ kJ/mol). It is counterintuitive to most chemists that a decrease in the total number of molecules should result in an increase in entropy, but the degree of torsional, rotational, and conformational freedom found in linear siloxane polymers is much greater than those found in cyclic siloxanes, which are confined in a ring structure. In many cases, the use of hexamethylcyclotrisiloxane (D_3) is the favored monomer for this polymerization as it does have some ring-strain to help drive this reaction toward polymerization.

a.) Initiation

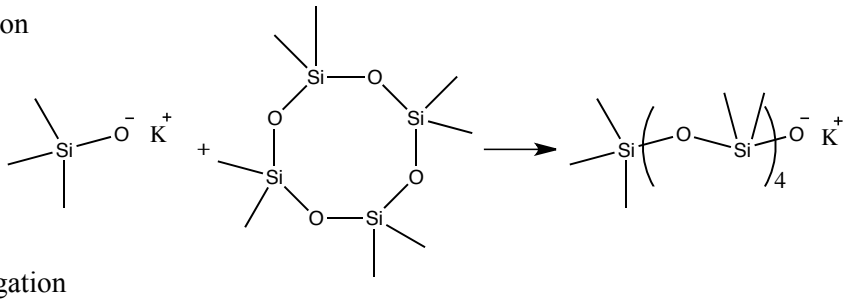

b.) Propogation

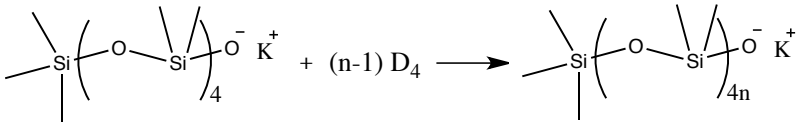

c.) Equilibration

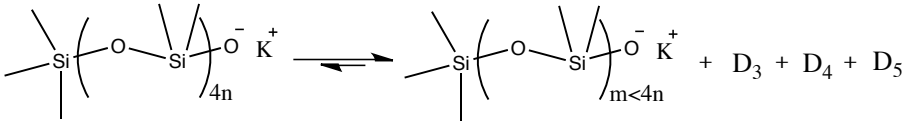

d.) Termination

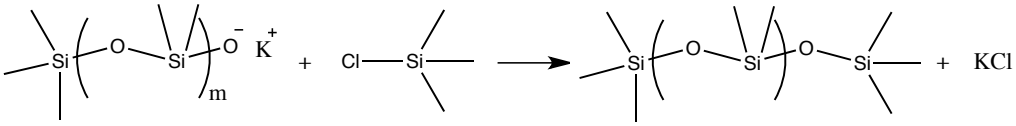

Figure 1.3. The initiation (a), propagation (b), equilibration (c), and termination (d) of a traditional ring-opening polymerization (ROP) of octamethylcyclotetrasiloxane (D_4) using a potassium trimethylsilanolate initiator.

Like the polycondensation of difunctional silanes, siloxane polymers will begin to equilibrate to shorter oligomers and cyclic siloxanes after high molecular weight has been achieved (Figure 1.3c). In order to produce high molecular weight poly(dimethylsiloxane), the

polymerization must be kinetically terminated, using an end-capping group such as a monofunctional silane (Figure 1.4d). However, end-capping siloxane polymers does not make them immune to equilibration to lower molecular weight species. As the siloxane bond is reactive with acid and base species, the addition of either of these into a silicone fluid will cause the scission of siloxane bonds (hydrolysis) and begin the equilibration process.

1.4 Silicone Materials and Composites

The term "PDMS" is used rather loosely when it comes to materials described in the literature. Poly(dimethylsiloxane) is a liquid at most temperatures, so the idea of PDMS used as a material is not an entirely accurate description, and the less specific designation of "silicone" material would be more appropriate. In order to be made into any sort of practical material, it is necessary to introduce crosslinks between siloxane polymer chains. The earliest methods for the crosslinking of PDMS involved bimolecular radical coupling of methyl groups using stoichiometric amounts of benzoyl peroxide to form silicone elastomers.[27] As it does not contain any β-hydrogens or β-C-C bonds, PDMS is particularly suited for crosslinking in this manner (fragmentation and disproportionation reactions do not compete as they typically do in hydrocarbon polymers). However, this method for crosslinking has largely been replaced by the more efficient hydrosilylation process.

Hydrosilylation (or hydrosilation) is the process of coupling hydridosilanes and carbon-carbon double bonds (typically terminal vinyl-groups) using a platinum catalyst (Figure 1.4a). While there are a variety of catalysts for hydrosilylation, the most common one is Karstedt's catalyst (Figure 1.4b).[28] Although the resulting products are identical (ethylene bridges), hydrosilylation has many advantages over radical coupling. First, being catalytic in nature, only small amounts of catalyst (parts per million quantities) are necessary. Second, hydrosilylation has a high degree of efficiency and control in terms of crosslinking. Because hydrosilylation occurs at vinyl and hydridosilane functionalities, fairly controlled structures can be formed. Finally,

hydrosilylation is so economically favorable due to its high efficiency that the recovery of the platinum catalyst is rarely attempted.

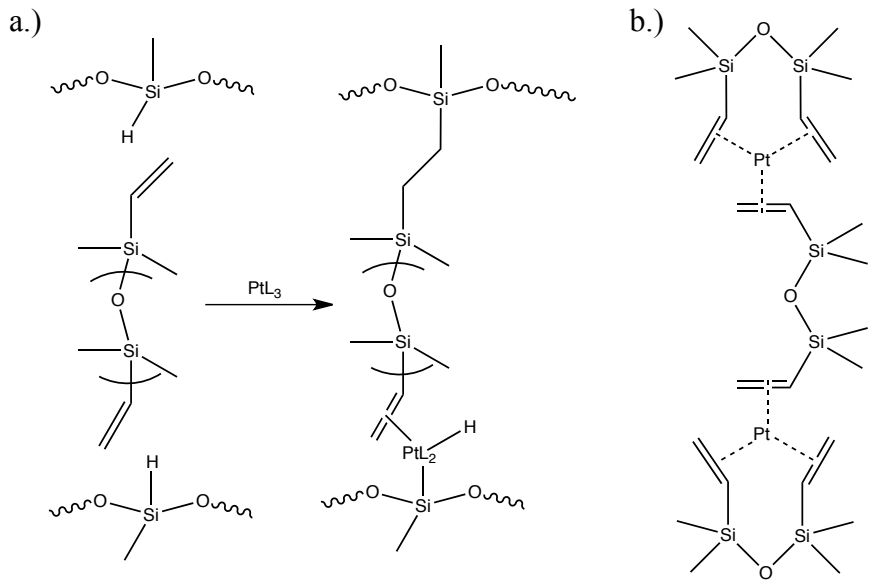

Figure 1.4. a.) Hydrosilylation of vinyl-terminated PDMS and hydridomethylsiloxane via platinum catalyst and b.) structure of Karstedt's catalyst.

More recently, the use of tris(pentafluorophenyl)borane for the coupling of hydridosilanes and terminal alcohols or ethers in the Piers-Rubinsztajn reaction has seen some use by Brook[29,30] *et al*. Although this method has yet to achieve popularity, the Piers-Rubinsztajn reaction offers a potential avenue for a variety of new silicone materials. Zheng in the McCarthy group recently developed several novel silicone materials utilizing the unique attributes of siloxane polymers. The use of low surface tension cyclic siloxane monomers to create highly crosslinked silicone materials has shown nanometric resolution as high temperature replicating materials for imprinting techniques.[31,32] Controlling siloxane equilibration within a crosslinked silicone was also shown to create a silicone material with self-healing properties.[33]

However, with the few exceptions mentioned above, silicone materials do not have robust bulk mechanical properties. This is largely due to the low cohesive energy of silicones. To overcome this problem, inorganic fillers are added to the silicone. Most common silicone elastomers typically contain over 50 vol.% fumed silica and other additives to give them more

robust physical properties and strength. Filler particles act as reinforcing agents and typically improve the modulus and in elastomers, overall elongation.[34] The size, shape, composition, and concentration of filler material greatly affects the effectiveness of the reinforcing agent and the final properties of the material. By using particles other than silica, it is possible to impart properties that are not found in the virgin silicone while retaining those properties which may be useful.

Incorporating inorganic particles within a polymer matrix, especially silicones, is not a trivial procedure. For successful, homogeneous dispersion, both sedimentation and aggregation processes must be overcome. In sedimentation, there are three major forces: buoyant (F_B), gravimetric (F_g) and drag (F_d) (Figure 1.5). The buoyant and gravimetric forces are directly opposing, and related to the particle mass and volume. The third force, drag, limits the movement of the particle in any direction through the system and is related to the viscosity of the matrix material and radius of the particle. Because of these three forces, nanometric particles are typically easier to homogeneously disperse and suspend in polymer materials. Aggregation is typically eliminated through the surface modification of the inorganic particle. The most useful surface modifiers, either surfactants or covalently attached layers, minimize inter-particle interactions (typically electrostatic for inorganic particles) and promote particle-matrix interactions. For these reasons, the effectiveness of surface modifiers for dispersion is highly system dependent.

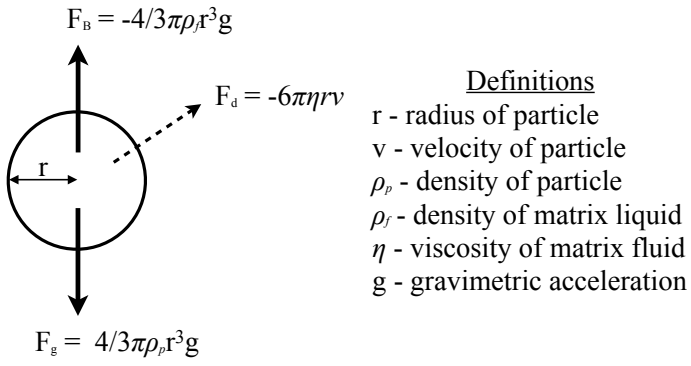

Figure 1.5. Buoyant (F_B), gravimetric (F_g), and drag (F_d) forces acting upon a particle in a polymer suspension which affect the sedimentation of these suspensions.

Typical procedures for homogeneously dispersing particles into polymers involves high shear force procedures. For silicone composites, the three mill roll was one of the earliest methods for the mixing of particles into the polymer and is still used today.[35] Another common method for making stable silicone suspensions is high shear mixing.[36] Ultrasound and vibrational agitation have also been used to disperse particles into silicones. In each of these cases, a great deal of mechanical mixing is required to achieve high levels of dispersion.

1.5 Absence of Siloxane Polymers from Academic Education

In the Preface of Reference 25, Eugene Rochow is quoted: "*Methyl silicone was so different in composition, in structure, and in physical and chemical properties that it was outside the ordinary day-to-day thinking of chemists and engineers fifty years ago.*" Unfortunately, this statement holds true for the majority of chemists today, as siloxane chemistry is not typically taught to newer generations of chemists and is not found in most basic organic, inorganic, or polymer chemistry textbooks. Given the widespread use of silicone polymers in materials, pharmaceuticals, cosmetics, adhesives, etc., it is surprising that modern chemists are not more adequately trained in this field. However, it is understandable (if not excusable) that siloxane chemistry does not find a greater place in education when considering both its history and chemical nature.

Aside from Kipping who dismissed the field as impractical and dead, the majority of silicones research was performed on the industrial level by two competitive companies. Coupled with the government mandate for secrecy in the field during the Second World War, information on silicone chemistry was kept as closely guarded trade and government secrets and not readily available to outside sources. These companies were first and foremost about business, and had no great concern with developing curricula. Regardless, the majority of academic institutions (in particular, materials science and chemistry departments) did not view polymers as a significant academic subject until many years after knowledge in the field was available.

Silicones and siloxane polymers also do not neatly fit into any specific area of organic, inorganic, or polymer chemistry. With a backbone comprised completely of inorganic elements, silicones do not readily fit into traditional organic chemistry, nor do they react in a completely traditional manner. The presence of organic side groups quickly dismisses them from inorganic chemistry. Siloxane polymers also behave so differently from other known organic polymers that it is difficult for most polymer chemists to find a place for them when teaching basic polymer science. Because of these factors, silicone chemistry often "slips through the cracks" of the normal chemist's education, and what was a well-understood field in the 1950s is currently far less understood.

1.6 Contact Angle Hysteresis

While not completely unrelated to the field of siloxane polymers, the interaction of liquids and solid surfaces (wetting) is a much older and broader field of research. This field has applications for adhesives, dispersions, and coatings. The first work concerning contact angles and wetting was performed by Thomas Young in 1804. In his work,[37] Young described the apparent interaction between liquids and solids to form "an appropriate angle of contact" for every solid/liquid pair. Though never explicitly written by Young, this relationship became known as Young's Equation (Eq. 1-3) in which the surface tensions of the solid-liquid, solid-vapor, and liquid-vapor interfaces are balanced.

$$\gamma_{LV} \cos \theta = \gamma_{SV} - \gamma_{SL} \qquad \text{(Eq. 1-3)}$$

$$\Delta\theta = \theta_A - \theta_R \qquad \text{(Eq. 1-4)}$$

However, Thomas Young assumed there was only one contact angle for each solid/liquid pair and did not account for contact angle hysteresis. Contact angle hysteresis represents a range of metastable contact angles, and is defined by the difference between the maximum contact angle value (advancing angle, θ_A) and the minimum value (receding angle, θ_R) (Eq. 1-4). This faulty assumption by Young has long been erroneously construed to confirm the existence of a finite equilibrium contact angle. There is no finite equilibrium contact angle. Bartell,[38] who

measured thousands of contact angles and always observed contact angle hysteresis in 1932, reported, "*We have since obtained good evidence that advancing angles and receding angles may each exist as definite, but different equilibrium angles.*"

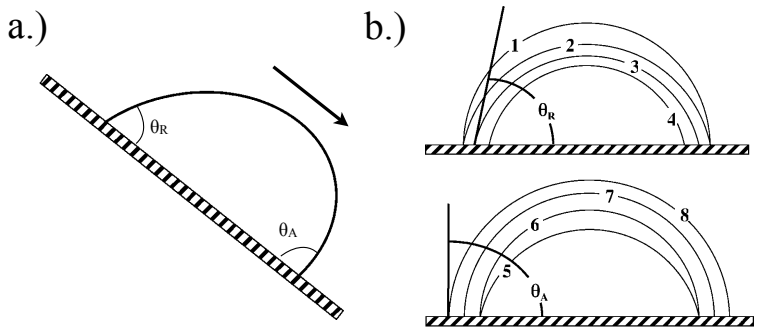

Figure 1.6. Advancing (θ_A) and receding (θ_R) contact angles of a.) a droplet sliding down a tilted surface, and b.) a sessile droplet with shrinking (1-4) and expanding (5-6) contact line diameters.

Figure 1.6[39] shows two common methods for measuring the advancing and receding contact angles. Any number of contact angles (θ_s) with values between the advancing and receding contact angle can be successfully formed and measured and are found to be quite stable. The advancing and receding contact angles, however, are unique, finite, and reproducible angles that are characteristic of an individual surface. For these reasons, contact angles (θ_A/θ_R) are one of the oldest and most useful characterization techniques for surfaces. Contact angle probe fluids are sensitive to molecular differences in surface structure (e.g. the difference between a methyl and ethyl group). Differences in these structures are reflected in the measured contact angle. Aside from surface characterization, advancing and receding angles also define the necessary conformations for droplet movement across a surface. A droplet cannot slide down a tilted surface without first the downhill side conforming to its advancing contact angle and the uphill side conforming to its receding contact angle (Figure 1.6a).

Despite the apparent utility of the advancing and receding contact angles, the problem of hysteresis has long plagued the field of wetting. There are many reasons for this. First, many researchers desire to fit thermodynamics onto something that is not at true equilibrium. For this reason, they interchange the surface tension (mN/m) used by Young and surface free energy (mJ/

m^2). [40] Although the units are equivalent, one is a measure of force while the other is the energy of an equilibrium state, and they are quite different in actual practice. Wenzel[41] in 1936 and Cassie and Baxter[42] in 1944 are perhaps some of the most influential researchers on others' perspectives on wetting. Their theories do not address hysteresis and have had an arguably destructive effect on wetting research and surface science education in the subsequent decades. This has led to a number of theoretical treatments which describe numerous differently defined contact angles,[43] and a general misconception of what hysteresis is, despite several experimental pursuits which have disproven the theories proposed by Wenzel and Cassie.[44,45]

With a few specially designed exceptions, all surfaces have and should have contact angle hysteresis, and this is actually a natural phenomenon. There are two traditional factors which contribute to contact angle hysteresis. The first is chemical heterogeneity. While this relates to different functional groups, such as amines or fluorinated alkyl chains, it also relates to the difference between ethylene groups and methyl groups in an alkyl chain. Chemical structure has also been demonstrated to be a factor contributing to hysteresis, such as the difference between *t*-butyl and *i*-butyl groups.[46] Since most molecules have some sort of definite structure, it is easy to see why hysteresis should be characteristic to most surfaces. The second factor is surface roughness. The roughening of a surface typically impacts and increases contact angle hysteresis.

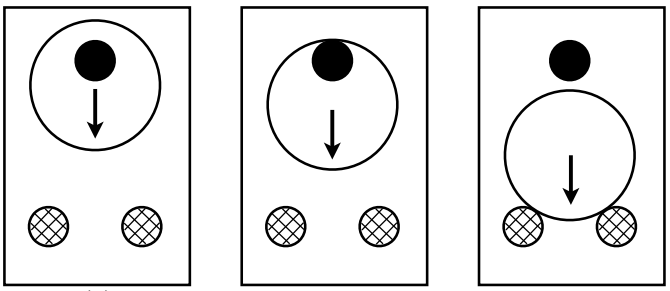

Figure 1.7. Schematic of a droplet sliding across a hypothetical hydrophobic surface with hydrophilic (solid circle) and superhydrophobic (thatched circles) defects in which a.) the defects do not contribute to the observed contact angles; b.) the hydrophilic defect pins the contact line at the receding contact angle and impedes the downward motion; and c.) the superhydrophobic defects impede the downward motion and necessitate a higher advancing contact angle for further movement.

However, only those factors which exist at the three phase contact line actively contribute to contact angle hysteresis, i.e. contact angle hysteresis is a 1-D issue.[47] For this reason, the areas underneath a droplet or on the surrounding surface do not affect the advancing and receding contact angles. The assumption that contact angles are area-dependent is one of the fundamental flaws in the Cassie-Baxter and Wenzel theories, and provides further evidence for the inaccuracies in their assumptions. Figure 1.7 gives a depiction of a droplet sliding down an hypothetical hydrophobic surface with multiple "defects". In Figure 1.7a, the solid (hydrophilic) and thatched (superhydrophobic) areas inside and outside the droplet contact line perimeter do not affect the observed advancing and receding contact angles. However, as the droplet slides downhill (Figure 1.7b), the solid (hydrophilic) defect impedes the recession of the droplet, as it must conform to a receding contact angle lower that its previous conformation before continuing downhill. Experimental results with similar parameters have been previously reported by Cheng[48] and this situation is commonly called "contact line pinning". Once the droplet conforms to the lower contact angle, it may continue downhill unimpeded until it reaches the "superhydrophobic" thatched circles with advancing contact angles greater than its previous conformation. The hydrophilic spot, no longer along the contact line perimeter, does not affect the contact angles. The thatched circles, on the other hand, pin the droplet until the advancing angle increases to a value with a conformation to move across these defects.

This understanding of contact line pinning and contact angle hysteresis has been further complicated by the recent focus on superhydrophobic surfaces. The most common method for the development of superhydrophobic surfaces is to impart secondary architecture, such as posts, onto the surface.[49] Depending on the structure, surfaces with very different properties can be developed, but others' attempts to define them with simple adjectives such as "slippy superhydrophobic" and "sticky superhydrophobic" does little to characterize and clarify the surface properties. This system of terminology has previously been criticized by the McCarthy group,[50] and the use of advancing and receding contact angles and hysteresis provides a much clearer system.

The motion of droplets across structured superhydrophobic surfaces is also much different. While droplets slide on perfectly smooth surfaces, on a superhydrophobic surface droplets roll in a tank-tread manner. This sliding and tank-tread rolling are, in fact, the two extremes for droplet motion and the actual motion of a droplet on a real surface most likely contains elements of both of these motions. As a final note, the motion of droplets requires both recession and advancing events which can occur concurrently or sequentially and can be concerted or individual. This is because the advancing and receding events are not necessarily the opposite or reverse of the other and typically have very different mechanisms.

1.7 References

1. Rochow, E.G., *Silicon and Silicones*. Spring-Verlag: Berlin; New York, **1987**.
2. Seyferth, D., *Organometallics*, **2001**, *20*, 4978-4992.
3. Liebhafsky, H.A., *Silicones Under the Monogram*. J. Wiley & Sons: New York, **1978**.
4. Warrick, E.L., *Forty Years of Firsts*. McGraw-Hill: New York, **1990**.
5. Berzelius, J.J., *Ann. Phys. Chem.*, **1824**, *1*, 169.
6. Thomson, T., *Annals of Philosophy*, **1814,** *3,* 450-454.
7. Sainte-Claire Deville, H.E., *Compt. rend. acad. sci.*, **1854**, *39*, 321.
8. Rochow, E.G., *Introduction to the Chemistry of the Silicones*. J. Wiley & Sons, Chapman & Hall: New York, London, **1946**.
9. Ladenburg, A., *Ann*., **1972**, *164*, 300.
10. Post, H.W., *Silicones and Other Organosilicon Compounds*. Reinhold: New York, **1949**.
11. Kipping, F.S., Lloyd, L.L., *J. Chem. Soc.*, **1901**, *79*, 449-459.
12. Kipping, F.S., *Proc. R. Soc. (London)*, **1937**, *159*, (A589), 0139-0148.
13. Stock, A., Somieski, C., *Ber. Dtsch. Chem. Ges.*, **1919**, *52*, 695-724.
14. Rochow, E.G., *J. Am. Chem. Soc.*, **1945**, *67*, 1772.
15. Pauling, L., *J. Am. Chem. Soc.*, **1932**, *54*, 3570-3582.
16. Pauling, L., *American Mineralogist*, **1980**, *65*, 321-323.
17. Mark, J.E., *Acc. Chem. Res.*, **2004**, *37*, 946.

18. Kantor, S.W., Grubb, W.T., Ostoff, R.C., *J. Am. Chem. Soc.*, **1954**, *76*, 5191.

19. Silicone Fluids, Gelest Catalog. 455-459.

20. Mark, J.E., ed., *Polymer Data Handbook*, Oxford University Press: New York; **1999**.

21. Dlubek, G., De, U., Pionetck, J., Arutyunov, N.Y., Edelmann, M., Krause-Rehberg, R., *Macromol. Chem. Phys.*, **2005**, *206*, 827-840.

22. Krumpfer, J.W., McCarthy, T.J., *Faraday Discuss*., **2010**, *146*, 103-111.

23. Bernardini, C., Stoyanov, S.D., Stuart, M.A.C., Arnaudov, L.N., Leermakers, F.A.M., *Langmuir,* **2011**, *27*, 2501-2508.

24. Graiver, D., Farminer, K.W., Narayan, R., *J. Polym. Environ.*, **2003**, *11*, 129-136.

25. Clarson, S.J., Semlyen, J.A., *Siloxane Polymers*. Prentice Hill: Englewood Cliffs; **1993**.

26. Odian, G. G., *Principles of Polymerization. 4th ed.*; Wiley: Hoboken, N.J., **2004**.

27. Marsden, J., U.S. Patent 2,445,794, July 27, **1948**.

28. Stein, J., Lewis, L. N., Gao, Y., Scott, R. A., *J*. *Am*. *Chem*. *Soc*., **1999**, *121*, 3693- 3703.

29. Brook, M.A., Grande, J.B., Ganachaund, F., *Adv. Polym. Sci.*, **2011**, *235*, 161-183.

30. Gretton, M.J., Kamino, B.A., Brook, M.A., Bender, T.P., *Macromol.*, **2012**, *45*, 723-728.

31. Zheng, P., McCarthy, T.J., *Langmuir*, **2011**, *27*, 7976-7979.

32. Zheng, P., McCarthy, T.J., *Langmuir*, **2010**, *26*, 18585-18590.

33. Zheng, P. McCarthy, T.J., *J. Am. Chem. Soc.*, **2012**, *134*, 2024-2027.

34. Paul, D.R., Mark, J.E., *Progress in Polymer Science*, **2010**, *35*, 893-901.

35. Maus, L., Walker, W.C., Zettlemoyer, A.C., *Industrial and Chemical Engineering*, **1955**, *47*, 696.

36. Schaer, E., Gagnard, C., Choplin, L., Canpont, D., *Powder Technology*, **2006**, *168*, 156.

37. Young, T., *Philos. Trans. R. Soc. London*, **1805**, *95*, 65.

38. Bartell, F.E., Whitney, C.E., *J. Phys. Chem.*, **1932**, *36*, 3115.

39. Gao, L., McCarthy, T.J., *Langmuir*, **2006**, *22*, 6234-6237.

40. Adamson, A.W., Gast, A.P., *Physical Chemistry of Surfaces*. J. Wiley & Sons: New York, **1997**.

41. Wenzel, R.N., *Ind. Eng. Chem.*, **1936**, *28*, 988.

42. Cassie, A.B.D., Baxter, S., *Trans. Faraday Soc.*, **1944**, *40*, 546.

43. Marmur, A., Bittoun, E., *Langmuir*, **2009**, *25*, 1277.

44. Gao, L., McCarthy, T.J., *Langmuir*, **2007,** *23*, 3762.

45. Gao, L., McCarthy, T.J., *Langmuir*, **2009**, *25*, 7249.

46. Fadeev, A.Y., McCarthy, T.J., *Langmuir*, **1999**, *15*, 3759-3766.

47. Pease, D.C., *J. Phys. Chem.*, **1945**, *49*, 107.

48. Cheng, D.F., McCarthy, T.J., *Langmuir*, **2011**, *27*, 3693-3697.

49. Öner, D., McCarthy, T.J., *Langmuir*, **2000**, *16*, 7777-7782.

50. Gao, L., McCarthy, T.J., *Langmuir*, **2008**, *24*, 9183.

CHAPTER 2

SURFACE MODIFICATION OF TITANIA USING HYDRIDOMETHYLSILOXANES

2.1 Introduction

2.1.1. Background.

Titania (TiO_2), the naturally occurring oxide of titanium, is the most widely used pigment material in the world, and approximately four million tons of pigment quality titania are produced annually.[1] Originally used as a non-toxic replacement to lead oxide pigments, titania is known for its bright white appearance and exceptionally high refractive index, and is used in paints (51% total production), plastic (19%) and paper (17%). More recently, titania has been used in food coloring (E-171), cosmetics, and toothpaste.[2] Titania also has several other important properties. It is known for its UV-absorbing properties and is found extensively in sunscreen lotions with high sun protection factors. Titania is also a photocatalytic material used in solar cell devices, anti-bacterial and self-cleaning materials, and as a catalyst in organic synthesis.[3] Finally, titania is a high resistance-end, semi-conducting material.[4]

Table 2.1 Bulk properties of rutile, anatase, and brookite titania.[1,4]

Titania	Crystal Structure	Density (g/cm^3)	Refractive Index (n_f)	Electrical Resistivity ($\Omega \cdot cm$)	Hardness (Mohs)
rutile	tetragonal	4.24	2.9467	$\sim 10\text{-}10^2$	5-6.5
anatase	tetragonal	3.83	2.5688	$\sim 10^5\text{-}10^6$	--
brookite	rhombohedral	4.17	2.809	$\sim 10^5\text{-}10^6$	--

Titania exists in several crystalline forms, with the three most common mineral forms being rutile, anatase and brookite. Rutile is the most common and stable form with a tetragonal crystal structure. Anatase and brookite are metastable (kinetically stable) phases with crystal structures of tetragonal and orthorhombic, respectively. Both the anatase and brookite forms can be easily converted to rutile by heating to temperatures above 800 °C. Table 2.1 gives several

common properties for these three phases of titania. From an application standpoint, only anatase and rutile have found significant usages.

There are several methods for the production of titania particles which directly affect the nature of the crystal structure obtained. The most common method for the production of anatase is the vapor-phase oxidation of titanium (IV) chloride ($TiCl_4$).[5] This produces a narrow particle size of approximately 20 nm, but often contains chlorine impurity. Furthermore, the anatase phase purity is not particularly high, generally containing close to 25% rutile (e.g. Degussa P25). The other most common commercial method, known as the "sulfate method", typically involves treatment of a titanium source (for instance, ilmenite, $FeTiO_3$) with sulfuric acid, followed by purification, hydrolysis and calcination.[6] This method also forms the anatase phase, but also may leave sulfur impurities. On a laboratory scale, pure anatase and rutile can be formed by the hydrolysis of titanium alkoxides or titanium tetrachloride and the crystal phase can be carefully controlled by temperature.[7]

Depending on the crystal phase, plane, and preparation (purity) method, the surface properties of titania can be quite variable and complex.[8,9] Generally speaking, like most other metal oxide surfaces, titania features terminal surface hydroxyl groups and is typically hydrated.[10] However, this does not exclude the existence of many other oxygen and titanium species, and in fact, titania surfaces feature a wide variety of neutral and charged species, which give titania many of its catalytic properties. Although typically tetracovalent, titanium, being a transition metal, can also easily be penta- and hexacovalent. This complex structure and wide variety of surface species lead to surfaces that have a much greater molecular roughness than those of silica. Because of the hydration and existence of charged species, titania also has a slightly acidic nature with point of zero charge (PZC) at pH's of approximately 5.5-6.5.[11]

Surface modification of titanium dioxide is very important to the fabrication of the materials mentioned in the first paragraph of this introduction. The surface modification is used to ease the dispersion of particles into materials.[12] It is also necessary in many applications, particularly as pigments in paints, to eliminate many of titania's photocatalytic properties to avoid

degradation of the matrix material. The most common method to completely eliminate the photocatalytic properties of titania is to coat the particles with silica,[13,14] followed by subsequent modification. Unfortunately, the use of chlorosilanes, popular surface modification reagents, cannot be used on titania surface, since the by-product of this reaction, HCl, is corrosive to titania surfaces. For this reason, a variety of other reagents have been used, such as phosphonic acids[15], sulfonic acids[16], and carboxylic acids[17]. However, these reagents have many drawbacks. They are typically much more costly than typical silane modifiers, and they do not produce particularly high quality monolayers.[18]

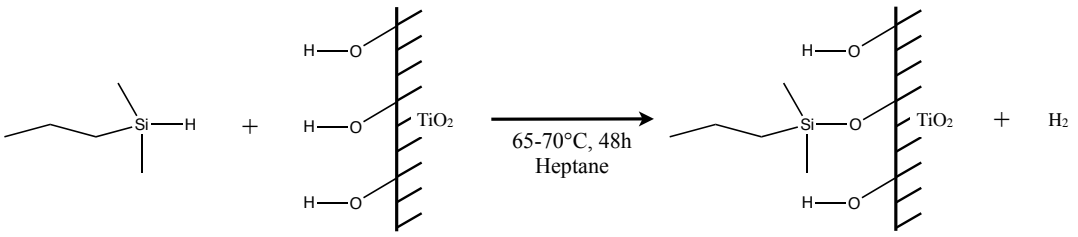

Figure 2.1. Reaction of alkylhydridosilanes with titania surfaces to form covalently attached monolayers and hydrogen gas by-product.

In 1999, Fadeev and McCarthy[19] reported the preparation of hydrophobic titania surfaces through the reaction with hydridosilanes, as seen in Figure 2.1, and the majority of our understanding of this reaction is derived from this work. They showed that this reaction produces monolayers with high grafting densities, high contact angles, and a stoichiometric by-product of hydrogen gas. This by-product is non-corrosive to titania and is environmentally friendly. These monolayers also show high thermal stability[20] with degradation beginning near 400 °C. Furthermore, hydridosilanes can be prepared through the reaction of lithium aluminum hydride with chlorosilanes,[21] allowing for surfaces with a wide variety of functionalities to be prepared. While not directly relevant to this topic on titania, hydridosilanes were also shown to be useful reagents for a wide number of metal surfaces.[22,23]

Despite the excellent surface properties, ease and versatility of preparation, and non-corrosive by-product produced by the reaction of hydridosilanes with titania surfaces, this preparation technique has found very little popularity with only a few reported usages.[24,25] There

have been a few reported cases of hydridomethylsiloxane reagents both prior and subsequent to the report by Fadeev. Tada[26,27] reported the use of 1,3,5,7-tetramethylcyclotetrasiloxane (TMCTS) for the modification of titania surfaces and creation of thin silicon oxide films on titania through subsequent annealing. Gentile[28] reported the use of hydrogen silsesquioxane as a chemical modifier, also for the preparation of thin silicon oxide films. In both of these cases, the thin silicon oxide films were created to control or eliminate the photocatalytic properties of titania. However, the reactions of hydridomethylsiloxanes are much more complicated than those of hydridosilanes (and more than these reports suggest) and this complication will be addressed in this and even more so in the following chapter.

2.1.2 Objectives.

The objectives of this work were to utilize and extend the reactions of hydridosilanes with titania to hydridomethylsiloxane polymers for the preparation of hydrophobic titania surfaces. This work was performed to reintroduce and promote this reaction to the research community and its benefits for further applications. The utility of these polymers as surface modifying reagents was addressed through comparison with small molecule reagents (e.g. silanes on silica). Hydridomethylsiloxanes offer another alternative to other reagents for the modification of titania and feature all of the previously mentioned benefits of siloxane polymers, such as thermal and chemical stability. Furthermore, it was the goal of this work to determine the use of these hydridomethylsiloxanes as a platform for subsequent modification techniques on titania surfaces. Finally, to investigate the use of hydridomethylsiloxane-*co*-dimethylsiloxane random copolymers as modifying reagents and to determine the necessary molar fraction of hydridosilane for the covalent attachment of these polymers.

2.2 Experimental Section

2.2.1 Materials

Silicon-supported titanium wafers, fabricated by the evaporation of titanium with titanium thicknesses of 500-550 microns, were purchased from International Wafer Service.

Poly(hydridomethylsilxonane)s (HMS), poly(hydridomethylsiloxane)-*co*-poly(dimethylsiloxane)s, poly(dimethylsiloxane) (MW~2,000 g/mol), 1,3,5,7-tetramethylcyclotetrasiloxane (TMCTS, D_4^H), and platinum-divinyldisiloxane complex (Karstedt's catalyst) were purchased from Gelest, Inc. and were used without further purification. Allylamine and (perfluorohexyl)ethylene were purchased from Sigma-Aldrich and used without further purification.

2.2.2 Reaction Conditions

Prior to reaction with hydridomethylsiloxanes, silicon-supported titanium wafers were cut into approximately 1.0 x 1.0 cm pieces and were exposed to an oxygen plasma using a Harrick Expanded Plasma Cleaner at 18W and 300 mTorr (flowing oxygen) for 30 min in order to produce clean surfaces. These surface were then submerged into 5% by volume solutions of the desired hydridomethylsiloxane in heptane in a sealed glass vessel, and heated at 100 °C for 72 hours. Although this reaction occurs slightly above the boiling point of heptane (b.p. ~ 98 °C), heptane does not boil inside the sealed vessels. After this, the wafers were removed from solution and rigorously rinsed with copious amounts of toluene, acetone, and water (in that order) from polyethylene squirt bottles. The surfaces were then dried under nitrogen.

Formation of silicon oxide surfaces on titania was performed on those surfaces reacted with hydridomethylsiloxane (MW~2,000 g/mol) and 1,3,5,7-tetramethylcyclotetrasiloxane prepared in the manner reported above. These surfaces were exposed to an oxygen plasma for 30 minutes at 18W and 300mTorr (flowing oxygen). Samples were rinsed with Milli-Q water immediately following this treatment, and dried under nitrogen.

Surface hydrosilylation was performed on surfaces prepared in the same fashion as above using hydridomethylsiloxane (MW~2,000 g/mol) in 5% by volume solutions in heptane and reacted at 100 °C for 4 hours. These samples were then submerged in 5% by volume solutions of either (perfluorohexyl)ethylene or allylamine in heptane containing $5 \cdot 10^{-4}$ g/mL Karstedt's catalyst and heated at 100 °C for 48 hours. Samples were then rinsed with copious amounts of

toluene, acetone, and water (in that order) from polyethylene squirt bottles, and dried under nitrogen.

2.2.3 Characterization

The primary characterization techniques for this work are dynamic contact angles and X-ray photoelectron spectroscopy (XPS). Dynamic contact angles were measured using a Rame-Hart telescopic goniometer and a Gilmont syringe with a 24-gauge, flat-tipped needle. Advancing (θ_A) and receding (θ_R) contact angles were recorded while the probe fluid (water) was added to and withdrawn from the sessile drop, respectively, in the fashion described in chapter 1.

X-ray photoelectron spectroscopy was performed using a Physical Electronics Quantum 2000 spectrometer to characterize the chemical composition of the surfaces at angles of 15° and 75° from the surface plane. A few brief notes to explain the mechanics of this characterization technique should be mentioned. During characterization, surfaces are bombarded with X-ray photons. X-rays impinge upon a surface, causing core electrons to be ejected. The difference between the energy of the photon and emitted electron detected is known as the binding energy, which is dependent upon and characteristic of the element and atomic orbital from which it was emitted. XPS is only useful in characterizing the surface of a material, rather than the bulk, as electrons statistically travel only a finite distance (mean free path) before striking an atom. Therefore, elements further in the bulk have a much lower probability of detection. However, there is some degree of control over the depth of the characterization by controlling the angle between the sample surface and the detector (referred to as the "take-off angle"). In this way, a take-off angle of 15° has a profile depth typically between 8-35Å, and a take-off angle of 75° has a profile depth between 30-130Å. Besides chemical composition of surfaces, this technique can also be used to give a rough estimate of the surface thickness of supported films.[29] This approximation is important, as traditional ellipsometry cannot be performed on titania samples. Further characterization using atomic force microscopy with a Digital Instruments Dimension 3000 was performed to give qualitative results of a few of the prepared surfaces.

2.3 Results and Discussion

2.3.1 Reactions of Linear Hydridomethylsiloxane Homopolymers

Commercially available, linear homopolymers of hydridomethylsiloxane (HMS) of various molecular weight (MW~1,600; 2,000; and 2,300 g/mol) were reacted with clean smooth silicon-supported titanium wafers at 100 °C for 72 hrs using 5 vol.% solutions in heptane. The surfaces of these titanium wafers feature a native oxide layer of amorphous titania (TiO_2) from exposure to air, and they are further treated with an oxygen-plasma prior to this reaction. Table 2.2 shows advancing (θ_A) and receding (θ_R) water contact angles for surfaces prepared using these three molecular weight HMS samples.

Table 2.2. Average advancing and receding water contact angles and X-ray photoelectron spectroscopy (15° take-off angle) %C/%Si elemental ratios for linear hydridomethylsiloxanes of various molecular weight reacted with smooth titania surfaces at 100 °C for 72 hrs using 5 vol.% solutions in heptane.

Molecular Weight (g/mol)	Reaction Time (h)	Water Contact Angle (θ_A/ θ_R)	Hysteresis ($\Delta\theta$)	XPS (15˚) %C/%Si
~1600	72	102 / 87	15	1.4
~2000	72	106 / 93	13	1.1
~2300	72	105 / 90	15	1.4

Standard deviation for the advancing and receding contact angles (σ_A/σ_R) reported were 2.13°/9.13° using MW~1,600 g/mol; 1.20°/1.64° using MW~2,000 g/mol; and 0.65°/2.45° using MW~2,300 g/mol. Figure 2-2 gives representative XPS spectra (15° and 75° take-off angles) for a titania surface modified with a linear hydridomethylsiloxane (MW~2,000 g/mol). From the X-ray photoelectron spectroscopy data, approximate thicknesses of 2 nm for these samples can be made using Eq 2-1,[29] in which *t* is the thickness, λ is the wavelength of the photon, and N_o and N are the intensities of a specific peak (here, using the Ti_{2p} peak) before and after modification respectively. This approximation is not an exact value, but does give a reasonable order of magnitude for these monolayer thicknesses.

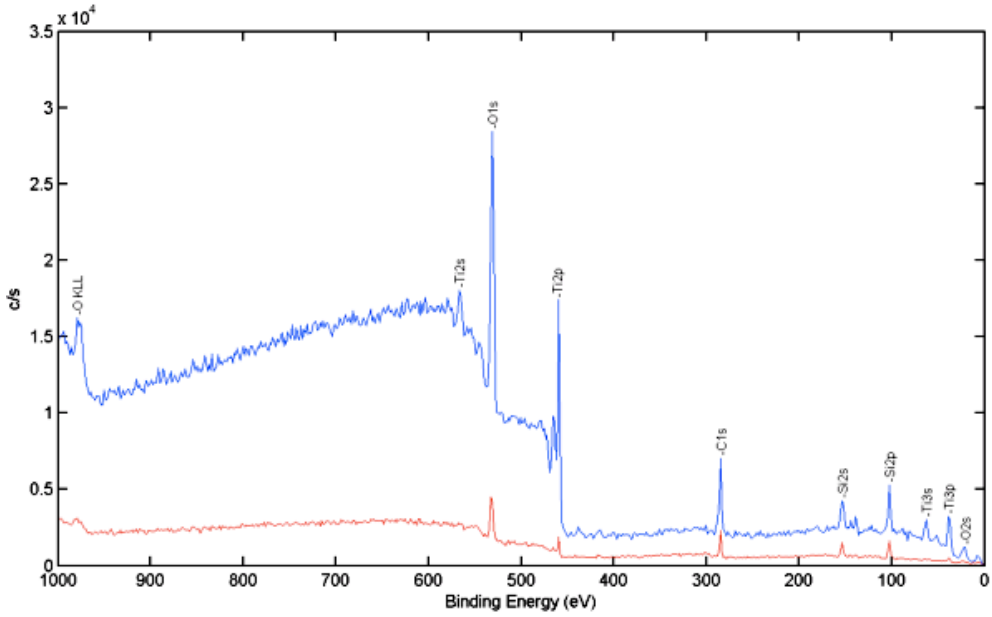

Figure 2.2. Representative X-ray photoelectron spectra of hydridomethylsiloxane (MW~2,000 g/mol) reacted with a smooth titania surface at 100 °C for 72 hrs using a 5 vol.% solution in heptane at 15° take-off angle (lower spectrum) and 75° take-off angle (upper spectrum).

$$t = \lambda \sin\theta / \ln(N_o/N) \qquad \text{(Eq 2-1)}$$

The surfaces fabricated using these three linear homopolymers give contact angle data comparable to those fabricated by hydridosilanes,[19] and there is not a significant difference between the surfaces prepared using the three different molecular weight samples. However, in general, the hydridomethylsiloxane (MW~2,000 g/mol) ($HMS^{2,000}$) showed slightly better surface characteristics in terms of the %C/%Si elemental ratio, contact angle hysteresis, and reproducibility than the other two homopolymers. The %C/%Si ratio for the $HMS^{2,000}$ was 1.1, which is close to the theoretical ratio of 1.0, rather than 1.4 for the others. The divergence from the theoretical ratio found in this and the other samples is ascribed to carbon contamination, which often occurs when exposed to the laboratory environment.

The contact angle hysteresis found in these samples is comparable to samples prepared by random covalent attachment of silanes with silica surfaces and suggests the presence of unreacted surface titanium hydroxyl groups.[30] These unreacted hydroxyl groups would act as molecular contact line pinning sites, accounting for the low receding contact angle. Furthermore, atomic

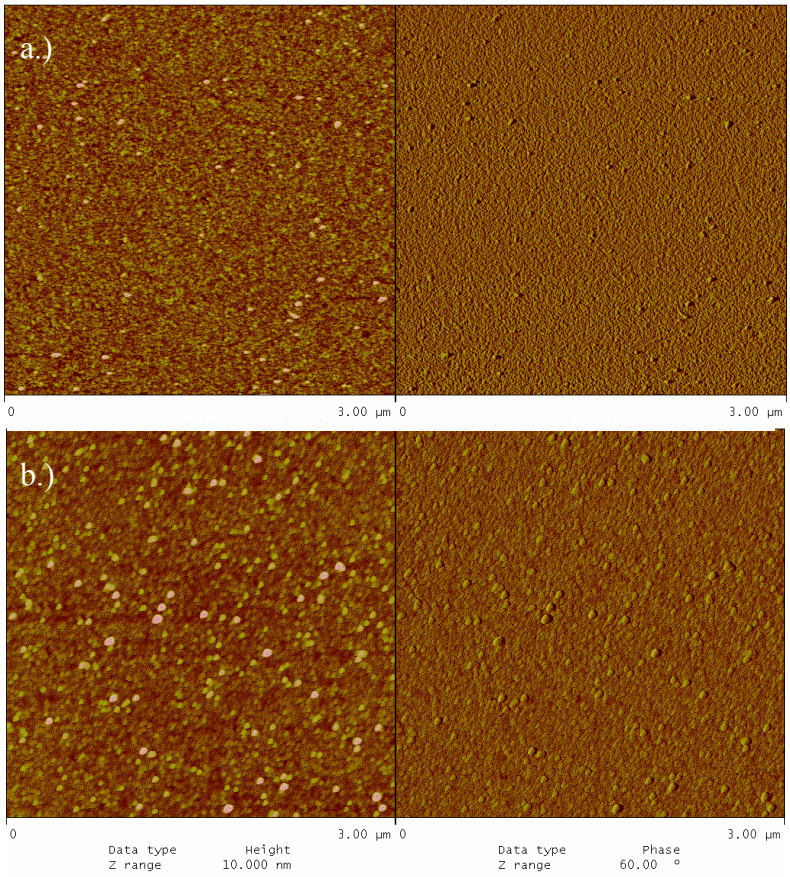

Figure 2.3. Atomic force microscopy height (left) and phase (right) images of a.) a clean silicon-supported titanium wafer and b.) silicon-supported titanium wafer reacted with hydridomethylsiloxane (MW~2,000 g/mol) at 100 °C for 72 hrs using a 5 vol.% solution in heptane.

force microscope images (Figure 2.3) show an increase in surface roughness after modification of the titania surface. While the morphology of the hydridomethylsiloxanes on titania surfaces was not directly ascertained, a number of globular shaped surface features seen in Figure 2.3b suggests that the hydridomethylsiloxanes do not simply lie flat (i.e. with the chain fully extended across the surface), but rather either overlap one another or form monomolecular bundles upon the surface with unreacted hydridosilane groups. It is also possible for hydridosilane bonds to react with one another in the presence of water to form crosslinks between chains. However, this reaction is believed to be slow and should not occur during the time scale of these experiments, but it is not entirely possible to discount. Regardless, this bundle/overlap structure would allow for the presence of unreacted titanium hydroxyl groups, since they would sterically limit other

chains to access unreacted titanium hydroxyl sites in a similar fashion to randomly attached monolayers. This would be consistent with the contact angle hysteresis found within these samples.

Table 2.3. Average advancing and receding water contact angles and X-ray photoelectron spectroscopy (15° take-off angle) %C/%Si elemental ratios for hydridomethylsiloxane (MW~2,000 g/mol) reacted with smooth titania surfaces at 100 °C using 5 vol.% solutions in heptane at various times.

Reaction Time (hr)	Water Contact Angle (θ_A/ θ_R) (°)	Standard Deviation (σ_A/σ_R)	Hysteresis ($\Delta\theta$)	XPS (15°) %C/%Si
0	0 / 0	n/a	n/a	n/a
0.25	104.3 / 87.8	1.23 / 1.70	16.5	1.89
0.5	104.8 / 88.0	1.06 / 5.29	16.8	1.89
0.75	105.9 / 87.3	1.12 / 8.86	18.6	2.49
1	107.6 / 95.2	1.14 / 2.80	12.4	1.90
2	107.5 / 87.7	1.57 / 6.97	19.8	1.86
4	103.2 / 81.1	1.17 / 3.23	22.1	1.70
6	104.6 / 84.1	1.04 / 2.05	20.4	1.72
12	103.1 / 81.4	0.96 / 2.53	21.7	1.11
24	102.0 / 80.4	3.38 / 1.70	21.6	1.42
48	102.3 / 82.1	2.95 / 2.55	20.2	1.27
72	104.0 / 93.2	1.20 / 1.64	10.8	1.14

Table 2.4. Advancing and receding water contact angles of trimethyl(dimethylamino)silane-treated silica surfaces using a 5 vol.% solution in toluene for various times at room temperature[31].

reacn time, h	θ_A/θ_R (°)	reacn time, h	θ_A/θ_R (°)
0.1	80/35	4	102/94
0.5	93/82	15	103/94
1	99/93	24	104/95
2	99/93	48	105/96
2.5	100/97	72	105/96
3	102/95	196	105/96

While no direct reasoning for the improved quality of $HMS^{2,000}$ over the other samples is offered, it may be simply due to higher quality of the reagent or less human error in preparation. Regardless, because of the slightly better quality of these samples in the data, this polymer was used for subsequent study of reaction conditions. Table 2.3 gives advancing and receding contact

angle (decimal places represent average values) and XPS %C/%Si elemental ratios for the reaction kinetics for $HMS^{2,000}$ at 100 °C using a 5 vol.% solution in heptane. As before, a comparison to randomly attached monolayers seems appropriate and is used here. Like the reaction kinetics of small molecule silanes on silica in random covalent attachment reported by Fadeev (Table 2.4),[31] reaction of $HMS^{2,000}$ with titania surfaces occurs rapidly in the first hour, as seen in the contact values. In fact, contact angles jump from 0°/0° for clean titania surfaces (water completely wets titania) to 104.3°/87.8° within 15 minutes.

Perhaps coincidentally, this reaction undergoes a relative minimum in contact angle hysteresis after approximately an hour of reaction, similar to the reaction of small silanes on silica. In the case of silanes on silica, this minimum of hysteresis was attributed to a higher degree of conformational freedom since the silanes can freely rotate around Si-O-Si bonds. However, unlike mono-functional silanes, hydridomethylsiloxanes are multi-functional and have a greater degree of conformational freedom which is typical of silicone polymers. Still, an argument for decreased conformational freedom can be made to explain this minimum.

At low reaction times, siloxane chains that have reacted with the surface still have a great deal of flexibility, since only a few of the hydridosilane groups bind the polymer to the surface. As the reaction time increases, further reaction of hydridosilane groups on the same polymer chain may occur with the surface, greatly limiting the conformational freedom of the polymer chain, and pinning it into a specific morphology. This resulting rigidity would lead to an increase in contact angle hysteresis. At increasing reaction times, unreacted titanium hydroxyl groups may become exposed to allow for further reaction and greater surface coverage, which would lead to the final minimum found at 72 hours.

Another difference between silane-silica and HMS-titania reactions is the rapidity in which the receding contact angle increases. This is attributed to the larger size and multi-functional nature of these polymers over small molecules. Hydridomethylsiloxane polymers can achieve much greater surface coverage through a single reaction than smaller molecules simply due to their bulk size. Also, due to the multi-functional nature of HMS polymers, there is a

higher probability for reaction per molecule than mono-functional reagents, although this is probably a negligible effect as the number of small molecules greatly exceeds those of polymers with higher molecular weights given equivalent solution concentration (mass/volume).

This reaction was also observed using X-ray photoelectron spectroscopy. Figure 2.4 shows changes in O_{1s}, Si_{2p}, and Ti_{2p} peaks of titania surfaces reacted with hydridomethylsiloxane (MW~2,000 g/mol) for various times. Figure 2.4a shows the difference in binding energy of oxygen bound with silica and titania at approximately 533 eV and 531 eV, respectively.

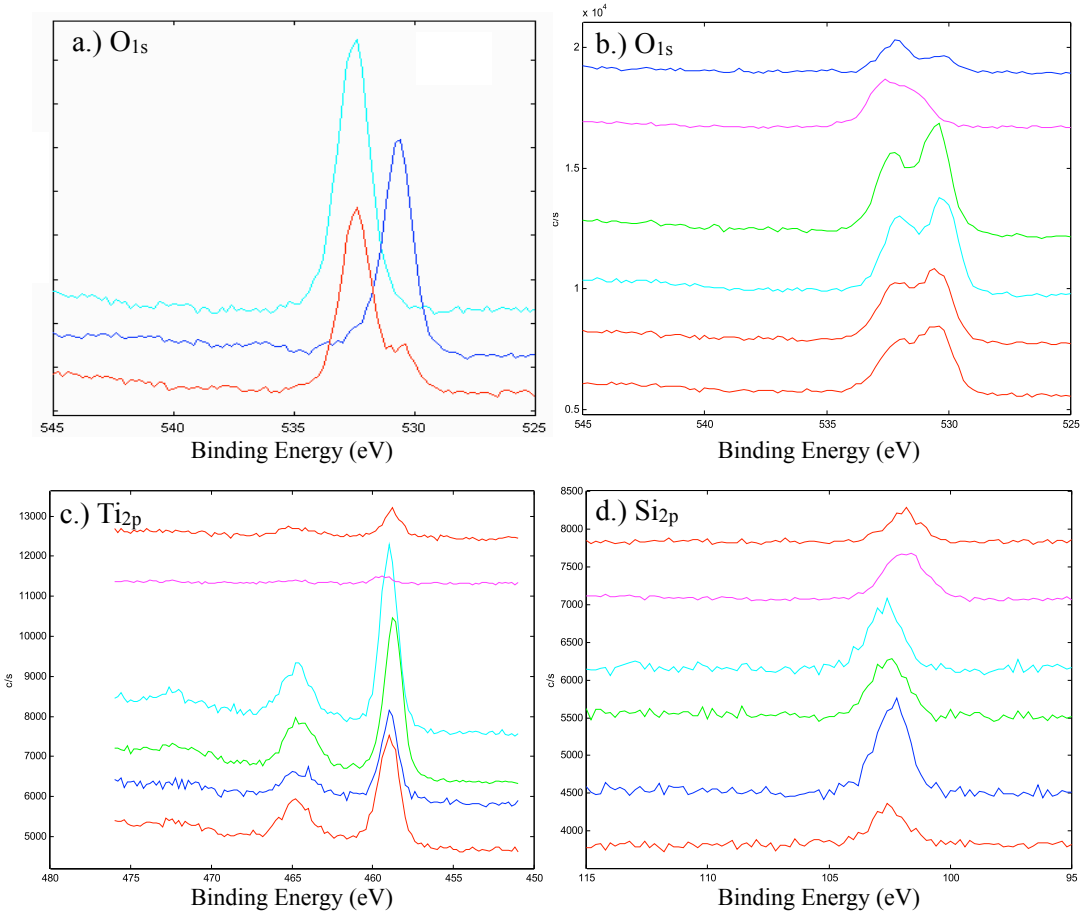

Figure 2.4. X-ray photoelectron spectra of a.) O_{1s} peaks of silica, titania, and hydridomethylsiloxane (top to bottom) on titania at a 75° take-off angle; and b.) O_{1s} peaks (15° take-off angle), c.) Ti_{2p} (15° take-off angle), and d.) Si_{2p} (15° take-off angle) peaks of titania surfaces reacted with hydridomethylsiloxanes (MW~2,000 g/mol) at 100 °C with 5 vol.% solutions in heptane for 0.5, 1, 4, 12, 14, and 72 hours (bottom to top).

The binding energy of oxygen in hydridomethylsiloxanes is similar to that of silica, and this 2 eV difference can be used to observe the growth of hydridomethylsiloxane monolayer on titania (Figure 2.4b), as the hydridomethylsiloxane O_{1s} peak increases over time. Due to the mean free path (8-35 Å) of X-ray photons at a 15° take-off angle, it is expected that as the monolayer thickness increases, the intensity of the Ti_{2p} should decrease and that of Si_{2p} should increase. This trend is observed in the XPS data, as seen in Figures 2.4c and 2.4d, respectively. The %C/%Si elemental ratios (Table 2.3) show a great deal of carbon contamination at low reaction times. This is expected as exposed titania surface should rapidly adsorb carbon contaminants when exposed to the laboratory environment. However, at longer reaction times, the %C/%Si ratio approaches the theoretical value of 1.0, signifying a much greater surface coverage and lack of contamination, and is consistent with the analysis of receding and advancing contact angles.

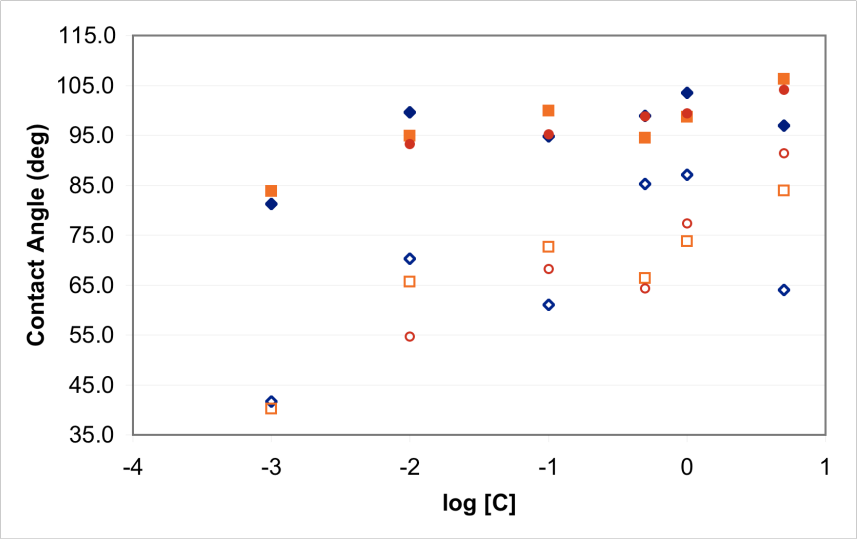

Figure 2.5. Advancing (closed) and receding (open) contact angles of hydridomethylsiloxane (MW~2,000 g/mol) reacted with titania surfaces at 100 °C for 24 (circles), 48 (squares), and 72 (diamonds) hours using different % vol. solutions in heptane.

The effect of solution concentration on the water contact angles of the surfaces prepared is shown in Figure 2.5. There is a definite upward trend in both advancing and receding contact angle with respect to both concentration and reaction time. Still, there is little decrease in

advancing contact angle when using concentrations even as low as 0.0l vol.%, and a much greater decrease is seen in the receding contact angles. This suggests a great deal of reaction which has not achieved maximum surface coverage, and may be attributed to the large size of the polymer modifying agents. It is probable that given longer reaction times, surfaces made with lower concentrations should achieve nearly equivalent properties as those made using 5 vol.% solutions. However, there is a significant change in the properties when using concentrations below 0.01 vol.%, and this may represent a limiting threshold.

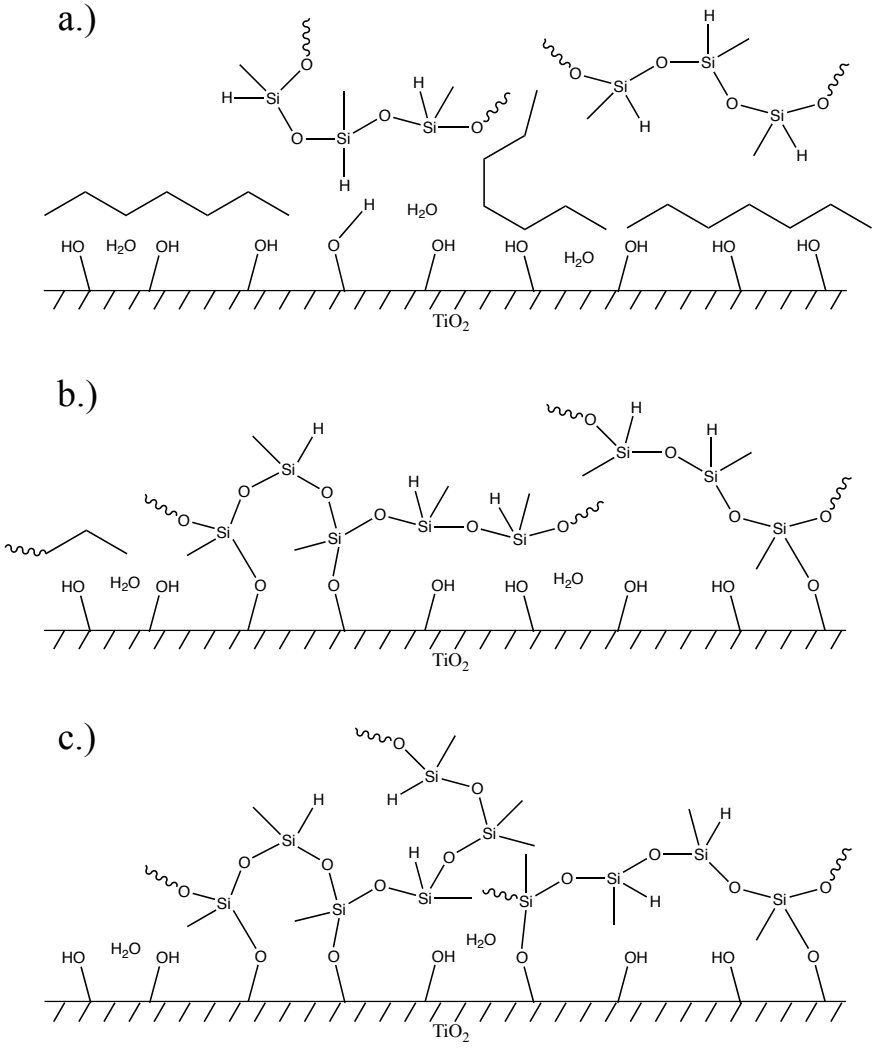

Figure 2.6. Scheme for the reaction of hydridomethylsiloxane polymers with titania surfaces beginning with a.) competitive adsorption with heptane solvent and initial reaction followed by b.) siloxane rearrangement and further reaction at low reaction times, and c.) limited conformational freedom and high surface coverage at high reaction times.

From this data, a general reaction scheme is developed (Figure 2.6). In the early stages of reaction, a competitive adsorption process occurs with the solvent followed by reaction (Figure 2.6a). It is uncertain whether reaction of the hydridosilane with titanium surface hydroxyl groups occurs directly or is catalyzed by surface bound water. Tethered only by only one covalent attachment (Figure 2.6b), the siloxane chain has a high degree of flexibility and may limit the access of other polymer chains to surface hydroxyl groups within its immediate vicinity. As the surface bound siloxane moves, it may open access to surface hydroxyl groups for the reaction of other polymer chains. It may also undergo further reaction with the surface with its remaining hydridosilane groups. This state represents the conditions seen after approximately one hour of reaction, in which there is a high degree of siloxane chain flexibility (i.e. low hydridosilane reaction), but a high degree of surface coverage is present. After this, further reaction of the polymer hydridosilane bonds occurs which limits the available conformations of the siloxane chain (Figure 2.6c), but may allow for further reactions by other polymers. This occurs until there are no accessible surface hydroxyl groups for reaction and represents the conditions found near reaction completion. Unbound chain ends and loops may account for the globular shapes found within the AFM data.

There are two secondary reactions which may occur in conjunction with the hydridosilane/titania surface reaction. The first is condensation between hydridosilane bonds in the presence of water, which may occur slowly. The second is covalent attachment between the polymer backbone and titania surface (not shown). This reaction is addressed in greater detail in the following chapter. It is also noted that this reaction scheme does not take into account any other surface species aside from surface hydroxyl groups, but models this reaction after a previously reported mechanism.[19]

A few comments on factors not directly addressed in this study should be noted which may have an effect on the reaction of HMS polymers with titania, the rapidity of monolayer formation, and the resulting surface properties. The rate of reaction of hydridosilanes with titania is expected to be different than those of chloro- or aminosilanes with silica, and this may account

for the comparative rapidity with which HMS polymers seem to react with titania. However, given that these polymers show significant surface reaction even using low concentrations, the effect of polymer size is believed to be more important. The role of surface hydration on this reaction of hydridosilanes with titania is unknown, and may or may not prove to be as significant as it is in the reaction of chlorosilanes with silica. Temperature is known to affect this reaction. The competitive adsorption of HMS and heptane on titania should impact the rate of this surface reaction. Heptane was chosen as solvent for these studies since it is a known good solvent for silicones. Finally, given the low intermolecular interactions exhibited by silicone polymers, it is believed that these surfaces are monolayers, and all unreacted polymer is easily rinsed away with solvents after reaction.

2.3.2 Subsequent Modification Techniques

Surfaces prepared using hydridomethylsiloxanes were used as a platform for a second modification to either add additional functionalities to the surface through hydrosilylation (discussed in Chapter 1) or to create silicon oxide films on the titania surface through oxygen plasma treatment. In this way, a greater degree of control may be exhibited over the surface properties of titania.

Table 2.5. Advancing and receding water contact angles and X-ray photoelectron spectroscopy elemental analysis for hydridomethylsiloxane surfaces both before and after hydrosilylation with allylamine (1-3) and (perfluorohexyl)ethylene (4-6) for 48 hours at 100 °C.

	Water Contact Angles (θ_A/ θ_R) (°)		XPS Elemental Analysis (15°) (initial / final)			
	Initial	Final	%C	%Si	%Ti	%N[a], %F[b]
1[a]	104.2 / 98.2	101.8 / 61.3	25.1 / 49.7	28.7 / 20.1	0.2 / 0.1	0.0 / 2.1
2[a]	105.3 / 91.8	92.7 / 51.8	36.4 / 46.7	17.1 / 15.0	5.4 / 2.1	0.0 / 3.6
3[a]	104.3 / 95.2	86.8 / 32.8	36.6 / 45.1	19.5 / 13.8	2.2 / 1.9	0.0 / 6.7
4[b]	103.3 / 81.5	108.7 / 80.2	21.0 / 27.7	12.8 / 14.6	13.9 / 5.9	0.0 / 7.3
5[b]	102.0 / 77.2	109.7 / 86.8	18.7 / 23.3	10.6 / 10.3	14.8 / 6.6	0.0 / 6.3
6[b]	104.3 / 84.7	108.7 / 89.0	21.4 / 26.6	13.0 / 11.9	13.0 / 5.7	0.0 / 6.2

Hydrosilylation was performed on titania surfaces reacted with linear hydridomethylsiloxane (MW~2,000 g/mol) for 4 hours. This time was chosen since it

represented a point at which a sufficient degree of reaction had occurred to cover enough of the surface, but residual hydridosilane groups may still be present. These samples were submerged in a solution containing either allylamine or (perfluorohexyl)ethylene. These two reagents were specifically chosen due to their identifiable elements, nitrogen and fluorine, respectively, which readily act as labeling elements in X-ray photoelectron spectroscopy. Table 2.5 gives advancing and receding water contact angles and XPS elemental analysis (15° take-off angle) data for samples prepared in this manner.

These samples show changes in both advancing and receding contact angles consistent with their respective changes in surface chemistry. In the case of those samples which underwent hydrosilylation with allylamine (1-3), a slight drop in advancing contact angles and much larger change in receding contact angle to create a more "hydrophilic" surface is observed. On the other hand, those samples (4-6) which underwent hydrosilylation with (perfluorohexyl)ethylene showed a general increase in both advancing and receding contact angles. Contact angles for both of these surfaces are similar to other reported[32] surfaces prepared using an aminopropylmethylsiloxane-*co*-dimethylsiloxane copolymer (99°/86°) and poly(trifluoropropolymethylsiloxane) (100°/89°). Differences between reported contact angles and these contact angles can be attributed to the comparative roughness of the titania surface to silica.

Despite clear changes in the contact angle data, the X-ray photoelectron spectroscopy data show only a slight addition of the labeling elements. This suggests that while there is some addition of the desired functional groups, there may not be enough residual hydridosilane groups exposed or available to undergo hydrosilylation for a larger degree of surface attachment. There is the expected increase in carbon, however, which may be attributed to this hydrosilylation process, and some unavoidable contamination.

Given this data, it is hard to determine whether hydrosilylation from HMS-modified titania surface is a "success". It is clear from the contact angle data and XPS data that hydrosilylation occurs from the surface and this affects the resulting properties. However, the

XPS data does not show a significant amount of the labeling element, signifying only a low % of attachment, and it is possible for a limited amount of modification to produce noticeable changes in wetting properties. Recently, Cheng *et al.*[33] reported the attachment of poly(dimethylsiloxane) brushs using a similar procedure using a much greater solution concentration for surface hydrosilylation. These data indicate that this technique is a good method for the post-modification of HMS surfaces to introduce new chemical functionalities and offers a greater control over surface properties, but is limited in the amount of modification which can occur.

Table 2.6. Advancing and receding water contact angles and X-ray photoelectron spectroscopy elemental analysis 1,3,5,7-tetramethylcyclotetrasiloxane (1-3) and poly(hydridomethylsiloxane) (HMS~2,000) (4-6) surfaces on titania before and after 30 minute oxygen plasma treatment.

	Water Contact Angles (θ_A/ θ_R) (°)		XPS Elemental Analysis (75°) (initial / final)		
	Initial	Final	%C	%Si	%Ti
1	98.3 / 64.0	29.8 / --	12.5 / 3.9	6.3 / 4.5	20.4 / 25.7
2	100.3 / 67.0	28.8 / --	11.3 / 6.4	7.3 / 5.2	20.8 / 25.0
3	99.0 / 62.0	36.0 / --	11.7 / 5.1	7.7 / 5.1	20.1 / 25.0
4	108.7 / 94.2	7.0 / --	16.7 / 1.8	10.1 / 10.4	14.8 / 14.2
5	105.8 / 93.7	10.7 / --	13.2 / 0.6	7.8 / 7.2	17.0 / 17.7
6	107.7 / 95.8	11.3 / --	14.2 / 5.3	10.0 / 9.4	15.1 / 15.6

The second technique for the subsequent modification of hydridomethlysiloxane-modified titania surfaces is the creation thin silicon oxide films using an oxygen plasma. This methodology is comparable to those of Tada[26,27] and Gentile[28]. Table 2.6 gives contact angle and X-ray photoelectron spectroscopy data of HMS-modified titania surfaces before and after a 30 minute oxygen-plasma treatment. The advancing and receding contact angles exhibit a sharp decrease to a much more hydrophilic surface in each of these samples. The double dashes in the receding contact angle data indicates that the contact line remains pinned upon removal of the water and represents an effective angle of 0°. However, those samples (1-3) prepared through the reaction of 1,3,5,7-tetramethylcyclotetrasiloxane (TMCTS) using a 5 vol.% solution in heptane at 100 °C for 72 hours show much higher advancing contact angles than those created with the

polymer (4-6). Initial contact angles for TMCTS surfaces show a great deal of hysteresis, indicating a low degree of surface coverage. The elevated advancing contact angles observed after oxygen plasma treatment of these sample may be due to the relative roughness of their surfaces and suggests that homogeneous coverage is not achieved, but rather patches of silicon oxide are developed on the titania surface.

The XPS data shown here are taken at a 75° take-off angle in order to show a deeper penetration depth. In each of these samples, there is a drop in elemental carbon found, indicating a "cleaner" surface and the oxidization of the hydridomethylsiloxanes. The relatively small changes in %Si and %Ti found in samples 4-6 suggest that there is little loss of siloxane during this technique and a relatively homogeneous silicon oxide layer is formed with a thickness of the same order of magnitude as the HMS monolayer. The advancing and receding contact angles for these samples are in agreement with this analysis, as a low advancing contact angle is observed. However, the decrease in %Si and increase in %Ti found in the TMCTS modified samples show that a loss of siloxane and that a thin silicon oxide layer formed. These data suggest that for the formation of silicon oxide films on titania, hydridomethylsiloxanes give more homogeneous films without loss of thickness, which is not observed using TMCTS.

Figure 2.7 gives survey spectra of titania, HMS-modified titania, and oxygen-plasma treated HMS-modified titania. Here, it is easy to observe the addition of HMS to titania through the addition of the Si_{2s} and Si_{2p} peaks (151 and 99 eV, respectively), and a decrease in $Ti_{2p3/2}$ peak (454 eV) relative intensity. After oxygen plasma treatment, there is a loss of the C_{1s} peak (285 eV), but the Si_{2p} peaks remain upon this surface. There is also a slight increase in the O_{1s} (531 eV) peak after oxygen plasma treatment, which is expected for the oxidation of siloxane polymers. Furthermore, there is little change in the relative intensity of the $Ti_{2p3/2}$ peak after oxygen plasma treatment, suggesting little change in the thickness of the modifying layer. This technique provides a simple method for the fabrication of thin silicon oxide layers on titania. Previous reports[26,27] have shown that these layers can be used to control the photo-oxidative

behavior of titania. Furthermore, it is possible that a silicon oxide film can act as a protective layer for titania surfaces and open avenues for the use of silica/silane chemistry.

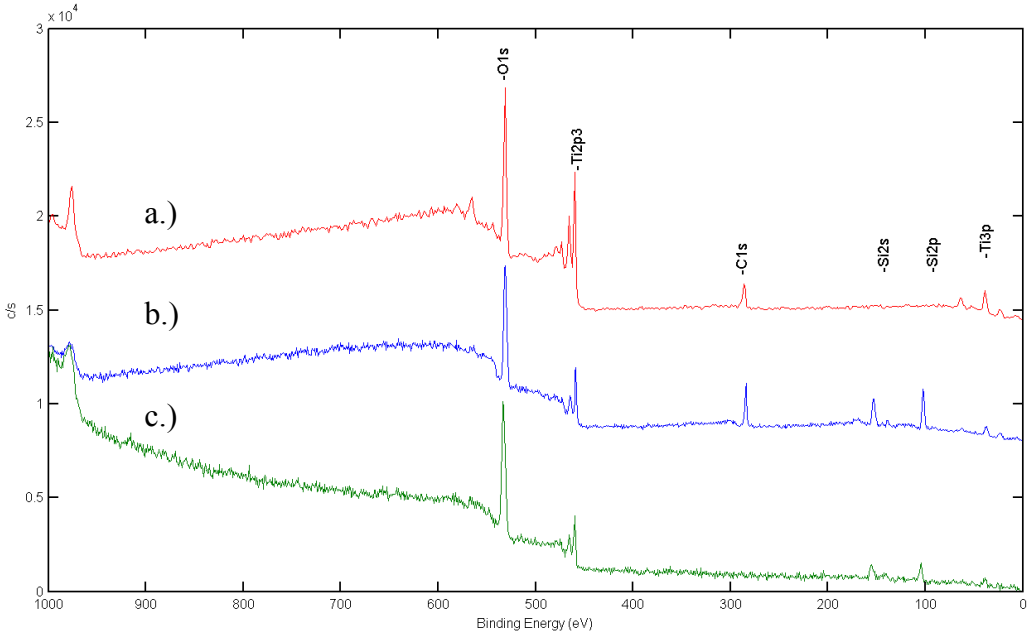

Figure 2.7. X-ray photoelectron survey spectra (75° take-off angle) of a.) titania surface (θ_A/ θ_R = 0°/0°), b.) hydridomethylsiloxane-modified titania surface (θ_A/ θ_R = 106°/93°), and c.) silicon oxide film generated by oxygen plasma treatment of hydridomethylsiloxane surface (θ_A/ θ_R = 11°/ 0°).

2.3.3 Reactions of Hydridomethylsiloxane-co-dimethylsiloxanes

While hydridomethysiloxane homopolymers have been shown to be good modifying agents for the surface of titania, the use of hydridomethylsiloxane-*co*-dimethylsiloxane (HMS-DMS) copolymers may be more beneficial. The largest benefit would be the absence of large amounts of residual hydridosilane groups. Hydridosilane groups are expected to react slowly with water vapor to change the surface properties over time, and generally decrease the hydrophobic nature of these surface. For this reason, the use of copolymers would decrease the quantity of residual hydridosilanes to make more stable surfaces.

Table 2.7 shows advancing and receding contact angle data for a range of copolymers featuring 55-3 mole percent hydridomethylsiloxane. Surface characteristics for the homopolymers (1-3) are reproduced here for easy comparison. From the data, it is shown that

copolymers (5-8) with as low as 3 mole percent hydridomethylsiloxane can be used to make surfaces with nearly equivalent wetting properties as the homopolymers. Figure 2.8 gives atomic force microscopy images of samples 6 and 9, which show features similar to those of titania surfaces modified with the homopolymer. There is a general increase in contact angle hysteresis with decreasing HMS mole percent. Although this change is only a few degrees, it does give significant information about the surfaces prepared. Given the similarities between the water contact angles of poly(hydridomethylsiloxane) (104°/103°) (Chapter 3, p. 73) and poly(dimethylsiloxane)[34] (104°/103°), analysis of these surfaces can be made in a similar fashion as the homopolymers.

Table 2.7. Advancing and receding water contact angle and X-ray photoelectron spectroscopy %C/%Si elemental ratios of poly(hydridomethylsiloxane) homopolymers (1-3), 1,3,5,7-tetramethylcyclotetrasiloxane (TMCTS) (4), poly(hydridomethylsiloxane)-*co*-poly(dimethylsiloxane) random copolymers (5-8), and poly(dimethylsiloxane) (9) reacted with titania surfaces at 100 °C for 72 hours using 5 vol.% solutions in heptane

	-SiMeH- (%)	Molecular Weight (g/mol)	Water Contact Angles (θ_A/ θ_R) (°)	Standard Deviation (σ_A/σ_R)	XPS (15˚) %C/%Si
1	98-100	~1600	102.2 / 86.6	2.13 / 9.13	1.38
2	98-100	~2000	104.0 / 93.2	1.20 / 1.64	1.14
3	98-100	~2300	104.8 / 89.9	0.65 / 2.45	1.40
4	100	240.51	98.5 / 63.3	1.71 / 8.53	1.01
5	50-55	900-1200	105.8 / 92.1	1.32 / 5.34	1.74
6	25-35	1600-2400	106.3 / 92.7	1.03 / 2.87	1.30
7	15-18	1900-2000	107.0 / 89.0	1.24 / 2.00	1.69
8	3-4	1600-2400	107.3 / 88.0	1.45 / 4.92	1.10
9	0	1600-2400	99.8 / 80.0	3.20 / 9.27	2.18

While these surface properties are similar to those of the homopolymers, the increase in contact angle hysteresis indicates an increasing amount of surface heterogeneity. The slight decrease in receding contact angle with decreasing hydridomethylsiloxane mole percent also indicates the presence of an increasing number of unreacted surface hydroxyl groups. This would

suggest a slightly lower degree of surface coverage, and therefore less hydridomethylsiloxane reaction, than found in the homopolymers. This would not be surprising given the lower amount of reactive groups found in these polymers. The XPS elemental data also supports this analysis. As the number of hydridosilane groups decreases, the elemental ratio of %C/%Si would be expected to converge toward 2 (9), the theoretical value found in poly(dimethylsiloxane), for surfaces with high degrees of surface coverage. This trend is not followed, and the copolymer with the lowest molar percent HMS (8), has a ratio of 1.10, indicating a low degree of reaction.

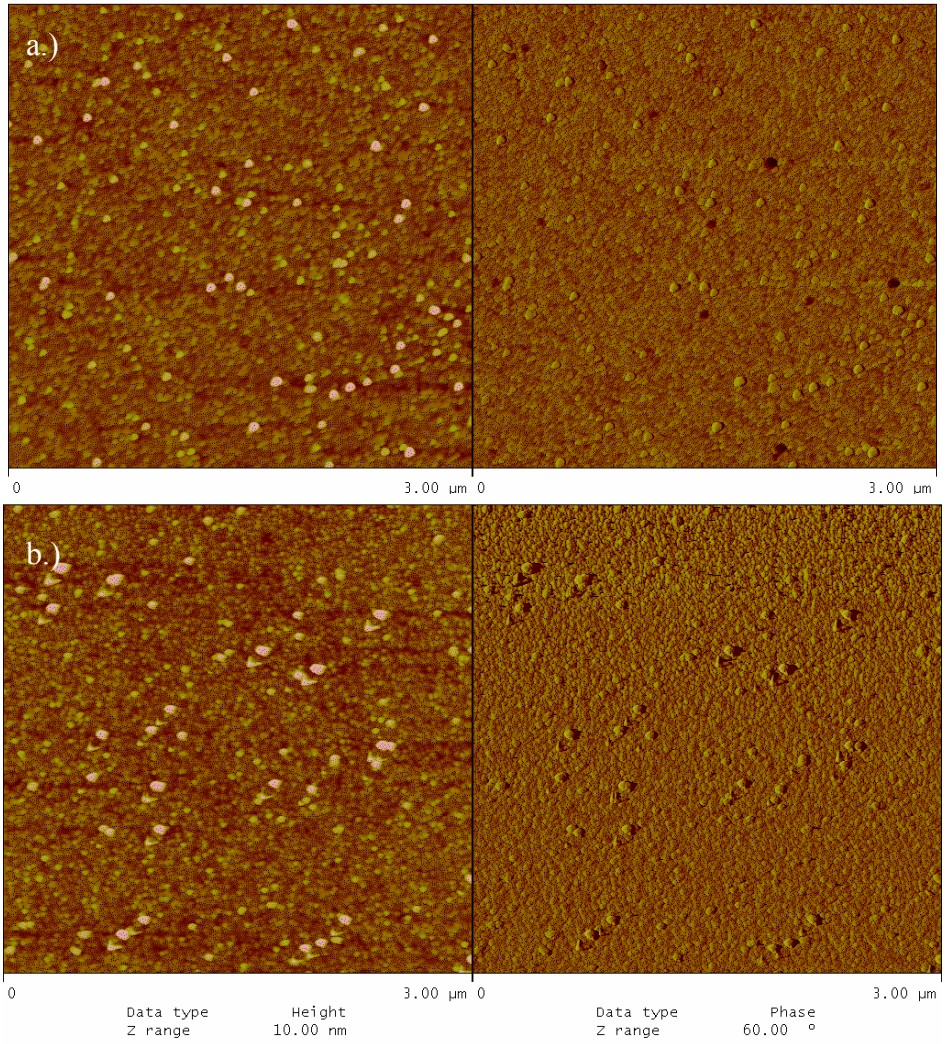

Figure 2.8. Atomic force microscope images of a.) 25-35% poly(hydridomethylsiloxane)-*co*-poly(dimethylsiloxane) (MW~1600-2400 g/mol) random copolymer and b.) poly(dimethylsiloxane) (MW~2,000 g/mol) on titania surface.

What is most surprising from this study, however, is the result of the poly(dimethylsiloxane) (PDMS) (9) control experiment, which has no hydridosilane functional groups. Under the same conditions as both the homopolymer and copolymers, PDMS-treated titania surfaces show surprisingly high contact angles, and its %C/%Si elemental ratio of 2.18 is very close to the theoretical value of 2. It was anticipated that no reaction would occur, and a titania surface with normal to high amounts carbon contamination would be produced with contact angles ranging between 40-60°, values typical of a "dirty" surface. Instead contact angles of approximately 100°/80° are observed even after thorough rinsing with solvents or prolonged submersion in heptane. This stability in regards to solvents and the unexpectedly high contact angles suggest a covalent attachment of the PDMS polymer. Yet, at the time of these experiments, there was no known reaction between PDMS and titania reported in the literature, and so these results were largely ignored due to our lack of understanding of the interaction of PDMS with titania or explained away by small amounts of silanol groups on the PDMS chain.

However, after further experimentation (Chapter 3), it was found that siloxane polymers can react with inorganic oxide surfaces through cleavage of the siloxane backbone. This reaction greatly complicates the analysis of the reactions of hydridomethylsiloxanes with titania surfaces, particularly in regards to the copolymers. It is impossible to truly establish the role of the quantity of hydridosilane groups on the copolymer chain, given that reaction can occur through the siloxane backbone without hydridosilanes reacting at all. Still, a comparison of the HMS homopolymers and PDMS shows that the homopolymers react much more readily with titania, and generally give surfaces with higher surface coverage, higher contact angles, and lower hysteresis given these reaction conditions. Yet, this control experiment proved to be significant and provided the foundation for further consideration of siloxane polymer interactions with inorganic oxide surfaces which is discussed in the following chapter.

2.4 Conclusions

Hydridomethylsiloxanes readily react with titania surfaces and create surfaces which exhibit high degrees of hydridomethylsiloxane surface coverage, as seen in the contact angle and X-ray photoelectron spectroscopy data, and this reaction does not produce any corrosive by-products. Furthermore, surfaces of these kinds can be used as a platform for secondary modification to introduce other chemical functionalities through the use of hydrosilylation. Oxygen plasma treatment of these surfaces is also shown to create thin silicon oxide films upon titania which can act as protective barrier layers. These two techniques represent further utility of these modifying reagents to control the surface properties of titania. Finally, the use of hydridomethylsiloxane-*co*-dimethylsiloxane copolymers, even those with only a few molar fraction of hydridosilane groups, create surfaces with nearly equivalent wetting properties as those of the homopolymer, although greater amounts of hydridosilane groups provide greater surface coverage more readily. The surprising result of poly(dimethylsiloxane) as a modifying reagent suggests that hydridomethylsiloxane polymers react with titania in other manners than through just the hydridosilane group.

2.5 References

1. Carp, O., Huismann, C.L., Reller, A., *Progress in Solid State Chemistry*, **2004**, *32*, 33-177.
2. Dufour, F., Cassaignon, S., Durupthy, O., Colbeau-Justin, C., Chaneac, C., *Euro. J. Inorganic Chem.*, **2012**, *16*, 2707-2715.
3. Allen, N.S., Edge, M., Sandoval, G., Verran, J., Stratton, J., Maltby, J., *Photochemistry and Photobiology*, **2005**, *81*, 279-290.
4. Kirstein, K., Reichmann, K., Preis, W., Mitsche, S., *J. European Ceramic Soc.*, **2011**, *31*, 2339-2349.
5. Tsantilis, S., Pratsinis, S.E., *Aerosol Science*, **2004**, *35*, 405-420.
6. Poznyak, S.K., Kokorin, A.I., Kulak, A.I., *J. Electroanal. Chem.*, **1998**, *442*, 99-105.
7. Wang, C., Ying, J.Y., *Chem. Mater.*, **1999**, *11*, 3113-3120.
8. Diebold, U., *Surf. Sci. Rep.*, **2003**, *48*, 53-229.

9. Martra, G., *Applied Catalysis A: General*, **2000**, *200***,** 275-285**.**

10. Henderson, M.A., *Surf. Sci. Rep.*, **2002,** *46,* 1.

11. Kosmulski, M., *Chemical Properties of Material Surfaces*, Cambridge University Press, Cambridge, 1994.

12. Morris, G.E., Skinner, W.A., Self, P.G., Marth, R., St.C., *Colloids Surfaces A: Physiochem. Eng. Aspects*, **1999**, *155*, 27-41.

13. Gamble, L. Hugenschmidt, M.B., Campbell, C.T., Jurgens, T.A., Rogers Jr., J.W., *J. Am. Chem. Soc.*, **1993**, *115*, 12096-12105.

14. Ballance, D.S., Camilletti, R.C., Gentle, T.E., U.S. Patent 5,145,723, Sept. 8, 1992.

15. Gao, W.; Dickinson, L.; Grozinger, C.; Morin, F.G.; Reven, L. *Langmuir*, **1996**, *12*, 6429.

16. Pettibone, J.M.; Cwiertny, D.M.; Scherer, M.; Grassian, V.H. *Langmuir*, **2008**, *24*, 6659.

17. Liu, Y., Liu, Ch., Zhang, Z., *Chem. Engin. J.*, **2008**, *138*, 596-601.

18. Helmy, R., Fadeev, A.Y., *Langmuir*, **2002**, *18*, 8924-8928.

19. Fadeev, A.Y., McCarthy, T.J., *J. Am. Chem. Soc.*, **1999**, *121*, 12184-12185.

20. McElwee, J., Helmy, R., Fadeev, A.Y., *J. Coll. Interf. Sci.*, **2005**, *285*, 551-556.

21. Finholt, A. E.; Bond, A. C.; Wilzbach, K. E.; Schlesinger, H. I., *J. Am. Chem. Soc.,* **1947**, *69*, 2692.

22. McCarthy, T.J., Fadeev, A.Y., U.S. Patent 6,331,329 B1, Dec. 18, 2001.

23. McCarthy, T.J., Fadeev, A.Y., U.S. Patent 6,673,459 B2, Jan. 6, 2004.

24. Shafi, K.V.P.M., Ulman, A., Yan, X, Yang, N., Himmelhaus, M., Grunze, M., *Langmuir*, **2001**, *17*, 1726-1730.

25. Arkles, B., Youlin, P., Kim, Y.M., Eisenbraun, E., Miller, C., Kaloyeros, A.E., *J. Adhesion Sci. Tech.*, **2011**, *26*, 41-54.

26. Tada, H., *Langmuir*, **1995**, *11*, 3281-3284.

27. Mukaihata, N., Matsui, H., Kawahara, T., Fukui, H., Tada, H., *J. Phys. Chem. C.*, **2008**, *112*, 8702-8707.

28. Gentile, T.E., U.S. Patent 5,165,955, Nov. 24, 1992.

29. Hofmann, S., Depth Profiling in AES, XPS, *Practical Surface Analysis*, Wiley Press, New York, 1996.

30. Gao, L., McCarthy, T.J., *Langmuir*, **2006**, *22*, 6234-6237.

31. Fadeev, A.Y., McCarthy, T.J., *Langmuir*, **1999**, *15*, 3759-3766.

32. Krumpfer, J.W., McCarthy, T.J., *Langmuir*, **2011**, *27*, 11514-11519.

33. Cheng, D., Urata, C., Masheder, B., Hozumi, A., *J. Am. Chem. Soc.*, **2012**, *134*, 10191-10199.

34. Krumpfer, J.W., McCarthy, T.J., *Faraday Discuss*., **2010**, *146*, 103-111.

CHAPTER 3

REACTIONS OF SILOXANE POLYMERS WITH INORGANIC OXIDE SURFACES

3.1 Introduction

3.1.1. Background

Many of the properties[1-4] of siloxane polymers, particularly poly(dimethylsiloxane) (PDMS), were discussed in the introduction (Chapter 1) of this dissertation, but a few pertinent properties are worth repeating. First, the difference in Pauling's electronegativity of oxygen (3.5) and silicon (1.8) impart an ionic nature to the siloxane backbone (51% ionic). This ionic nature gives PDMS a high thermal stability (T_d ~ 350 °C), yet makes silicones much more susceptible to hydrolysis by acids and bases. Second, PDMS has greater bond lengths and angles than carbon-based polymers which allow high degrees of rotational and vibrational freedom. This gives siloxane polymers a much more flexible backbone. Third, PDMS is a liquid at room temperature (T_g ~ -125 °C) with unusually weak intermolecular forces that give rise to a low surface tension (γ ~ 20 dyn/cm). It is also a traditional hydrophobic coating (water-repellent), yet has a high water permeability. Finally, silicone elastomers typically have poor mechanical properties, and inorganic oxide fillers are often used to make useful rubbers.

Since nearly all useful silicone materials feature inorganic oxide filler materials, understanding the interactions between the inorganic oxide surface and the matrix material would be important in controlling physical properties of these composites. The most common filler material for silicones is silica (SiO_2). The most common, current opinion on the interaction of silica reinforcing agents in silicone is best described by Bokobza:[5] "PDMS is traditionally reinforced with silica and the interactions between the two phases is ensured by hydrogen bonds between the silanols on the silica surface and the oxygen atoms of the polymer chains." Similar statements[6-8] can be found in much of the literature across a wide range of disciplines. Şerbescu *et al.*[8] found that fumed silica (25 wt.%) can induce network formation in linear PDMS after heating at 90 °C for 48 hours, and they propose this network formation to be caused by multiple

hydrogen bonding of the PDMS chains. Furthermore, many have claimed that without the presence of functional groups, such as terminal silanol groups, covalent attachment of PMDS chains to silica surfaces does not occur, and only hydrogen bonding is possible.[9,10]

However, silica-silicone materials often undergo strange aging phenomena.[11-13] These aging effects are most pronounced in uncured silicone composites. There is no universal agreement on the causes of these aging phenomena, nor is there agreement on the actual effects. Degroot and Marcosko[9] claim hydrogen bonding of silicone to silica surfaces can bind multiple particles to a single polymer chain and cause reagglomeration. Cohen-Addad and deGennes[14] ascribe these aging phenomena to silica surface "poison" water molecules, which slowly desorb from the silica surface over time, and allow for greater hydrogen bonding of the polymer to the silica surface. However, neither of these models satisfactorily describes why the rate of this aging effect seems dependent on molecular weight of the silicone in a polymer melt.[15] Two methods have been shown to eliminate these aging effects. The first is through heating the silica-silicone mixture to elevated temperatures.[8] The second is to chemically modify the surface of the silica.[13]

Figure 3.1[16] gives a list of silicon-based compounds which are vital components to many applications where surface modification is required. Aminopropyltriethoxysilanes[17] (a) and similar derivatives are the most common coupling agents for inorganic-polymer composite materials. *n*-Alkyltrichlorosilanes[18] (b) form self-assembled monolayers on silica. The mono-functional (aminobutyl)dimethylmethoxysilane[19] (c) forms amine-containing monolayers for polyelectrolyte adsorption. Hexamethyldisilazane[20] (d) is widely used to hydrophobize silica particles. Hydridosilanes[21] (e) react with most metal oxide surfaces to form covalently attached monolayers. While many of these reagents were designed for the modification of silica for polymer composites, these reagents are often used without prejudice on other metal oxide surfaces (of which this author is also guilty). Despite the varied nature of these modifying reagents, it is surprising that the siloxane bond of silicone polymers (f) is generally considered to be unreactive while these other reagents are and that modern literature seems to insist that siloxane polymers must only hydrogen bond to surfaces.

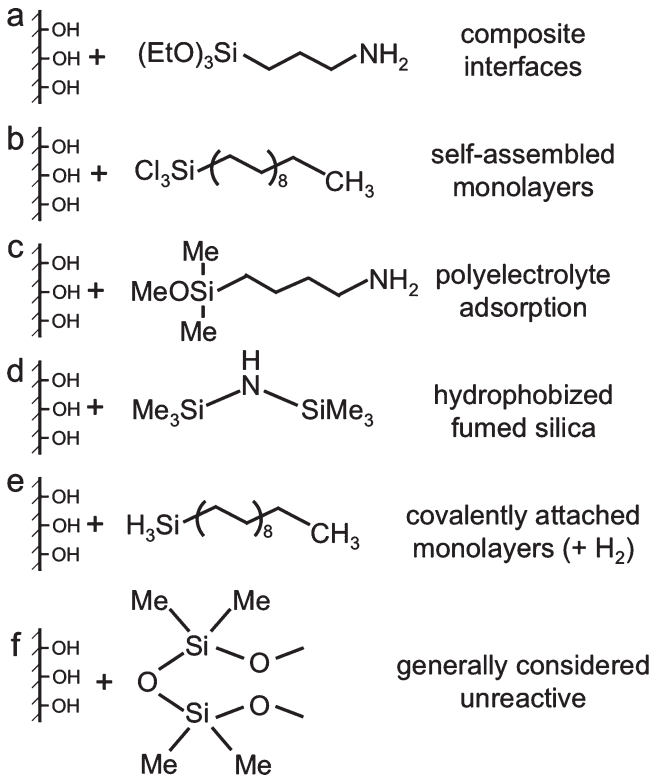

Figure 3.1. Common silicon-based reagents for the surface modification of silica and their applications (a-e), and a siloxane polymer (f) which is generally considered unreactive.

The surfaces of inorganic oxides have many interesting and complex properties which have been studied in great detail in the fields of chromatography[22] and catalysis[23,24]. Of all inorganic oxides, silica (SiO_2) is perhaps the most well-studied given its relative abundance and low cost. All inorganic oxide surfaces generally show significant amounts of hydration and this surface-bound water affects many catalytic processes and equilibrium.[25,26] Silica is a known desiccant, and dry silica absorbs water from all solvents with the exception of supercritical carbon dioxide, which dehydrates silica surfaces.[27,28] Given the strong association of water with silica surfaces, it would seem that the "poison water" model[14] for the aging phenomena of silica-silicone composites would be unlikely.

The hydration layer on silica is known to be an important component for many processes which occur at the silica interface. Surface bound water is known to be important for the self-assembly of alkyltrichlorosilanes and covalent attachment of functional silanes, as these groups

must hydrolyze before condensation with surface silanols. Covalently-attached monofunctional silane monolayers are also known to equilibrate at silica interfaces through the hydrolysis of the siloxane bond,[29] although the exact role of the hydration layer in this process is unknown. In fact, silica itself is soluble in water and reacts via the silicic acid equilibration shown in Figure 3.2.[16] It would not be surprising that all inorganic oxide surfaces should undergo some equilibration process with surface bound water, but the exact nature of these equilibria would be highly dependent on the chemistry and structure of the surface.

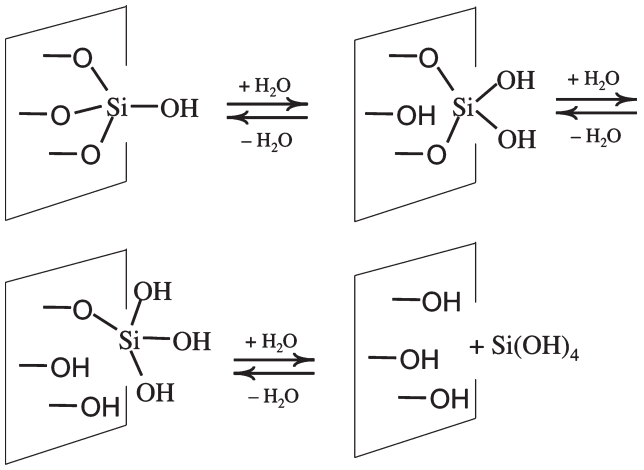

Figure 3.2. Equilibration of silica surfaces with water to form silicic acid.

Table 3.1. Point of zero charge (pH_o) of several inorganic oxide surfaces.

M_xO_y	SiO_2	TiO_2	Fe_2O_3	Fe_3O_4	α-Al_2O_3	γ-Al_2O_3	CuO	ZnO	NiO
PZC (pH_o)	2-4	5.5-6.5	5.5-8.5	6.4-7.1	7.2-8.8	8.8-9.1	8.5-9.7	9.3-9.8	9.8-11.3

Another important characteristic of silica surfaces is the acidic nature of this interface. This quality is a very important consideration in the chromatography field. It should not be surprising, then, that all inorganic oxide surfaces exhibit some acidic or basic characteristics. Table 3.1[30] gives the point-of-zero-charge (PZC) for several common inorganic oxides. The PZC is the pH value of a solution at which an immersed surface of the inorganic oxide is neutral. While inorganic oxide surfaces are often depicted as smooth interfaces with regularly ordered dangling hydroxyl groups for simplicity (and the same is done in this work), these surfaces are

much more complex than these idealized versions suggest. Figure 3.3[31] gives an example of a more realistic view of the surface of alumina (Al_2O_3). Inorganic surfaces typically feature a number of cation and anion species which can act as Lewis acid or base sites, and these are found to be important in catalytic functions. While the manner in which surface hydroxyl groups disassociate from the surface (i.e. the loss of a proton or hydroxide anion) is typically used to rationalize the acidic/basic nature of inorganic surfaces, these other Lewis acidic and basic site also affect this. It has also been found that the reactivity of inorganic oxide surfaces is greatly affected by temperature, and increased temperature increases surface reactivity.[31,32]

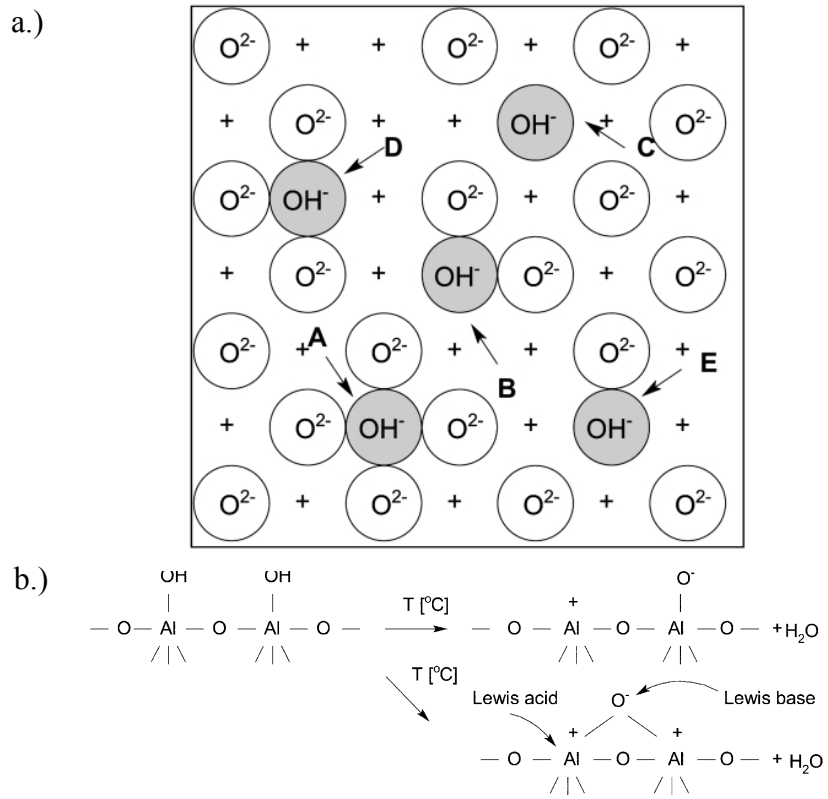

Figure 3.3. Depiction of ionic species on the surface of alumina (a) (+ symbols denote Al^{3+} species), and development of Lewis acid and base sites upon heating (b)[31].

Given the high degrees of surface hydration, acidity/basicity of surfaces, and the known equilibria of silica and siloxane bonds at the interface, it is surprising that the interaction of siloxane polymers with inorganic oxide surfaces is not interpreted as an interfacial equilibration of the siloxane bond. Poly(dimethylsiloxane) is known to equilibrate in the presence of acids and

bases[33], and there are reports of naturally occurring minerals (montmorillonite, kaolite) that can function as heterogeneous catalysts for silicone equilibration.[34,35] Galembeck[36,37] has shown the reaction of iron oxide particles in silicone oils at 250 °C. However, he accounts for this as the reaction of silanol terminated species developed by the thermal degradation of PDMS. Silicones are also known to react with water, although this is not directly addressed in the literature. Steam causes silicone rubbers to degrade and lose mechanical stability.[38,39] A few reports[40] do exist which suggest the covalent attachment of cyclic siloxanes to inorganic oxide surfaces, but these are by far a minority in the literature.

3.1.2 Objectives

The objective of this work was to examine the reactions of inorganic oxide surface with poly(dimethylsiloxane)s, and provide a simple alternative method for the modification of inorganic oxide surfaces. Conditions for reactions of siloxanes with inorganic oxide surfaces were also examined, including the effects of time and temperature. Furthermore, the fabrication of surfaces exhibiting negligible contact angle hysteresis is shown to be straightforward with high reproducibility using poly(dimethylsiloxane) and smooth silica surfaces. In addition to this, it was the goal of this work to show that this reaction is general to siloxane polymers and inorganic oxide surfaces, and that covalent attachment of the polymer is established through hydrolysis of the polymer backbone by interfacial water or surface acid/base sites. In this way, surfaces exhibiting various wetting and chemical characteristics could be easily fabricated.

3.2 Experimental Section

3.2.1 Materials

The following siloxane reagents were purchased from Gelest, Inc., and used without further purification: trimethylsiloxy-terminated poly(dimethylsiloxane)s of various molecular weights, hydridomethylsiloxane (MW~2,000 g/mol), 1,3,5,7-tetramethylcyclotetrasiloxane, hexamethylcyclotrisiloxane, octamethylcyclotetrasiloxane, pentamethylcyclopentasiloxane, poly[(3,3,3-trifluoropropyl)methylsiloxane] (MW~2,400 g/mol), poly[(3-

aminopropyl)methylsiloxane-co-dimethylsiloxane] (MW~ 4,500 g/mol) with 6-7 mol.% 3-aminopropylsiloxane, poly[phenylmethylsiloxane-co-dimethylsiloxane] (MW~2,000 g/mol) with 50-55 mol.% phenylmethylsiloxane, and poly(dimethylsiloxane-block-ethylene oxide) (MW~3,600 g/mol) with 80-85% non-siloxane. The following silane reagents were purchased from Gelest, Inc and used without further purification: octylsilane, octadecylsilane, trimethyl(dimethylamino)silane, trimethylchlorosilane, and octadecyltrichlorosilane. Silicon wafers as well as titanium-, aluminum-, and nickel-coated wafers were obtained from International Wafer Services, Inc. The nickel and titanium layers were 100 nm thick. The aluminum layer (100nm) was coated over a 30 nm thick titanium binding layer. Nickel powder (4SP-10, ~3-6 micron diameter) were received from Novamet. Nanometric titania (P25) particles was received from Degussa. Alumina particles (50 nm diameter, Premalox) were received from Ocean State Abrasives, Inc.

3.2.2 Reaction Conditions

Prior to reaction, silicon wafers and silicon-supported metal wafers were cut into approximately 1.0 x 1.0 cm pieces and exposed to an oxygen plasma using a Harrick Expanded Plasma Cleaner at 18W and 300 mTorr (flowing oxygen) for 30 minutes in order to produce clean surfaces.

Reactions of neat silicone fluids with inorganic oxide surfaces were performed by wetting the surface of a clean inorganic oxide wafer typically with a drop or two of silicone fluid. Reactions were carried out within a scintillation vial (Fisher) with screw-on caps. The scintillation vials used for these experiments are prepared in clean room environments and sealed by the manufacturer so that they provide ultra-clean reaction vessels which is particularly important for the preparation of surfaces with low contact angle hysteresis. The sealed scintillation vials with the inorganic oxide surfaces wet by a silicone fluid are placed inside an oven at the desired temperature for a desired amount of time, typically 100 °C for 24 hours. Wafers were then rinsed with copious amounts of toluene, acetone, and water (in this order) and dried in a stream of nitrogen.

Surfaces exhibiting negligible contact angle hysteresis were fabricated using poly(dimethylsiloxane)s with molecular weights of either ~2,000 or ~9,430 g/mol and the conditions described above.

Vapor phase reactions of cyclic siloxanes and inorganic oxide surfaces were performed by exposing clean inorganic oxide wafers to the vapor of the cyclic siloxane at 150 °C for the desired amount of time, typically 72 hours, within a sealed vessel. It should be noted that at no point does the inorganic oxide wafer come into direct contact with cyclic siloxane bulk liquid. This is typically done by placing a smaller vial with cyclic siloxane in a larger sealed vessel with the inorganic oxide wafers. After reaction, the wafers were rinsed with copious amounts of toluene, acetone, and water (in this order) and dried under a stream of nitrogen.

Solution-based reactions of silanes and hydridomethylsiloxanes with clean nickel surfaces were performed using 5 vol.% solutions of reagent in toluene at 65 or 100 °C for 72 hours in a sealed vessel. Wafers were then rinsed with copious amounts of toluene, acetone, and water (in this order) and dried under nitrogen.

Vapor phase reactions of dimethyldichlorosilane or dimethylsilandiol41 with clean silica surfaces were performed by exposing a clean silicon wafer with the silane vapor at 70 °C for 72 hours in a sealed vessel. Wafers were then rinsed with copious amounts of toluene, acetone, and water (in this order) and dried under nitrogen.

3.2.3 Characterization

Advancing and receding contact angles (θ_A/ θ_R) of water, hexadecane, and methylene iodide were measured using a Ramé-Hart telescopic goniometer. Contact angle values reported in the tables are, in general, averages of ~15 measurements made on three separately prepared samples. Exceptions to this are surfaces prepared with PDMS (MW~2,000 g/mol) and PDMS (MW~9,430) at 100 °C, which are averages of 216 measurements on 12 samples and 180 measurements on 10 samples, respectively. X-ray photoelectron spectroscopy (XPS) was performed using a Physical Electronics Quantum 2000. Ellipsometry measurements were made using a Rudolph research model auto SL-II automatic ellipsometer by reported42 procedures.

Atomic force microscopy was performed on select surfaces to determine root-mean-square roughness (RMS) using a Digital Instruments Dimensions 3000.

3.3 Results and Discussion

3.3.1 Preliminary Nickel Surface Modification Techniques

This work originated as an extension of the studies on the reactions of hydridomethylsiloxanes on titania (Chapter 2) for modification of nickel surfaces due to the lack of surface modification techniques for nickel surfaces. While only tangentially related to the reactions of poly(dimethylsiloxane)s with inorganic oxide surfaces, the results from these experiments, along with the control experiment of poly(dimethylsiloxane) on titania surfaces, provided the impetus for the careful consideration of the reactions discussed later in this chapter. As such, the data presented here represents the earliest work performed on this topic, highlights the process by which siloxane bonds were considered to be reactive functional groups, and was not necessarily directed to focus on silicones.

Table 3.2. Advancing and receding water contact angles and X-ray photoelectron spectroscopy elemental analysis (15° and 75° take-off angles) for preliminary modification of smooth nickel surfaces (1-6) using silanes and hydridomethylsiloxanes using 5 vol.% solution in toluene at 65 °C for 48 hours and (7-8) hydridomethylsiloxanes using 5 vol.% solutions in toluene at 100 °C for 48 hours.

		Reaction Temp.	Water Contact Angles	XPS (15° / 75°)		
	Reagent	(°C)	(θ_A/ θ_R) (°)	%Si	%C	%Ni
1	$(CH_3)_3SiCl$	65	51.5 / --	6.8 / 2.7	32.5 / 24.4	15.3 / 31.1
2	$(CH_3)_3SiN(CH_3)_2$	65	92.3 / 45.7	4.0 / 3.7	47.6 / 26.1	15.3 / 25.4
3	$C_{18}H_{37}SiCl_3$	65	71.3 / --	2.0 / 4.1	26.4 / 29.0	7.9 / 14.6
4	$C_8H_{17}SiH_3$	65	103.5 / 44.2	0.1 / 3.3	38.9 / 23.6	9.7 / 26.6
5	$C_{18}H_{37}SiH_3$	65	101.5 / 50.0	10.8 / 3.2	45.7 / 27.3	20.2 / 33.4
6	HMS (MW~2,000)	65	95.3 / 43.3	3.9 / 3.4	23.3 / 18.4	21.3 / 35.4
7	D_4^H	100	93.6 / 45.5	11.4 / 5.1	23.9 / 11.6	12.6 / 25.9
8	HMS (MW~2,000)	100	105.2 / 83.3	14.5 / 8.9	23.0 / 18.5	7.3 / 18.5

Table 3.2. gives advancing and receding water contact angles and elemental analysis for various silane and siloxane reagents reacted with smooth nickel surfaces. Oxygen (not shown)

represents the remainder of the surface elements in the X-ray photoelectron spectroscopy (XPS) data. Reaction conditions for samples 1-6 were chosen based on previously reported reactions of silanes with silica surfaces.[43] Reaction conditions for samples 7-8 were chosen based on previous techniques for the reaction of hydridomethylsiloxanes with titania surfaces (Chapter 2). These reactions were terminated after 48 hours since this was believed to be prior to reaction completion in order to gain insight into the relative reactivities of these reagents. The silicon-supported nickel wafers were found to have an oxide layer (NixOy) at the surface, and these surfaces are believed to be hydrated and feature surface hydroxyl groups in a similar fashion to most other metal oxide surfaces.

From the data, chloro- and dimethylaminosilanes (1-3) had the lowest degree of surface modification given their low contact angles, high hysteresis and low quantity of %Si from the elemental analysis and are not particularly useful modifying reagents for nickel surfaces given these conditions. The double dash marks for the receding contact angles of samples 1 and 3 indicate that the contact line remained pinned upon removal of water from the droplet and represents an effective contact angle of 0°. Those samples with hydridosilane groups (4-8) show much higher surface coverage, with greater advancing and receding contact angles, and an increase in the %Si found on the surface. Hydridosilanes were previously shown to be good nickel modifying agents by Fadeev,[21] who reacted octadecylsilane with nickel foils, and as such, these data show reactions of hydridosilanes as a versatile modification technique for metal oxides. A comparison of samples 6 and 8 shows a substantial change in surface properties with elevated temperatures. The increase in contact angles, decrease in contact angle hysteresis, and increase in %Si on the surface suggests a greater deal of surface coverage given this reaction time, and indicates this reaction is greatly influenced by reaction temperature.

Although the hydridomethylsiloxane (MW~2,000) showed higher contact angles with a lower contact angle hysteresis, it was decided to investigate the use of the cyclic monomer, 1,3,5,7-tetramethylcylcotetrasiloxane (D_4^H) for further study. There is one major advantage to using the smaller monomer rather than the polymer, and it comes from its ability to vaporize for

use in vapor phase reactions. Vapor phase reactions are particularly enticing as they do not require a solvent medium and typically do not require large amounts of reagent. Furthermore, the lack of solvent allows for much higher reaction temperatures without concerns for the solvent boiling. Table 3.3 shows advancing and receding water contact angles and X-ray photoelectron spectroscopy data for the vapor phase reaction of D_4^H at 150 °C for various times. It should be noted that at no point does the nickel surface come into contact with bulk liquid D_4^H, but is only ever exposed to the vapor.

Table 3.3. Advancing and receding water contact angle and X-ray photoelectron spectroscopy elemental analysis (15° and 75° take-off angles) for silicon-supported smooth nickel surfaces reacted with 1,3,5,7-tetramethylcyclotetrasiloxane vapor at 150 °C for various times.

Reaction Time	Water Contact Angles	XPS (15° / 75°)		
(hr)	(θ_A/ θ_R) (°)	%Si	%C	%Ni
0.25	97.9 / 67.6	14.6 / 8.1	38.7 / 21.7	5.1 / 17.3
0.5	104.3 / 83.9	19.4 / 11.1	33.9 / 22.4	2.9 / 11.7
0.75	107.1 / 93.8	28.9 / 22.4	29.2 / 26.1	0.1 / 1.2
1	115.2 / 93.3	28.7 / 24.5	33.1 / 32.4	0.2 / 0.1
2	110.5 / 98.4	26.3 / 23.5	38.9 / 37.9	0.2 / 0.5
4	108.0 / 101.9	25.3 / 31.9	31.9 / 26.1	0.7 / 3.7
6	106.2 / 102.9	26.5 / 18.8	33.3 / 27.0	0.7 / 3.7
12	104.2 / 77.1	29.3 / 26.8	29.4 / 28.8	0.5 / 0.6

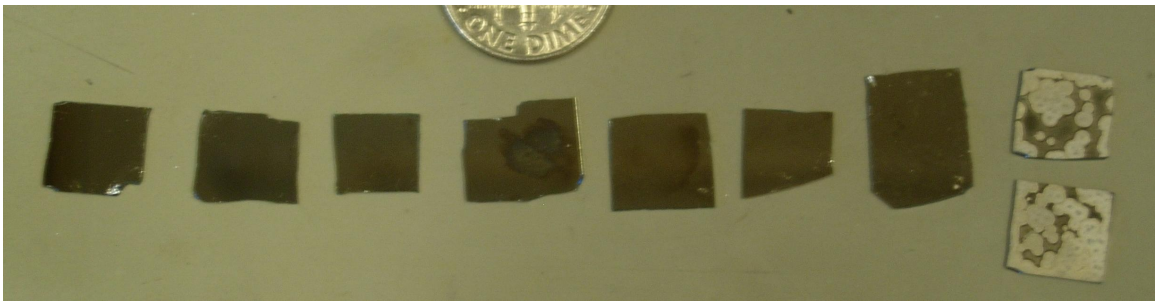

Figure 3.4. Image of wafers reacted with 1,3,5,7-tetramethylcyclotetrasiloxane through the vapor phase at 150 °C for 0.25, 0.5, 0.75, 1, 2, 4, 6, and 12 hours (left to right).

From the contact angle data, rapid modification occurs within minutes of exposure of the nickel surface with D_4^H vapor at 150 °C. After 15 minutes of reaction, water contact angles are

already significantly higher than those reacted after 48 hours in heptane at 100 °C (Table 3.3, 7). This drastic difference is attributed to the elevated reaction temperature, and the absence of competitive adsorption with the heptane solvent. After reaction for over 45 minutes, the D_4^H thickness becomes large enough that little elemental nickel is detected on the surface by XPS. This represents a "monolayer" on the order of ~ 10 nm in thickness.[44] This is much larger than anticipated for a monolayer. In addition to this, the %C/%Si elemental ratio is approximately 1, the theoretical value for hydridomethylsiloxanes, and remains relatively constant after this point. This ratio and the absence of elemental nickel from the surface indicates complete coverage of the surface by D_4^H. After 45 minutes of reaction, the data should be analyzed in conjunction with the visual observations of the surfaces (Figure 3.4).

At 1 hour of reaction time, visual discoloration of the surface becomes apparent, and represents an uneven modification of the sample and the formation of a visibly thick D_4^H layer. This is also seen in the elevated advancing contact angle which suggests a rougher surface than at shorter reaction times. Contact angle hysteresis undergoes a minimum after six hours of reaction, followed by a large increase in hysteresis after 12 hours. This increase in contact angle hysteresis is attributed to the great deal of roughness which is visible on the surface in Figure 3.4. The circular, white shapes which appeared on surfaces reacted for 12 hours resemble the results of nucleation and growth processes occurring at the interface.

The large thickness, absence of nickel from the surface, %C/%Si ratio, and unexpected surface features all suggest a reaction other than hydridosilanes with the nickel surface. This is a reasonable assumption as a monomolecular D_4^H film should have a maximum thickness on the order of several angstroms (~8 Å) if standing on a single Si-O-Ni bond with the ring plane standing perpendicular to the surface plane, elemental nickel should be seen at that length scale, and discoloration should not be apparent for a monolayer. In order to discount the condensation reactions of D_4^H through the hydridosilane bonds, octamethylcyclotetrasiloxane (D_4), the monomer of PDMS for ring-opening polymerization (ROP) and a "non-functional" siloxane, was reacted in the vapor phase under the same conditions. This reaction yielded a surface with water

contact angles (θ_A/ θ_R) of 107° / 96°, a %C/%Si elemental ratio (15° take-off angle) of 2.01, and very little elemental nickel was visible in the XPS spectra, but did not show the discoloration seen when using D_4^H. With the absence of traditional functional groups, it would seem the reaction of D_4 with nickel would most likely undergo a ring-opening mechanism.

It was at this point that a more careful consideration of the interactions of siloxane polymers with inorganic oxide surfaces seemed necessary. In retrospect, when considering the control experiment of PDMS with titania along with these results, the cleavage of the siloxane bond to form covalent bonds should have been more obvious given the known reactions of silicones with acids and bases. However, this reaction had little to no precedence in the scientific literature, and actually seemed contrary to reports of the interactions of PDMS with inorganic oxides. Under the hypothesis that siloxanes can undergo hydrolysis and covalent attachment through surface cations and anions (Lewis acids and bases), this reaction should be general for most inorganic oxide surface, and this is addressed in the following sections.

3.3.2 Poly(dimethylsiloxane) Reactions with Inorganic Oxide Surfaces

As knowledge of the silica interface is well-established and our understanding of it is much greater than other inorganic oxide surfaces, many of the fundamental studies on the reactions of poly(dimethylsiloxane)s with inorganic oxide surfaces were performed on silica. Smooth silica surfaces have particular advantages as well, as they can be prepared with finite oxide layers and molecularly smooth interfaces to help eliminate the effects of roughness. Reactions using neat silicone fluids were chosen in order to eliminate competitive adsorption processes with solvents. As such, there is no solvent for this reaction, which simplifies the reaction procedure, decreases cost, and produces less waste.

Table 3.4 gives advancing and receding contact angles of water, methylene iodide, and hexadecane, along with ellipsometric thicknesses for surfaces reacted with poly(dimethylsiloxane) with a molecular weight of 2,000 g/mol ($PDMS^{2000}$) in sealed scintillation vials. The probe fluids chosen are traditional liquids used for contact angle measurements and represent a polar, ionic liquid (water), a polar, non-ionic liquid (methylene iodide), and a non-

polar, non-ionic liquid (hexadecane). The 24 h/ 100 °C data are repeated to facilitate comparisons. X-ray photoelectron spectroscopy elemental analysis is not included as differentiating the elements of silicones and silica is not possible due to their similarities in atomic composition.

Table 3.4. Advancing and receding contact angles of various probe fluids and ellipsometric thickness of silica surfaces reacted with neat poly(dimethylsiloxane) (MW~2,000 g/mol) at various times and temperatures.

		Contact Angles (θ_A/θ_R) (°)			
Time (h)	Temp (°C)	H_2O	CH_2I_2	$C_{16}H_{34}$	Thickness (nm)
24	25	94 / 80	71 / 61	37 / 30	0.67
24	60	102 / 93	72 / 65	37 / 34	0.72
24	100	104 / 102	76 / 74	36 / 35	1.15
24	150	105 / 102	75 / 72	37 / 33	3.1
1	100	91 / 71	71 / 60	35 / 29	1.1
6	100	98 / 85	74 / 69	36 / 34	1.22
24	100	104 / 102	76 / 74	36 / 35	1.15

Prior to reaction of PDMS, silica wafers are wet (θ_A/θ_R = ~0° / 0°) by each of these probe fluids. In addition to this, silicones applied to silica surfaces at room temperature can be easily removed by rinsing with solvents shortly after application and show carbon contamination on the lines of rinsing with organic solvents. Therefore, it can be seen that a significant increase in contact angles occurs for each of these reaction conditions. However, analysis of the receding contact angle data and hysteresis suggests there are significant differences between these surfaces, and that both time and temperature are important for this reaction. Surfaces prepared at 25 and 60 °C show much larger contact angle hysteresis for each of the probe fluids than those prepared at higher temperatures. This is analyzed in a previously reported manner[45] and suggests the presence of unreacted surface silanols which pin the receding contact angle and indicate a low degree of surface coverage at these temperatures. Therefore, it would seem that temperature

greatly influences this reaction, and below 100 °C, this reaction proceeds slowly. The general increase in ellipsometric thicknesses with respect to temperature, also suggests a greater deal of surface reaction at elevated temperatures.

Time also appears to play an important role in this reaction. From the data, it appears that PDMS reacts rapidly with silica surfaces at 100 °C, showing a large increase in advancing and receding contact angles after 1 hour of reaction, and an eventual minimization of contact angle hysteresis after 24 hours of reaction. More careful kinetics were not performed since reaction conditions of 24 hour / 100 °C produced surfaces with highly reproducible surface properties with standard deviations of advancing and receding contact angles (σ_A/ σ_R) of 0.68° / 1.43° (H_2O); 0.63° / 0.75° (CH_2I_2); and 0.54° / 0.51° ($C_{16}H_{34}$). Standard deviation of the sample thickness for these conditions was 0.13 nm. These statistics were performed using over 200 individual measurements.

In general, the differences in thickness between those samples which show high degrees of surface coverage is not entirely significant for this molecular weight. Assuming reaction between the poly(dimethylsiloxane) and silica surface, there should be random attachment along the polymer chain, and depending on where on the polymer chain this covalent attachment occurs should dictate the thickness of the grafted PDMS layer. In other words, if reaction occurs near the end of the polymer chain, a short PDMS chain and a long PDMS chain are both likely to be covalently attached to the surface. On the other hand, if reaction occurs in the exact center of the polymer chain, two equally long PDMS chains may be attached. Ellipsometric thicknesses are the average thickness of a millimetric sized spots, and should represent a great number of different grafted PDMS chain lengths. As such, the thickness measured should be a statistical average for different grafted chain lengths upon the surface and should represent chain lengths of approximately half of the total polymer chain length as it would appear when covalently attached to the silica surface. If this is the case, there should be a definite dependence on molecular weight of the PDMS used in regards to the monolayer thickness that is observed. It would be expected that larger molecular weight poly(dimethylsiloxane)s should give thicker monolayers on silica.

Table 3.5 gives advancing and receding contact angles of various probe fluids, ellipsometric thicknesses, and atomic force microscopy root-mean-square roughness (RMS) for smooth silica surfaces reacted with poly(dimethylsiloxane)s of various molecular weights reacted at 100 °C for 24 hours. From this data, a very clear trend is seen in the ellipsometric thickness in regards to PDMS molecular weight. As expected, larger molecular weights produce much thicker monolayers. However, based on the contact angle data for PDMS oligomers with molecular weights of 310.69 and 770 g/mol, low molecular weight PDMS does not produce surfaces with high surface coverage, as evidenced by the low contact angles and high hysteresis. Furthermore, the RMS roughness for these samples is almost identical to those of unmodified silica surfaces. This lower surface modification is attributed to the lower number of available chain conformations and the steric hindrance caused by the the bulky trimethylsilyl-chain ends.

Table 3.5. Advancing and receding contact angles of various probe fluids, ellipsometric thickness, and atomic force microscopy root-mean-square (RMS) roughness for silica surfaces reacted with neat poly(dimethylsiloxane)s of various molecular weights (MW) at 100 °C for 24 hours.

	Contact Angles (θ_A/θ_R) (°)				
MW (g/mol)	H_2O	CH_2I_2	$C_{16}H_{34}$	Thickness (nm)	RMS (nm)
310.69	70.4 / 48.9	52.3 / 26.6	23.2 / 10.9	0.47	0.101
770	92.7 / 79.2	66.5 / 57.4	33.9 / 26.8	0.58	0.101
2,000	104.0 / 102.4	75.5 / 73.9	36.1 / 34.8	1.15	0.160
9,430	105.6 / 104.8	76.1 / 73.1	33.5 / 32.8	5.05	0.133
116,000	112.7 / 94.2	94.5 / 51.9	33.0 / 16.1	12.48	0.253

This data also shows a range of poly(dimethylsiloxane)s which produce surfaces with low contact angle hysteresis (MW~2,000 - 9,430). Despite differences in ellipsometric thickness, both of these surfaces exhibit RMS roughness only slightly greater than the unmodified silica wafer. The low contact angle hysteresis and relative smoothness give rise to what is termed a "liquid-like" surface.[46] This quality and its importance in the development of low hysteresis surfaces is discussed in greater detail in the following section. There is an increase in contact

angle hysteresis and roughness seen in the samples prepared using PDMS (MW~116,000 g/mol). In regards to the water contact angle hysteresis, this increase is attributed to the formation of a water lens upon this thicker PDMS surface (i.e. the water droplet sinks into the PDMS monolayer) which impedes the advancement and recession of the three-phase contact line. Another possible explanation for this increased hysteresis could be the stretching of PDMS chains onto the water-air interface. Given the longer polymer chain length and that PDMS is known[47] to form monolayer films on water, extension of these chains could also account for an increase in hysteresis, although determining if this chain extension occurs was not attempted. The large increase in methylene iodide and hexadecane contact angle hysteresis is attributed to swelling of the PMDS monolayer, as both of these solvents are soluble in silicone oil.

A few qualitative experiments were performed to determine the stability of these monolayers on silica surfaces. Samples prepared using PDMS^{2000} on silica wafers reacted at 100 °C for 24 hours were then immersed in 20 mL of several solvents for 1 week at room temperature to compare the surface properties after prolonged exposure to these solvent conditions. Samples immersed in toluene and heptane exhibited no change in water contact angles after one week. It was expected that, should strong adsorption be responsible for interaction between PDMS and silica, some change in surface properties, however minor, should be observed when using liquids that are known to be good solvents for silicones. Furthermore, as these samples are rinsed after reaction by shooting a stream of toluene, acetone, and water from a polyethylene squirt bottles, these surfaces appear surprisingly robust in regards to organic solvents. Samples immersed in water after one week showed a drop in receding contact angles from θ_A/θ_R = 105° / 102° to θ_A/θ_R = 104° / 94°. Water is known as a poor solvent for PDMS (they are immiscible), and so desorption of the PDMS chain in water is not expected. This drop in contact angles, then, is seen as evidence of monolayer restructuring or hydrolysis of the siloxane backbone via water. It is possible that formation of dimethylsilandiol,[48,49] a water soluble compound and the major degradation product of silicones in soils,[50] is a degradation product of these surfaces when immersed in water for long periods of time, although this was never investigated. Finally, these

surfaces which are stored in sealed scintillation vials without solvents show no visible change in surface properties over the course of two years.

A few more experiments were performed which do not offer further insight into the interaction of poly(dimethylsiloxane)s with silica surfaces but do produce some interesting results worth commenting. The reaction of PDMS^{2000} with silica wafers was performed at 100 °C for 24 hours in the presence of various vapors, by placing a smaller vial with 0.5mL of either acetic acid, ammonium hydroxide, water, or tridecafluoro-1,1,2,2-hydrooctyl(dimethyl)chlorosilane in the 20 mL scintillation vial in which the reaction occurs. In this way, the PDMS does not come into contact with the bulk liquid, but is exposed to a vapor. In the case of the first three vapor materials, a drop in contact angles was observed, forming surfaces with water contact angles (θ_A/ θ_R) of 98° / 85°, 103° / 93°, and 96° / 87° for acetic acid, ammonium hydroxide, and water, respectively. This drop in contact angles is not surprising, since these reagents are known to degrade PDMS and also suggests that humidity may be an important parameter in these reactions, although it was not further investigated. Surfaces made using the chlorosilane exhibited an increase in advancing water contact angles to form surfaces with θ_A/θ_R = 113° / 105°, an ellipsometric thickness of ~2 nm, and a fluorine peak visible in X-ray photoelectron spectroscopy. Interpretation of this data is difficult since a number of known reactions may occur between silicones, silica, silanes, and hydrochloric acid (the by-product of chlorosilanes), but may suggest some solubility of silanes though the silicone fluid or the equilibration of the PDMS surface with the fluorinated silane.

Given the stability of these surfaces, and the effects of reaction time and temperature on the properties of the surfaces produced, two possible reaction schemes for the reaction of PDMS with silica surfaces are proposed in Figure 3.5. Silica has a known isoelectric point in water[30] of ~3 and likely functions as an acid catalyst in both of these mechanisms. Since these reactions were performed using neat PDMS liquid which wet the clean silica surface, traditional adsorption processes are not considered important using this procedure. Shown on the left, the siloxane backbone reacts directly with the acidic surface silanol to cleave the siloxane backbone through

silanolysis and undergoes direct covalent attachment. The equilibration of siloxane polymers with acid catalysts is well-known, and this reaction is consistent with that knowledge.

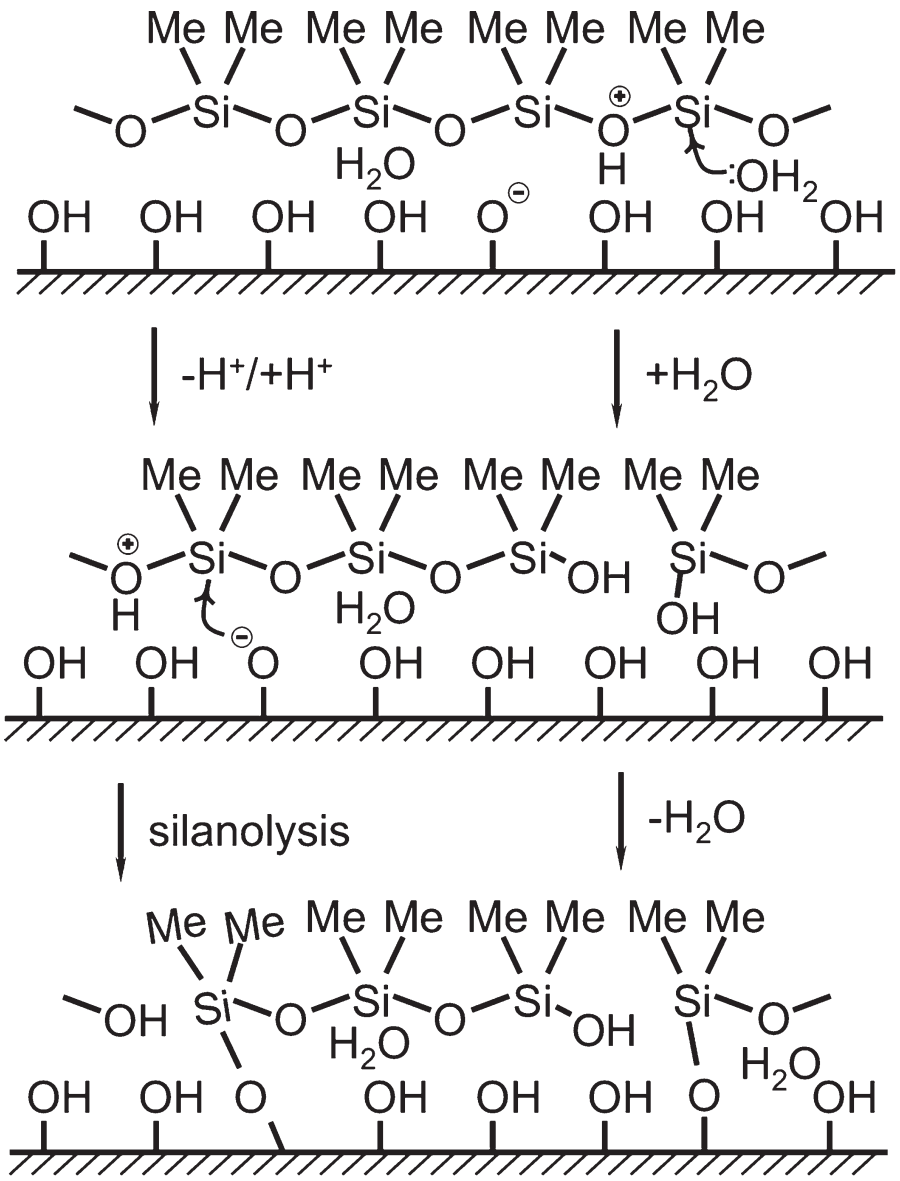

Figure 3.5. Scheme for the covalent attachment of poly(dimethylsiloxane) with silica surfaces through the cleavage of the siloxane backbone through acid silanolysis using the silica as the acid and a silanolate as the nucleophile (left) or hydrolysis by surface-bound water followed by condensation of silanols (right).[16]

On the right, the siloxane backbone undergoes hydrolysis with surface bound water to form silanol groups on the PDMS chain which may then condense with free surface silanols to

form covalent attachment. This reaction is consistent with the reported reaction of siloxane polymers with water and the well-known condensation of silanol groups. In each of these mechanisms, a second silanol-terminated PDMS chain is formed which may also condense with free adjacent surface silanols to covalently attach to the silica surface

Based on the dependence of the grafted layer thickness on molecular weight (Table 3.5), the equilibration of the grafted silicone chains is believed to be very slow when compared to the coequilibration of surface silanols. This would be consistent with silica as a catalyst, which is bound to the interface, and would prevent the continued equilibration of the bulk of the siloxane polymer monolayer into shorter oligomers. This is also consistent with the relatively constant thicknesses of PDMS monolayers reacted at 100 °C for different lengths of time (Table 3.4). Finally, since both silica and siloxanes are known to equilibrate with water, it should also be noted that these two reaction schemes are most probably simplifications of more complex equilibria of water, silica, and siloxanes at the interface, but represent two probable interactions which may occur.

Table 3.6. Advancing and receding water contact angles of inorganic oxide surfaces reacted with neat poly(dimethylsiloxane) (MW~2,000 g/mol) at various temperatures for 24 hours.

	H_2O Contact Angles (θ_A/θ_R) (°)			
Temp (°C)	SiO_2	TiO_2	Al_2O_3	NiO
25	94/80	77/34	75/35	84/37
60	102/93	89/54	87/44	90/57
100	104/102	97/67	92/51	95/74
150	105/102	101/84	106/100	103/85

Given these mechanisms, the covalent attachment of PDMS should be general for all inorganic oxide surfaces since they all have Lewis acid or base sites and are highly hydrated. Table 3.6 gives water contact angles for inorganic oxide surfaces reacted with $PDMS^{2000}$ for 24 hours at various temperatures. Data for silica wafers is repeated for easy comparison. From this data, it is seen that each of these surfaces reacts with PDMS between 25 and 150 °C. The

differences in extent of reaction can be seen in the differences in contact angle hysteresis with respect to reaction temperature. This suggests that these reactions are thermally activated, as was observed with silica. This is also consistent with the known increase in reactivity for several of these surfaces.

The data points for the surfaces reacted at 150 °C suggest that conditions can be optimized to result in more useful modification procedures for these metals. However, it is expected that the reactivities of each of these surfaces are very different with different optimized conditions. Silica (SiO_2) and titania (TiO_2) are surfaces known to have an acidic nature, while nickel oxide (NiO) is known to have a basic nature, as evidenced by their point-of-zero charge values (Table 3.1). Due to the difference in chemical nature of these surfaces, optimization of reaction conditions for each was not pursued. Still, the surfaces presented here give a good enough representation of metal oxide surfaces with different properties to suggest that the covalent attachment of PDMS should occur with any inorganic oxide surface.

3.3.3 Low Hysteresis Surfaces

The initial results of a surface that exhibited nearly no contact angle hysteresis was so unexpected that wetting properties for these surfaces had to be verified by several other researchers before fully believing them. In retrospect, it should have been obvious that PDMS was particularly suited for the development of surfaces with no contact angle hysteresis. However, given previous reports on the fabrication of surfaces exhibiting low contact angle hysteresis which used extremely complex apparati[51] or dubious techniques for measuring contact angles,[52,53] it was surprising that these surfaces could be made by such a simple, reproducible method.

Previously reported techniques for the fabrication of hydrophobic surfaces exhibiting low contact angle hysteresis have employed monolayer flexibility to minimize hysteresis. Chen et al. employed[54] the use of tris(trimethylsiloxy)silylethyldimethylchlorosilane to create a "liquid-like" surface which exhibited low water contact angle hysteresis (θ_A/θ_R = 104° / 103°). The surfaces prepared using this reagent had an "umbrella"-like structure which could freely rotate around the

Table 3.7 Advancing and receding contact angles of water, hexadecane, and methylene iodide for smooth silica surfaces reacted with PDMS (MW ~ 2,000 g/mol) at 100 °C for 24 hours.

	Contact Angles (θ_A/θ_R) (°)			
	Water	$C_{16}H_{38}$	CH_2I_2	Thickn.(nm)
α	104.7 / 102.3	--	--	--
β	105.8 / 105.0	--	--	--
γ	104.2 / 103.2	--	--	--
1	104.3 / 103.7	35.7 / 34.3	76.0 / 74.7	1.2 / 1.2
2	103.7 / 103.2	36.5 / 35.2	75.0 / 73.2	1.1 / 0.9
3	104.2 / 100.2	36.7 / 34.7	74.8 / 73.8	1.5 / 1.0
4	104.0 / 102.2	36.0 / 34.0	75.5 / 73.0	2.3 / 2.2
5	104.2 / 102.7	35.8 / 34.3	75.2 / 73.2	2.1 / 2.0
6	103.3 / 99.8	36.2 / 35.0	75.0 / 73.0	2.3 2.6
7	103.7 / 102.0	37.0 / 35.0	75.3 / 72.7	2.5 / 2.3
8	103.3 / 101.7	36.5 / 35.5	75.2 / 74.0	2.6 / 2.6
9	103.2 / 102.7	36.2 / 34.2	75.5 / 73.5	2.3 / 2.3
Ave. Δθ	1.7	1.6	1.8	

Table 3.8 Advancing and receding contact angles of water, hexadecane, and methylene iodide for smooth silica surfaces reacted with PDMS (MW ~ 9,430 g/mol) at 100 °C for 24 hours.

	Contact Angles (θ_A/θ_R) (°)			
	Water	$C_{16}H_{38}$	CH_2I_2	Thickn.(nm)
1	105.0 / 105.0	28.0 / 28.0	78.0 / 73.2	5.9 / 5.5
2	106.0 / 105.7	35.5 / 34.2	74.7 / 72.2	4.8 / 4.3
3	106.0 / 104.0	35.3 / 34.8	75.2 / 73.0	4.9 / 5.1
4	106.0 / 106.0	35.0 / 34.0	77.3 / 74.7	5.0 / 4.8
5	106.5 / 106.3	33.8 / 32.8	75.2 / 72.3	5.1 / 5.1
6	104.3 / 103.7	33.5 / 32.0	77.7 / 73.8	5.0 / 5.0
7	105.7 / 104.2	33.5 / 33.0	76.7 / 73.7	5.3 / 5.4
8	105.0 / 104.3	34.0 / 32.7	77.0 / 73.5	5.2 / 5.1
9	105.5 / 103.8	35.0 / 32.7	77.3 / 73.0	5.5 / 5.7
10	105.8 / 104.5	34.8 / 32.8	77.3 / 73.8	6.0 / 6.0
Ave. Δθ	0.8	1.1	3.3	

ethylene bond to create dynamic monolayers which prevents pinning at the three-phase contact line. Surfaces equivalent to those shown here were also prepared using dimethyldichlorosilane[55] and chloro-terminated siloxane oligomers[54,56] showing water contact angles of 104° / 103°. However, the surfaces prepared using the method presented in this chapter do not produce corrosive by-products (HCl), nor require skill in silane chemistry.

Tables 3.7 and 3.8 give the advancing and receding contact angles of various probe fluids and ellipsometric thicknesses for smooth, clean silica surfaces wet by poly(dimethylsiloxane) (MW ~ 2,000 and 9,430 g/mol, respectively), sealed in a scintillation vial and heated at 100 °C for 24 hours. The samples designated with Greek letters represent the first three samples of this kind prepared and did not undergo robust characterization. While the data in these two tables are slightly redundant, they emphasize the reproducibility and ease of this modification procedure. From this data, surfaces reacted with PDMS^{2000} have less than 2° of contact angle hysteresis for each of these probe fluids, and many of these surfaces show hysteresis less than 1°. Surfaces reacted with poly(dimethylsiloxane) (MW ~ 9,430 g/mol) (PDMS^{9430}) show even lower average hysteresis for water and methylene iodide probe fluids. The increase in average hysteresis of hexadecane is attributed to solubility of hexadecane in the thicker PDMS monolayer.

The extremely low contact angle hysteresis exhibited by both of these PDMS monolayers also provides insight into the structure of the grafted polymer chains. Traditionally, two factors must first be overcome to minimize contact angle hysteresis: surface roughness and chemical heterogeneity. Given the hysteresis shown by these surfaces, the monolayers of PDMS must be molecularly smooth and no silanols from the silica surfaces must be exposed. Atomic force microscopy images of these two surfaces are shown in Figure 3.6 to show very smooth surfaces, with roughness only slightly greater than the silica surface to which they are covalently attached. However, minimization of roughness does not necessarily mean negligible hysteresis. Like previous reports,[54-56] these monolayers must also be mobile and "liquid-like" to create a three-phase contact line that is dynamic at room temperature.

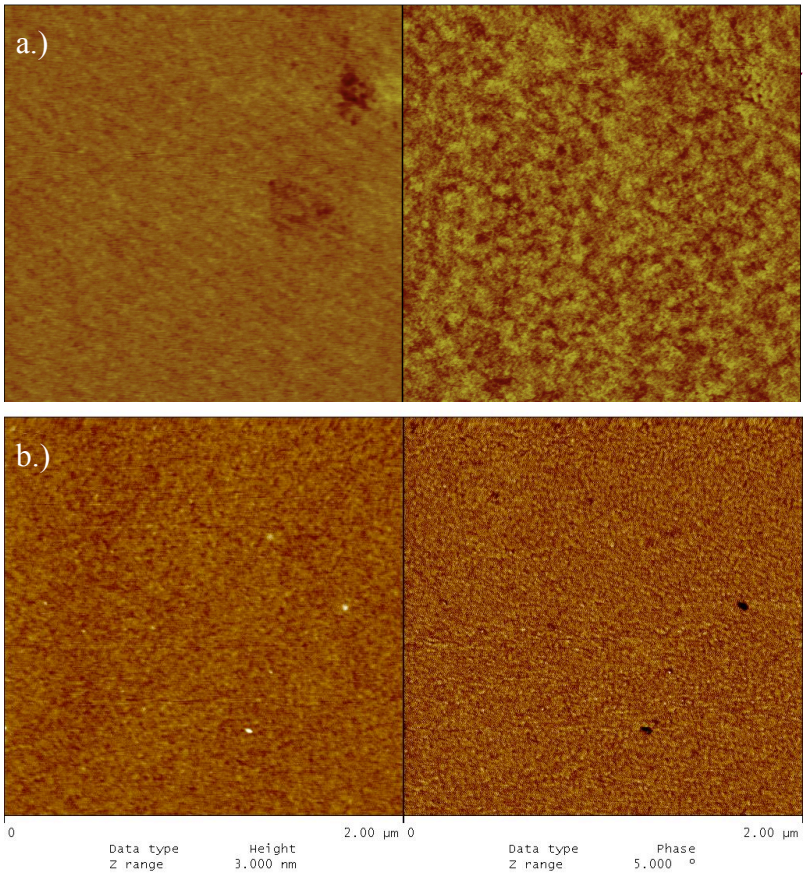

Figure 3.6 Atomic force microscopy images of silica surfaces reacted with poly(dimethylsiloxane) of molecular weights of a.) 2,000 and b.) 9,430 g/mol for 24 hours at 100 °C.

Poly(dimethylsiloxane) is particularly suited to forming monolayers with these qualities. The flexibility of the siloxane backbone allows for a monolayer that can constantly contort and remain mobile to create a dynamic three-phase contact line. Furthermore, the size of these polymer chains along with their flexibility ensures that a great deal of surface coverage is achieved as these polymer chains can spread across the surface to prevent any unreacted surface silanols from being exposed to probe fluids. Poly(dimethylsiloxane)s also has a low T_g and is liquid at room temperature. The AFM root-mean-square roughness for these two monolayers is extremely low, suggesting a liquid-like nature to the monolayers (although the exact physical state of a polymer chain grafted to a solid interface is debatable). Finally, the low surface tension of PDMS means these surfaces are highly water-repellent. From the viewpoint of droplet motion,

droplets of liquids easily slide off these surfaces with the slightest tilt angles. In this manner, they are perfectly "shear hydrophobic".

Hydridomethylsiloxane polymers (MW~2,000) also create surface with low contact angle hysteresis using these conditions. Three samples were made with advancing and receding water contact angles of 104.3° / 103.3°, 103.7° / 103.2°, and 105.3° / 104.5°. However, these surfaces typically show a decrease in receding contact angles and increase in hysteresis ($\Delta\theta \sim 7°$ at last measurement) a few weeks after preparation, indicating that these surfaces do not have the long-term stability that PDMS surfaces have. This is attributed to the reaction of hydridosilane groups with the silica surface which limits the flexibility of the siloxane chain or the slow reaction with water vapor to create silanol groups which would lower the receding contact angle. Because of the lack of stability observed in these samples, they were not further considered as good candidates for low hysteresis surfaces and no careful examination of these surfaces was performed, although similar results were also observed by another researcher.[57]

Water contact angles for poly(dimethylsiloxane) surfaces have been reported[58] to range from 95 - 117.5°. This wide range of contact angles is most likely evidence of the looseness in which the term PDMS is used by many researchers, as many silicone materials are compounded with silica. Furthermore, it has been shown that silicones can conform to their reaction vessels upon crosslinking,[59] and this can impart textures into silicone surfaces that affect the contact angles. Because of these factors, it has been hard to isolate what the true contact angles for PDMS should be. However, the values presented here are of surfaces that do not exhibit surface texturing, feature no polymer chain crosslinking, and are not compounded with silica. For these reasons, the contact angle values of surfaces prepared using PDMS^{2000} and PDMS^{9430} give evidence that these are the true contact angles of this polymer.

This reaction does not require the use of air-sensitive silanes; there is no cleaning of glassware; it is not dependent on air humidity (to our current knowledge) or the water content of solvents; and it does not require the skills of an experienced chemist. Since these experiments were first performed, this reaction has been performed numerous times by many researchers in

various fields to produce surfaces with identical properties as those presented in Tables 3.7 and 3.8, and suggests that this high reproducibility is attributed to the ease of the reaction procedure and not any special skills of this particular researcher.

3.3.4 Reactions of Functional Silicones

The reaction of poly(dimethylsiloxane)s with silica is a convenient method for creating hydrophobic monolayers. However, the reaction of siloxane polymers with inorganic oxide surfaces is not limited to PDMS, but rather can be performed using any polymer with sufficient siloxane backbone. The silicone polymers used in this study each have very different properties and applications.[60] Poly(phenylmethylsiloxane-co-dimethylsiloxane) (PPMS-PDMS) is an aromatic siloxane polymer with high thermal stability used for mechanical and heat transfer applications. Poly[3-aminopropyl)methylsiloxane-co-dimethylsiloxane) (PAMS-PDMS) is a reactive siloxane polymer used in epoxies and urethanes. Poly[(3,3,3-trifluoropropyl)] (PFMS) is a fluorinated siloxane miscible in fluoropolymers and often used as a lubricant. Finally, poly(dimethylsiloxane)-block-poly(ethylene oxide) (PDMS-PEO) is a hydrophilic siloxane polymer often used as a surfactant and with higher water solubility than traditional silicones. PAMS-PDMS and PFMS also have readily identifiable elements in X-ray photoelectron spectroscopy. Because of the very different properties of the siloxane polymers, surfaces with different chemical natures and wetting properties were fabricated using this technique.

Table 3.9. Advancing and receding water contact angles, X-ray photoelectron spectroscopy (15° take-off) elemental analysis, and ellipsometric thickness of smooth silica wafers reacted with poly(phenylmethylsiloxane-*co*-dimethylsiloxane) (PPMS-PDMS), poly[(3-aminopropyl)methylsiloxane-*co*-dimethylsiloxane] (PAMS-PDMS), poly[(3,3,3-trifluoropropyl)methylsiloxane] (PFMS), and poly(dimethylsiloxane)-*block*-poly(ethylene oxide) (PDMS-PEO) at 100 °C for 24 hours.

	MW (g/mol)	Water Contact Angles (θ_A/ θ_R) (°)	XPS (15°)		Thickness (nm)
			%C	%N[a], %F[b]	
PPDM-PDMS	2,100	94.6 / 87.3	45.7	--	2.56
PAMS-PDMS	4,500	99.4 / 86.4	45.6	0.61[a]	4.33
PFMS	2,400	99.4 / 89.4	25.9	19.75[b]	2.15
PDMS-PEO	3,600	55.5 / 35.5	45.9	--	2.00

Table 3.9 gives advancing and receding contact angles, X-ray photoelectron elemental analysis, and ellipsometric thicknesses of silica wafers reacted with a variety of siloxane copolymers. The wetting properties exhibited by the water contact angles show surfaces with much different wetting properties than PDMS, and give a good indication of the effects of the additional functional groups present on these surfaces. This is most pronounced in the PAMS-PDMS contact angles in which a small amount of aminopropyl groups produces lower advancing and receding contact angles than those seen in the PDMS homopolymer. While it is possible that the amino groups in the 3-aminopropylmethylsiloxane repeat units may be reactive with the silica surface, they are present in a small mole percent (6-7 mol.%), and this is evident in the low %N seen in the XPS elemental analysis. The PFMS homopolymer also shows different wetting properties and has a %F/%C elemental ratio of 0.76. This is approximately equal to the theoretical ratio of 0.75 for this polymer. Finally, the PDMS-PEO produces a hydrophilic surface. These low contact angles are not attributed to low surface coverage as the standard deviations for the water contact angles (σ_A / σ_R) are 0.58° / 0.58° and for ellipsometric thickness, 0.69 Å, indicate good reproducibility for these surfaces. For these reasons, the low contact angles are attributed to the low contact angles traditionally associated with poly(ethylene oxide). Like the PDMS homopolymers, these siloxanes show a general increase in monolayer thickness with molecular weight with the exception of the PDMS-PEO copolymer. This is most likely due to the low mole percent siloxane in this copolymer, and the differences between PEO and PDMS flexibility and surface structures.

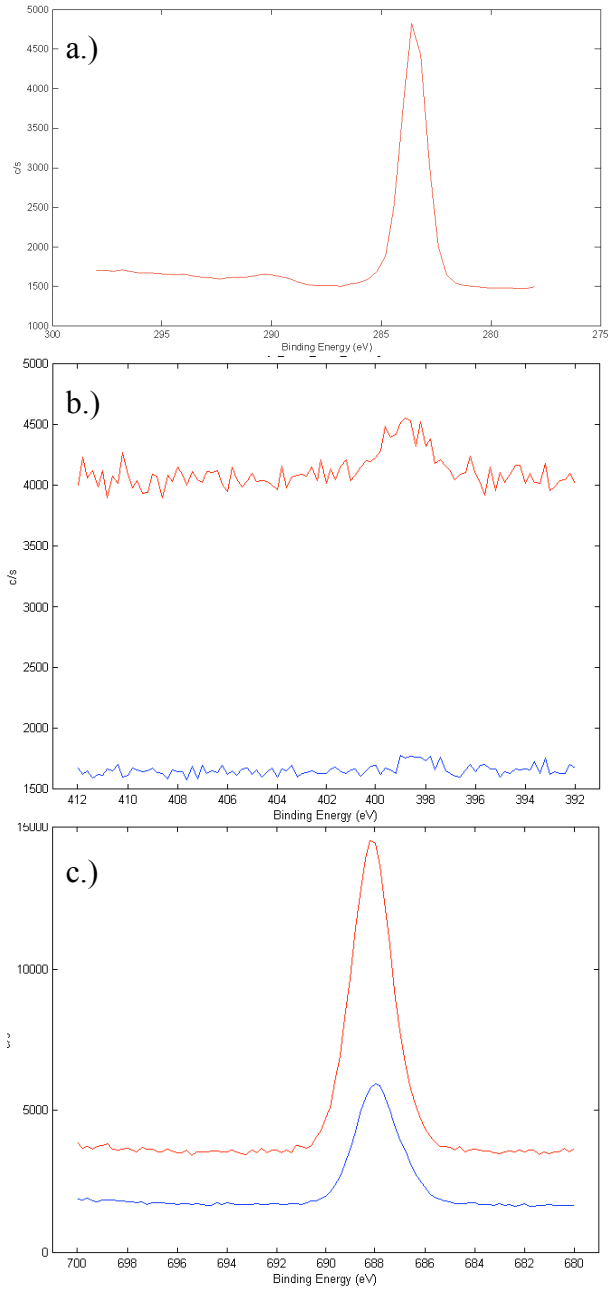

Figure 3.7. Identifiable elemental peaks for a.) π-π* shake-up spectrum (75° take-off angle) in the C_{1s} spectra of (phenylmethylsiloxane-*co*-dimethylsiloxane), and b.) N_{1s} peak in the spectra of poly[(3-aminopropyl)methylsiloxane-*co*-dimethylsiloxane] and c.) F_{1s} peak in the spectra of poly[(3,3,3-trifluoropropyl)methylsiloxane]

X-ray photoelectron spectroscopy was performed to identify specific labeling elements. Figure 3.7 shows these elemental peaks. Figure 3.7a is a high resolution scan of the C_{1s} peak of PPMS-PDMS taken at a 75° take-off angle. Here, a π-π* shake-up peak can be see at ~290.9 eV,

which is indicative of aromatic carbon rings. Figure 3.7b shows the low intensity of the N_{1s} peak at ~399 eV found in PAMS-PDMS, specifically at the 75° take-off angle (upper spectra). Finally, the F_{1s} peak is clearly seen at ~688 eV for PFMS samples. These identifiable elemental peaks give good indication that covalent attachment of siloxane polymers are a useful and simple method for creating surfaces with unique properties and chemical functionalities.

3.3.5 Vapor Phase Reactions of Cyclic Siloxanes

As mentioned previously in this chapter, vapor phase reactions have many advantages over solution based reactions. The vapor phase reactions of cyclic siloxanes also helps highlight the reactivity of the siloxane bond with inorganic oxide surfaces. Table 3.10 gives advancing and receding water contact angles, XPS %C/%Si elemental ratios and ellipsometric thickness of four different inorganic oxide surfaces reacted with hexamethylcyclotrisiloxane (D_3), octamethylcyclotetrasiloxane (D_4) and decamethylcyclopentasiloxane (D_5) through the vapor phase at 150 °C for 72 hours. Similar to the other vapor phase reactions reported in this chapter, the inorganic oxide surface does not come into direct contact with the bulk siloxane liquid.

Table 3.10. Advancing and receding water contact angles, X-ray photoelectron spectroscopy (XPS) %C/%Si elemental ratios (15° take-off angle), and ellipsometric thickness for surfaces modified with hexamethylcyclotrisiloxane (D_3), octamethylcyclotetrasiloxane (D_4), and decamethylcyclopentasiloxane (D_5) through the vapor phase at 150 °C for 72 hours.

	H_2O Contact Angles (θ_A/θ_R) (°)				XPS (15°) %C/%Si			Thickness (nm)
	SiO_2	TiO_2	Al_2O_3	NiO	TiO_2	Al_2O_3	NiO	SiO_2
D_3	106.8 / 104.5	113.0 / 102.7	101.0 / 89.5	96.3 / 71.3	1.96	1.95	1.9	5.02
D_4	97.6 / 83.4	101.0 / 72.3	105.6 / 77.2	107.0 / 98.3	2.14	2.24	2.24	3.40
D_5	104.7 / 102.5	96.3 / 60.4	106.4 / 88.0	109.0 / 87.6	2.11	1.9	1.71	4.17

For each of these inorganic oxide surfaces, advancing and receding water contact angles show a great deal of surface coverage. The hysteresis present in the metal oxide surfaces is attributed to the roughness of the unmodified substrate and the differences in reactivity between the surfaces. The XPS %C/%Si elemental ratio is approximately 2 regardless of which cyclic

siloxane which is the theoretical ratio for both the cyclic siloxanes and PDMS. These cyclic siloxanes are appear to grow thick films upon the surface of silica ranging from 3-5 nm. These thicknesses are much greater than those which would be observed from the adsorption of cyclic siloxanes bound to the surface through irreversible hydrogen bonding. Rather, these thicknesses are more comparable to polymer chains upon the surface and indicate the growth of PDMS polymers from the inorganic oxide surface, most probably through the ring-opening polymerization of these monomers.

The relative reactivities of these cyclic siloxanes can be seen in the differences in ellipsometric thickness and contact angle hysteresis. The thickness of these siloxanes on silica follows the trend of $D_3 > D_5 > D_4$. Similarly, D_3 generally shows higher contact angles and lower hysteresis than the other two cyclic monomers. These differences in surface properties are interpreted as indication of the reactivity of these monomers as related to their respective ring strains. The ring strain of these monomers follows the same trend as the ellipsometric thickness, with D_4 having negligible ring strain and the lowest reactivity. Because of this ring strain, these monomers are believed to be more reactive than linear siloxane polymers.

The ring-opening polymerization of cyclic siloxanes demonstrates the reactivity of the siloxane bond with inorganic oxides and gives further evidence that PDMS reacts with these surfaces. In fact, D_4-treated hydrophobic silica particles are commercially available, although these products never suggest that these siloxanes are covalently attached to the surfaces. Cyclic siloxanes are useful for the modification of inorganic oxide powders, since they are small molecules which can diffuse through particle interstices to provide more conformal coating without the need for solvents. Figure 3.8 shows several metal oxide powders before (left column) and after (right column) treatment with D_4 vapor. In each spectra of the modified metal oxide, a decrease in the intensity of the inorganic substrate peak can be seen suggesting a conformal coating on the order of several nanometers upon the particles.

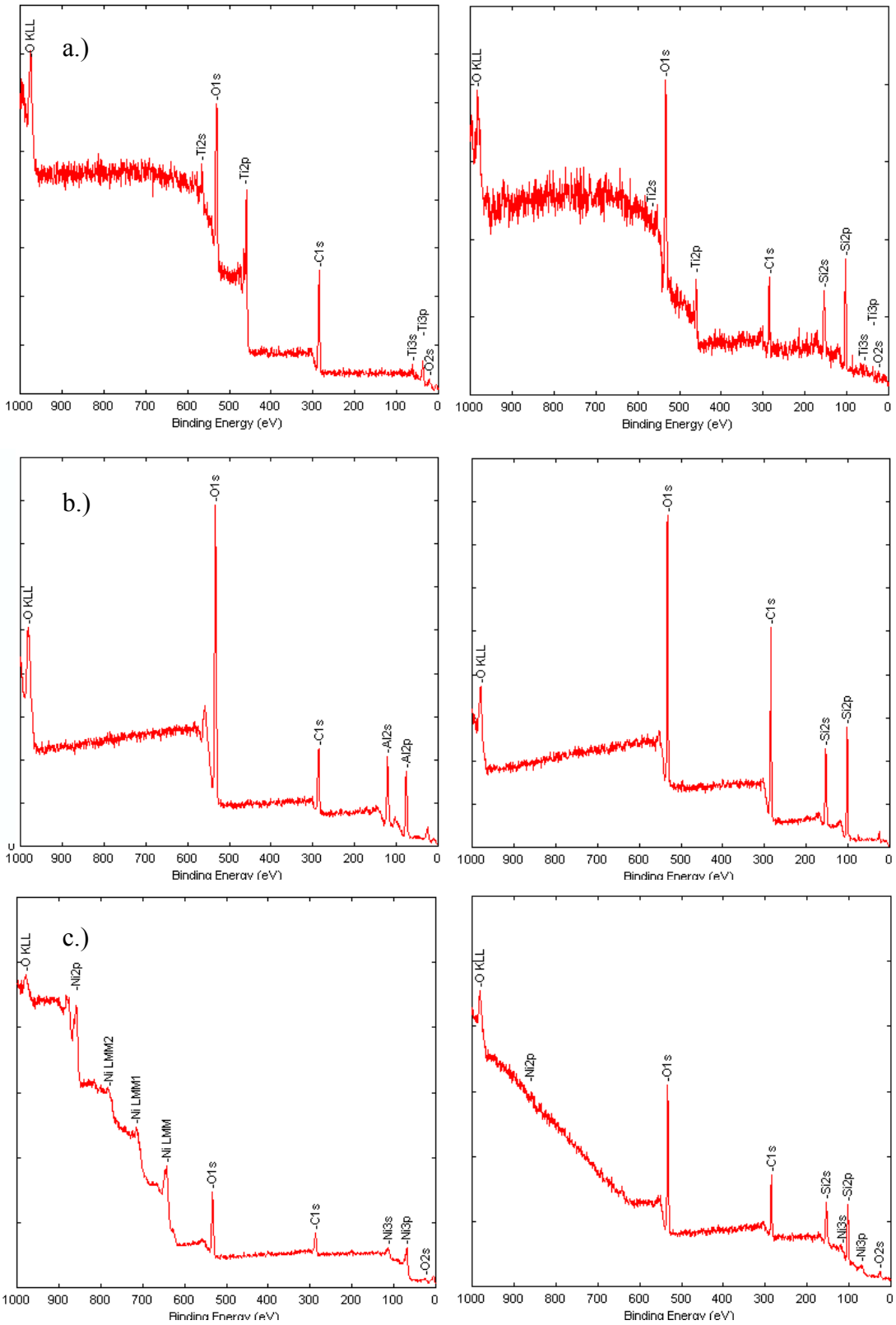

Figure 3.8. X-ray photoelectron spectra of unmodified (left column) and D_4-vapor modified (right column) particles of a.) titania, b.) alumina, and c.) nickel taken at a 10° take-off angle.

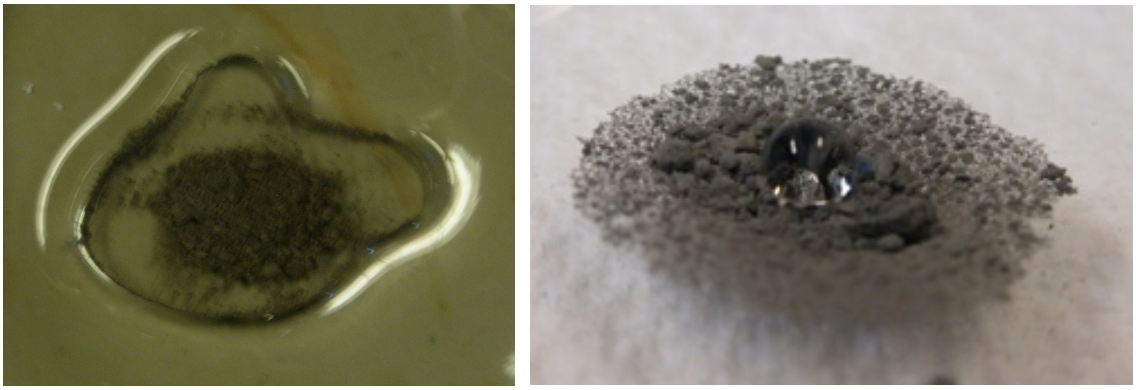

Figure 3.9. Images of nickel powder modified with D_4-vapor for 72 hours at 150 °C illustrating their hydrophobicity by pushing water away preventing the spreading of water on glass (left) and creating a hydrophobic raft floating on water and supporting a water droplet.

Figure 3.9 shows some qualitative images of the hydrophobicity of micronic nickel particles modified in this manner. Nickel has a density of ~8.9 g/mL, and these particles typical sediment to the bottom of any aqueous solution given their size and weight. However, upon treatment of D_4 vapor, they easily float on water to form particle rafts which may support the weight of water droplets (right). Furthermore, water added to a glass dish with this powder is prevented from spreading across the glass surface and nickel particles create a coating on the water-air interface similar to liquid marbles61 which further prevents this spreading.

3.3.6 Comparison of Preparative Techniques of PDMS Surfaces

While the reactions of PDMS with inorganic oxide surfaces are presented in this chapter as a new surface modification technique, surfaces with covalently attached poly(dimethylsiloxane) chains have been reported many times prior to this work, and to those with experience and skill produce surfaces with identical properties to those reported in this chapter.

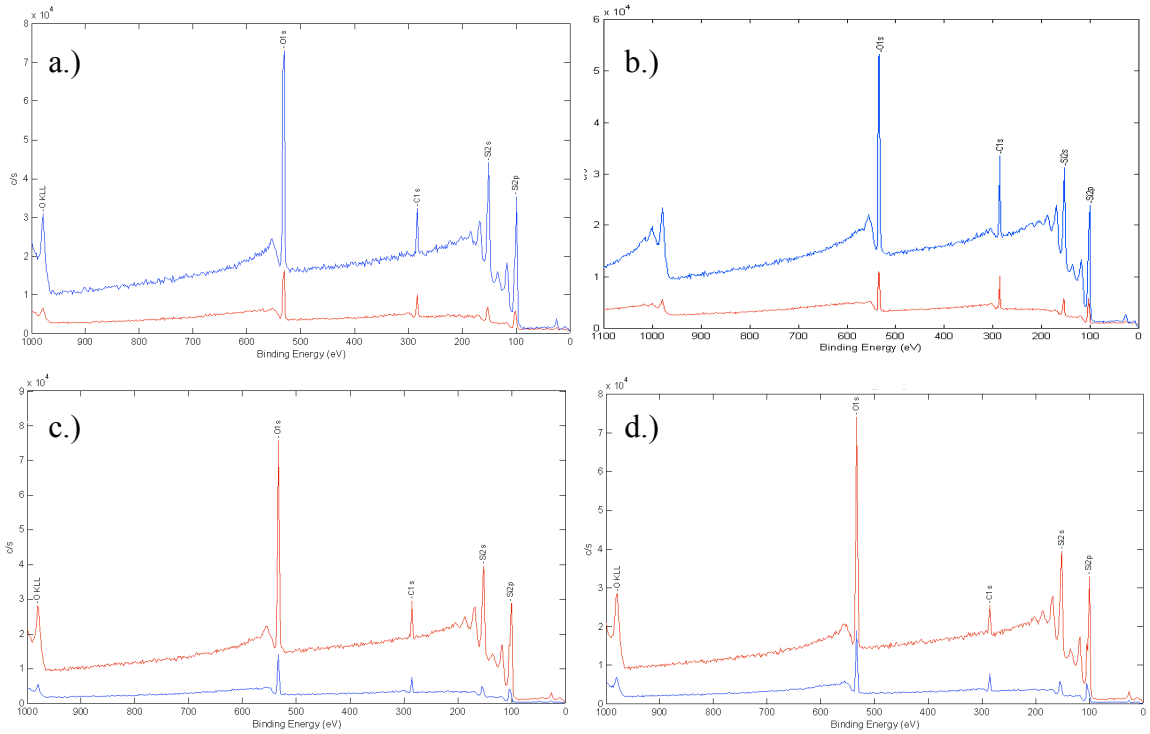

Figure 3.10. X-ray photoelectron spectra for PDMS surfaces prepared on smooth silica using 1.) poly(dimethylsiloxane) with molecular weight ~2,000 g/mol($PDMS^{2000}$); 2.) octamethylcyclotetrasiloxane (D_4); 3.) dimethyldichlorosilane, $(CH_3)_2SiCl_2$; and 4.) dimethylsilandiol $(CH_3)_2Si(OH)_2$ taken at 15° (bottom spectrum) and 75° (upper spectrum) take-off angles.

Figure 3.10 gives X-ray photoelectron survey spectra of poly(dimethylsiloxane) surfaces on silica wafers prepared using different starting reagents and techniques. The surface in Figure 3.10a was created[46] using $PDMS^{2000}$ at 100 °C for 24 hours. The surface in Figure 3.10b was created using D_4 through a vapor phase reaction at 150 °C for 72 hours. The surface in Figure 3.10c was created[55] using dimethyldichlorosilane through the vapor phase at 70 °C for 72 hours, and the surface in 3.10d was created[41] using dimethylsilandiol through the vapor phase at 70 °C for 72 hours.

Admittedly, Figure 3.10 is not particularly interesting and gives no real useful information to distinguish any of these surfaces. Without careful labeling, any of these spectra could easily represent any of the others. Table 3.11 gives more distinguishing characteristics of these surfaces showing water contact angle values and ellipsometric thicknesses for PDMS

surfaces prepared using these four different reagents and conditions. Even with this data, the surfaces prepared using $PDMS^{2000}$ and dimethyldichlorosilane are nearly identical in both contact angles and thickness. In fact, surfaces prepared using dimethyldichlorosilane have been reported[55] with contact angles of 104° / 103°. The lower contact angles found using D_4 and dimethylsilandiol are attributed to their lower reactivities and lower surface coverages.

Table 3.11. Advancing and receding water contact angles and ellipsometric thicknesses for PDMS surfaces prepared on smooth silica using 1.) poly(dimethylsiloxane) with molecular weight ~2,000 g/mol ($PDMS^{2000}$); 2.) octamethylcyclotetrasiloxane (D_4); 3.) dimethyldichlorosilane, $(CH_3)_2SiCl_2$; and 4.) dimethylsilandiol $(CH_3)_2Si(OH)_2$.

Reagent	H_2O Contact Angles (θ_A/θ_R) (°)	Thickness (nm)
$PDMS^{2000}$	104 / 103	1.00
D_4	98 / 83	3.40
$(CH_3)_2SiCl_2$	104 / 102	1.97
$(CH_3)_2Si(OH)_2$	94 / 85	0.44

This comparison was made to show that the PDMS surface prepared using poly(dimethylsiloxane) polymers as the starting reagent does not create a surface that cannot be made by using other techniques. Rather, they are consistent with other preparative methods, and the only advantages of using PDMS polymers as the starting reagent lie solely in the higher reproducibility found in this technique and the simplicity of its preparative procedure.

3.3.7 On Covalent Attachment vs. Hydrogen Bonding

It is not the intent of this work to altogether disprove the existence of the hydrogen bonding between silicone polymers and inorganic oxide surfaces, and in fact no comment is made on whether this occurs or not. Rather, this work was done to suggest that siloxane polymers react with inorganic oxide surfaces, and that this interpretation of the interaction between siloxane polymers and inorganic oxides is more consistent with the known properties and reactivities of inorganic oxide surfaces and silicone polymers. While there is no direct proof that siloxane polymers covalently attach to inorganic oxide surfaces (i.e. no proof is provided showing the exact existence of a M-O-Si bond, which would be difficult to clearly identify), there is enough

evidence to suggest that this occurs and that it explains many of the interactions between silicones and inorganic oxide surfaces.

The high contact angles and low hysteresis of these surfaces suggests a high surface coverage, and their stability in solvents suggests that adsorption is not the primary interaction between these two materials. Further, that this reaction seems general to inorganic oxide surfaces and siloxane polymers, and not just PDMS and silica, gives further support for the cleavage and covalent attachment of siloxane polymers with inorganic oxide surface Lewis acid/base sites. The reactions of cyclic siloxanes, particularly D_4 which has almost no ring-strain, that grow thick PMDS monolayers also highlight that inorganic oxide surfaces are reactive with siloxane bonds. The mechanism of irreversible adsorption through hydrogen bonding does not satisfactorily explain the results obtained using these cyclic siloxanes.

For these reasons, it is surprising that the interpretation using hydrogen bonding as the primary interaction between PDMS and silica, particularly after heating to elevated temperatures, is so prevalent in the modern scientific literature. This was not the case in the late 1940s, though. In a 1947 paper,[62] authors from Dow Chemical, Corning Glass Works, and Bell Telephone Laboratories reported tests of dozens of silanes applied to different types of glass to form silicone films. These authors report: "In contrast to wax films, the dimethylsiloxane film is fixed when cured at high temperatures, probably by surface reaction; after that it is resistant to solvents and only slightly injured by elevated temperatures short of 500 °C." These observations are consistent with the surfaces prepared in this chapter, and the analysis of surface reaction is further supported here.

3.4 Conclusions

Linear silicones, containing siloxane (Si-O-Si) bonds in their main chain, react with inorganic oxide surfaces (silicon, titanium, aluminum and nickel) by a simple thermally activated equilibration reaction to form M-O-Si bonds and covalently attached silicone chains. In particular, surfaces prepared using poly(dimethylsiloxane)s with molecular weights of 2,000 and

9,430 g/mol react with silicon wafers to produce surfaces with low contact angle hysteresis in a highly reproducible manner that are indistinguishable from surfaces prepared using difunctional reagents, such as dimethyldichlorosilane. Thickness of the silicone layer on silica can be easily controlled with the PDMS molecular weight. The use of functional silicones and siloxane copolymers can also provide a versatile method for introducing chemical functionalities or controlling wetting properties. Results of these copolymer reactions suggest that this reaction is general for all siloxane polymers and inorganic oxide surfaces. Furthermore, cyclic siloxanes are also shown to react through the vapor phase to create conformal PDMS coatings on both smooth and particulate surfaces. The reaction of poly(dimethylsiloxane) with silica surfaces is attributed to the presence of water at the silica-silicone interface and the known reactions between water and both silica and silicones as the likely cause of reactivity. Finally, this method is proposed as a simple method for the modification of inorganic oxides that does not require skills normally associated with chemists, does not require the use of solvents, and shows a high degree of reproducibility.

3.5 References

1. Rochow, E.G., Introduction to the Chemistry of Silicones, Wiley, New York, 1946 (1st ed.), 1953 (2nd ed.)
2. Clarson, S.J., Semlyen, J.A., Siloxane Polymers, Prentice Hall, Englewood Cliffs, 1993.
3. McGregor, R.R., Silicones and Their Uses, McGraw-Hill, New York, 1954.
4. Seyferth, D., Organometallics, 2001, 20, 4978.
5. Bokobza, L., J. Applied Polym. Sci., 2004, 93, 2095-2104.
6. Smith, J.S., Borodin, O., Smith, G.D., Kober, E.M., J. Polym. Sci. B: Polym. Phys., 2007, 45, 1599-1615.
7. Aranguren, M.I., Mora, E., Macosko, C.W., J. Coll. Interf. Sci., 1997, 195, 329-337.
8. Şerbescu, A., Saalwächter, K., Polymer, 2010, 50, 5434-5442.
9. Leger, L., Hervet, H., Deruelle, M., Adsorption on Silica Surfaces, Marcel Dekker, New York, 2000.
10. Marinova, K.G., Christova, D., Tcholakova, S., Efremov, E., Denkov, N.D., Langmuir, 2005, 21, 11729.

11. DeGroot, Jr., J.V., Macosko, C.W., J. Coll. Interf. Sci., 1999, 217, 86-93.

12. Osaheni, J.A., Truby, K.E., Silvi, N., Macromol. Symp., 2001, 169, 216-268.

13. Hu, Y., Hadziomerspahic, A., Wang, Y., Macromolecules, 2010, 43, 8233-8238.

14. Cohen-Addad, J. P., de Gennes, P. G., C. R. Acad. Sci. Paris, Ser. II, 1994, 319, 25–30.

15. Selimovic, S., Maynard, S. M., Hu, Y. J., Rheol., 2007, 51, 325–340.

16. Krumpfer, J.W., McCarthy, T.J., Langmuir, 2011, 27, 11514-11519.

17. Plueddemann, E.P., Silane Coupling Agents, Plenum Press, New York, 1982.

18. Wasserman, S.R., Tao, Y.-T., Whitesides, W.G., Langmuir, 1989, 5, 1074.

19. Losche, M., Schmitt, J., Decher, G., Bouwman, W.G., Kjaer, K., Macromolecules, 1998, 5, 1074.

20. Hertl, W., Hair, M.L., J. Phys. Chem., 1971, 75, 2181.

21. Fadeev, A.Y., McCarthy, T.J., J. Am. Chem. Soc., 1999, 121, 12184-12185.

22. Mendez, A., Bosch, E., Roses, M., Neue, U.D., J. Chromatography A, 2003, 986, 33-44.

23. Morterra, C., Magnacca, G., Catalysis Today, 1996, 27, 497-532.

24. Martra, G., Applied Catalysis A: General, 2000, 200, 275-285.

25. Tamura, H., Mita, K., Tanaka, A., Ito, M., J. Colloid and Interf. Sci., 2001, 243, 202.

26. Hiemstra, T., Van Riemsdijk, W.H., J. Colloid and Interf. Sci., 2006, 301, 1.

27. Tripp, C., P., Combes, J.R., Langmuir, 1998, 14, 7348.

28. Cao, C., Fadeev, A.Y., McCarthy, T.J., Langmuir, 2001, 17, 757.

29. Krumpfer, J.W., Fadeev, A.Y., Langmuir, 2006, 22, 8271-8272.

30. Kosmulski, M., Chemical Properties of Material Surfaces, Marcel Dekker, Inc., New York, 2001.

31. Kasprzyk-Hordern, B., Advances Coll. Interf. Sci., 2004, 110, 19-48.

32. Morterra, C., Magnacca, G., Catalysis Today, 1996, 27, 497-532.

33. Kantor, S.W., Grubb, W.T., Ostoff, R.C., J. Am. Chem. Soc., 1954, 76, 5191.

34. Bageli, N., N., Bryk, M.T., Ukr. Khim. Zh., 1981, 47, 409.

35. Xu, S., Lehmann, R.G., Miller, J.R., Chanra, G., Environ. Sci. Technol., 1998, 32, 1199.

36. Soares, R.F., Leite, C.A.P., Botter, Jr., W., Galembeck, F., J. Applied Polym. Sci., 1996, 60, 2001-2006.

37. Vichi, F.M., Galembeck, F., J. Adhesion Sci. Technol., 1999, 13, 973-982.

38. Kole, S., Srivasta, S.K., Tripathy, D.K., Showmick, A.K., J. Appl. Polym. Sci., 2003, 54, 1329.

39. Lai, S.K., Batra, A., Cohen, C., Polymer, 2005, 46, 4204.

40. Nawrocki, J., Chem. Anal. (Warsaw), 1995, 40, 183-193.

41. Liu, Y., Wang, L., Krumpfer, J.W., Watkins, J.J., McCarthy, T.J., J. Am. Chem. Soc., 2012, submitted.

42. Fadeev, A.Y., McCarthy, T.J., Langmuir, 2000, 16, 7268.

43. Fadeev, A.Y., McCarthy, T.J., Langmuir, 1999, 15, 3759-3766.

44. Hoffman, S., Depth Profiling in AES, XPS, Practical Surface Analysis, Wiley Press, New York, 1996.

45. Fadeev, A.Y., McCarthy, T.J., Langmuir, 1999, 15, 7238.

46. Krumpfer, J.W., McCarthy, T.J., Faraday Discuss., 2010, 146, 103-111.

47. Fox, H.W., Taylor, P.W., Zisman, W.A., Indust. Engin. Chem., 1947, 39, 1401-1409.

48. Hyde, J.F., J. Am. Chem. Soc., 1953, 75, 2166-2167.

49. Kantor, S.W., J. Am. Chem. Soc., 1953, 75, 2712-2714.

50. Veraprath, S., Lehmann, R.G., J. Env. Polym. Degrad., 1997, 5, 17-31.

51. Brzoska, J.B., Azouz, I.B., Rondelez, F., Langmuir, 1994, 10, 4367.

52. Gupta, P., Ulman, A., Fanfan, S., Korniakov, A., Loos, K., J. Am. Chem. Soc., 2005, 127, 4.

53. Schmidt, D.L., Cobern, C.E., DeKoven, B.M., Potter, G.E., Meyers, G.F., Fischer, D.A., Nature, 1994, 368, 39.

54. Chen, W., Fadeev, A.Y., Hsieh, M.C., Öner, D., Youngblood, J., McCarthy, T.J., Langmuir, 1999, 15, 3395-3399.

55. Fadeev, A.Y., McCarthy, T.J., Langmuir, 2000, 16, 7268-7274.

56. Fadeev, A.Y., Kazakevich, Y.V., Langmuir, 2002, 18, 2665-2672.

57. Zheng, P., unpublished results.

58. Mark, J.E., ed., Polymer Data Handbook, Oxford University Press: New York; 1999.

59. Zheng, P., McCarthy, T.J., Langmuir, 2010, 26, 18585-18590.

60. Arkles, B., Larson, G., eds., Silicon Compounds: Silanes and Silicones Catalogue, 2nd ed., Gelest, Inc., Morrisville, 2008.

61. Gao, L.C., McCarthy, T.J., Langmuir, 2007, 23, 10445-10447.

62. Hunter, M.J., Gordon, M.S., Barry, A.J., Hyde, J.F., Heidenreich, R.D., Ind. Eng. Chem., 1947, 39, 1389.

CHAPTER 4

ELECTRICALLY CONDUCTIVE SILICONE COMPOSITE FILMS

4.1 Introduction

4.1.1 Background

Compounding is one of the most common and useful methods for imparting and improving polymer material properties. Inorganic particles, such as silica, alumina and titania, are the most common additives to materials, largely due to their relative abundance, low cost, and unique properties. For example, alumina is a hard material often added in the processing of ceramics.[1] Titania has a remarkably high refractive index and is added to nearly all paints.[2] Other particles, such as nickel, silver, and copper, can be added to materials to impart electrical conductivity. Magnetite (Fe_3O_4) is used for the creation of ferrofluids for automobile suspension dampeners.[3,4] The wide variety of materials which can be produced from compounding makes this process extremely valuable and enticing.

Silicone materials are nearly all composite materials, featuring silica as a reinforcing agent. Silicones are known for their high thermal stability and chemical resistance.[5] In this way, silicone materials can be made robust and useful as adhesives, elastomers, or sealants. Like many other polymeric materials, a wide variety of particles have been added to silicones to give them properties that are not typically associated with the virgin polymer. The heat-conductance properties of silicone materials have been increased by the addition of alumina while retaining electrical resistance of silicones.[6] The electrical conductivity has been increased through the addition of carbon black[7] and nickel particles[8]. Magnetite added to silicone rubbers have created magnetically responsive silicones which act as microheaters upon application of an alternating-current (AC) field.[9]

However, as with all compounded materials, dispersion of particles into the matrix material is crucial in imparting the desired properties. Poor dispersion often results in subpar materials with poor reproducibility. While the topic of dispersing particles into materials was

briefly discussed in the Introduction of this dissertation, many of points of this topic will be repeated here. There are two primary issues which face the dispersion of particles in a matrix material, and these are sedimentation and aggregation.[10] Sedimentation is the settling of particles at the bottom of a vessel. The forces affecting the sedimentation of particles are gravity, buoyancy, and drag (Figure 1.5). The balance of gravity and buoyancy is completely due to the differences in density of the particle and matrix material. For composites of inorganic particles in polymer materials, the density of the particle is almost always greater than polymer matrix. There are two methods for overcoming this sedimentation. The first is to increase the viscosity of the matrix material. By increasing the viscosity, the force of drag is increased which prevents the movement of particles within the matrix and prevents sedimentation. However, starting with a high viscosity matrix material makes the initial dispersion of particles difficult since particles must be able to freely move to form a suspension.

The second technique is the use of small particles, typically with sub-micron diameters. By reducing the radius, the forces of gravity and buoyancy are greatly diminished. For this reason, the effect of gravity, buoyancy, and drag are often ignored for extremely small particles. However, careful analysis of the forces presented in Figure 1.5 shows that all particles should sediment given a long enough time scale. However, what is not presented in Figure 1.5 is the effect of interfacial forces which can greatly affect the stability of a suspension. Good particle-matrix compatibility can make a particle suspension indefinitely stable, and this is seen in the dispersion and suspension stability of surface functionalized colloids, such as gold, in various systems.[11]

This leads to the second issue in the dispersion of particles: aggregation, also known as flocculation or coagulation. In a two component particle-matrix system, there are three interactions which determine whether aggregation will occur or not. These three interactions are particle-particle, matrix-matrix, and polymer-matrix. For most inorganic oxides, the particle-particle interactions are typically dominated by long-range electrostatic attraction and short-range repulsion,[12] although both van der Waals and hydrodynamic interactions are possible, and these

electrostatic interactions are generally much stronger than the other two possible interactions which leads to aggregation. Simply put, if the particle-particle or matrix-matrix interactions are stronger than the polymer-matrix interactions, aggregation occurs. Aggregation also often leads to sedimentation, as the sudden growth in the size of the aggregate is greatly affected by gravity. For this reason, the most common method for controlling the interactions between these two materials is the surface modification of the filler material. Using good surface modifiers, this technique does two things. First, it shields the electrostatic interactions between particles, thus lowering the particle-particle interactions. Second, it increases the particle-polymer interactions.

A great deal of study has been performed on the aggregation mechanisms of suspended particles.[13,14] While it is not appropriate here for an in-depth discussion on aggregation kinetics, a few brief notes should be made which may elucidate this process. There are two discrete steps in the aggregation of particles: transport and attachment. In other words, two particles must move through a matrix and then collide with one another. Depending on whether this collision is inelastic or elastic, aggregation of the two particles will either occur or not. For chemists, this is an analogue of binary reaction kinetics. Equation 4-1[13] gives an expression for the rate of aggregation, in which α is the collision efficiency, β is the collision frequency between particles of size i and j, and n_i and n_j are the particle concentrations for particles of size i and j. More simply, α can be seen as the strength of particle-particle interactions, and β can be seen as a function of matrix viscosity (transport) and particle size. At equivalent particle number concentrations, smaller particles should aggregate less rapidly than larger particles. However, this should not be confused with equivalent weight or volume concentrations.

$$\text{rate of aggregation} = \alpha\,\beta(i,j)n_i n_j \qquad \text{(Eq. 4-1)}$$

Despite the importance of good dispersion in creating composite materials, quantification of a suspension is particularly difficult, especially at typical loading concentrations needed to impart the desired properties or when the particles are opaque. This problem has long been a problem in the paint industry[15] since the high refractive index of titania and opacity of the composite limits the transmission of light, and eliminates many optical characterization

techniques such as light scattering and transmission microscopies. Because of this, qualitative or indirect determinations of dispersion are most common in composite industries and literature.

The most common methods for determining the quality of dispersion in a material are scanning electron microscopy (SEM) and optical reflectance microscopy (OM). These techniques are useful for obtaining a qualitative view of the dispersed particles in a matrix material. However, because these are two-dimensional images of a three dimensional structure, there are limitations to how much information can be gathered from these techniques. There are other methods to determine the quality of a particle suspension.

The spatula rub-out test[16] (ASTM-D281) is a qualitative method for determination of the oil absorption of pigment particles. Daniel and Goldman[17] have shown that the flow of an oil after pigment absorption from the spatula rub-out test can be used to determine the quality of the dispersion as good, fair, or poor. It was shown that for good dispersions a substantial portion of a composite paste will flow down a vertically held spatula without leaving any jagged flow edges. In poor dispersion, the paste will drip off the spatula or flow with edges that are not smooth. This is simply an observation of the rheological behavior to determine the dispersion characteristics. A technique similar to this is used in this work. More robust rheological techniques[18] can also be used to indirectly determine the quality of particle dispersions, although this can prove difficult for crosslinking systems.

Conductive composites represent a more specific division of composite materials. When dealing with conductive composites, either thermally or electrically conductive, percolation becomes a significant parameter which governs the properties of these materials. In this class of materials, percolation is defined as the formation of a continuous conductive region.[20] Percolation is typically defined by a percolation threshold below which a continuous path or region does not exist and above which a continuous path or region does exist. Because of this, the percolation threshold represents a sudden change in material properties, often exhibited by an S-curve (Figure 4.1),[19] which above and below the inflection point, there is only a relatively small change in properties.

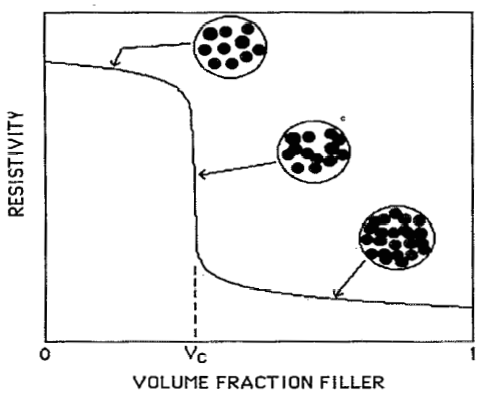

Figure 4.1. Common resistivity dependence on volume fraction of filler material in conductive composites in which there is a drastic change in properties at the percolation threshold (b.), above (c.) and below (a.) which there is only a slight change in properties with respect to volume fraction.[19]

A great deal of work has been performed in regards to the theory of percolation.[21,22] Percolation theory has been well-established over the last fifty years in fields of mathematics and has found a great deal of application in materials sciences, especially with conductive composites. Percolation theory dictates that for an infinite system with a specific lattice orientation and dimensionality, there is a specific fraction of lattice sites that when randomly occupied create a continuous occupied path through the system.

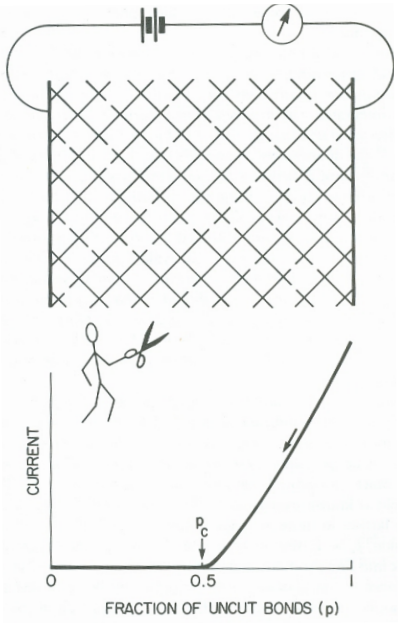

Figure 4.2. "The Mad Man with the Scissors".[23]

A classical example of percolation theory is known as "The Mad Man with the Scissors" and is shown in Figure 4.2.[23] This is known as "bond percolation" since it involves the existence or absence of bonds to connect two lattice sites. Here, a man with a pair of scissors randomly cuts a very large fence that is conducting an electrical current (even though he is a mad man, he is wearing special gear to not be electrocuted). Percolation theory states that if he is truly cutting the wires at random, the probability of this fence no longer having a conductive path is at its highest after the man cuts 50% of the bonds. If this were an infinitely large fence, this fence would stop conducting exactly after 50% of the bonds were cut, and this is known as the percolation threshold.

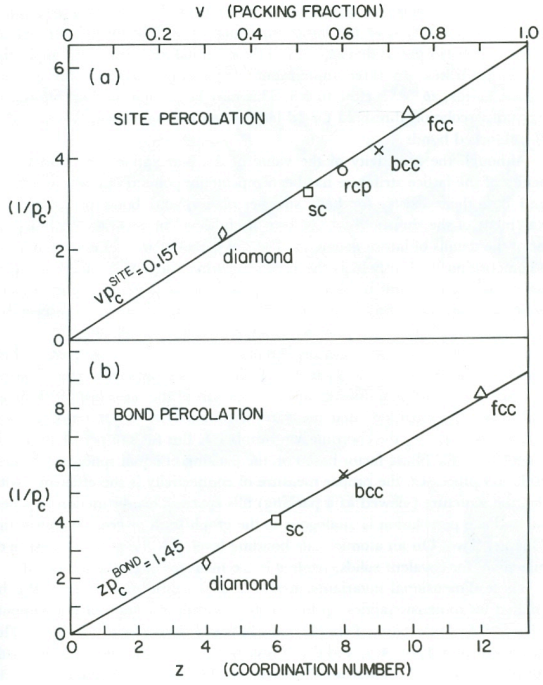

Figure 4.3. The Schar-Zallen Invariant in which the volume fraction of the percolation is a product of a packing parameter (v for 3D systems and z for 2D systems) and the number percolation threshold (p_c).[23]

Percolation theory becomes more complex with increasing dimensions and lattice sites. However, Schar and Zallen[23] have mathematically shown that while the number of occupied sites necessary for percolation is dependent on lattice, the volume fraction for percolation is dependent only on the dimensionality of the system, not related to the lattice structure with which it is

framed, and is in fact constant. This is known as the Schar-Zallen Invariant. Figure 4.3 shows the site percolation and bond percolations for several different lattice. The volume fraction for percolation (φ_c) in three-dimensional lattices is always 0.157 and is the product of the packing factor (v) and the site percolation fraction (p_c) for that specific lattice. Because the percolation volume fraction is not dependent on the system lattice, it can be used to describe any randomly dispersed system, such as particles in a polymer matrix, and for this reason has found such wide acceptance in the materials science of composites.

Furthermore, this theoretical volume fraction of approximately 16% has been found to be consistent with experimental results, which are not infinite systems. For this reason, a universality principle is applied to composite systems.[24] While not accepted by all,[25] the universality principle states that a given finite fraction of an infinite system is not dependent on other fractions outside of its boundaries, and this finite fraction should be representative of the entire infinite system. In other words, percolation theory should work just as well in finite systems as it does in infinite systems assuming randomness and homogeneity.

All these things being said, there are a few assumptions made using this theory in composite materials. The first assumption is that all filler materials are uniform in size and shape, typically spherical. In practical applications, this is almost never the case which leads to deviation from the theoretical value. Furthermore, increase of the aspect ratio of a particle (i.e., spheres to wires to flakes) decreases the percolation threshold as the probability of the two particles touching increases.[26] The second assumption is that the particles are not the same order of magnitude as the entire material. This assumption is typically ignored, as most particles are several orders of magnitude smaller than the composite material. The third assumption is that there is no aggregation phenomena and the particles are randomly dispersed. This is a significant assumption as even in well dispersed materials there is typically small degrees of aggregation.

There are other factors which effect how a composite material conducts electricity. Conductance is defined as the degree of ease which an electric current may pass through a system, and is measured in units of Siemens (S).[27] The inverse of conductance is resistance, the

opposition to the passage of an electric current through a system, and is measured in Ohm's (Ω). Two other definitions should be made. Voltage is defined as the difference in potential between two points of a conductive path (i.e. the force by which a current is passed through a material) and is measured in either volts (V) or joules per coulomb. The closest analogy to voltage is a water pumped through a closed circuit, in which differences in water pressure cause the water to flow through the circuit. Finally, electric current is the flow of an electric charge through a medium and is measured in amperes (A) or coulombs per second. The relationship between current and voltage is given by Ohm's Law (Eq. 4-2).

$$V = IR \quad \text{(Ohm's Law)} \qquad \text{(Eq. 4-2)}$$

$$\rho = RA / l \qquad \text{(Eq. 4-3)}$$

However, conductance and resistance are not material properties, since the size and shape of a system can effect the resistance and conductance measured. Instead, conductivity and resistivity are material properties. Eq. 4-3 gives the expression for resistivity (ρ) in which R is the measured resistance, A is the cross-sectional area over which the resistance is measured and l is the length over which the resistance is measured. Resistivity is given in units of Ohm·m. Since resistivity is a bulk material property, it is often used to classify materials. Although there is no universal definitions for these conductive materials, they are generally classified as conductors ($\rho < \sim 10^{-3}$), semi-conductors ($\sim 10^{-3} < \rho < \sim 10^{3}$), and resistors ($\rho > \sim 10^{3}$). Metals are good conductors with conductivities on the order of 10^{8} or greater. Silicones are good insulators with conductivities on the order of 10^{-13}.

$$\rho = 2\pi r V/I \qquad \text{(Eq. 4-4)}$$

After reviewing Eq. 4-3, though, special consideration must be made to measure and classify the resistivity of thin films, since the cross-sectional area shrinks to zero. For these reasons, a separate definition for resistivity has been developed to account for these geometric limitations (Eq. 4-4),[28] in which r is the distance between two points, and V and I are the voltage and current measured over r, respectively. This is the fundamental equation used in two-point and four-point conductivity measurements of a surface.

There are other system considerations which can affect the measured resistance. The first of these is known as contact resistance, which is an increase in the apparent resistance due to the probe materials and their contact to the surface. Similar to this is constriction resistance which is caused by the bottle-necking of current flow which occurs at contact points, such as the contact of two particles. Finally, there is tunneling resistance which is the resistance found by the coating of a material or the presence of a insulating oxide film. While the contact resistance is purely an experimental issue, constriction resistance and tunneling resistance are material issues. Because of these factors, the resistance of a percolated composite is almost always higher than those of the pure conductive filler material.

In this study, the electrical properties of silicone films loaded with nickel and titania are discussed. Silicones are a traditional electrically insulating material ($\rho \sim 10^{13}$) with a high dielectric strength of 135-217 kV/cm. Dielectric strength can be seen as the required voltage to make a certain length of material become conductive. For perspective, the dielectric strength of nylon 6,6[29] is ~260; poly(propylene) is ~217-300; vacuum is ~400; and air is ~30 kV/cm, although the value for air is highly dependent on humidity.[30] Nickel, however, is a transition metal and a good conductor. Titania (anatase, P25) is an insulating material, although its resistivity has been measured[31] as $7.7 \cdot 10^5$, lower than most good insulating materials, and is often classified as a semi-conductor. Many studies have been performed on conductive silicone composites. However, most of these studies involve silicone elastomers[32,33] and the use of films coated on substrates has not been a focus of study.

4.1.2 Objectives

The objective of this work was to develop nickel particle-silicone composite films which exhibited electrically conductive characteristics. The influence of particle volume fraction on the properties of these films is investigated, and adherence to percolation theory is determined. Furthermore, the influence of particle geometry on conductance and percolation of these films is examined. Vinyl-terminated silicones of various molecular weights were used to make crosslinked films to investigate the effects of crosslink molecular weight and crosslink density on

electrical properties was also examined. Finally, the addition of titania into the nickel-silicone composite was performed to observe the effects of small particle insulators on the electrical properties of this system.

4.2 Experimental Section

4.2.1 Materials

Hydridomethylsiloxane (MW ~ 2,000 g/mol) ($HMS^{2,000}$), vinyl-terminated poly(dimethylsiloxane)s of molecular weights of 187 g/mol (0.7 cSt.), 6,000 g/mol (100 cSt.), 28,000 g/mol (1000 cSt.), and 62,700 g/mol (10,000 cSt.), and platinum-divinyltetramethylsiloxane complex (Karstedt's Catalyst) (3-3.5% platinum concentration in vinyl-terminated siloxane, 1000 cSt.) were purchased from Gelest, Inc. Spherical conductive nickel particles (4SP-10) and conductive nickel flake Type HCA-1 were purchased from Novamet. Anatase titania nanoparticles (P25) were purchased from Degussa. For the nickel wire synthesis, ethylene glycol, nickel (II) chloride hexahydrate, and sodium hydroxide were purchased from Fisher Scientific. Hydrazine hydrate was purchased from Arcos Organics. Xstatic antipad test boards were provided by Shocking Technologies.

4.2.2. Particle Dispersion and Film Preparation

Catalyst solutions of Karstedt's catalyst (Figure 1.4b) in toluene were made, such that the platinum concentration was $5 \cdot 10^{-4}$ g Pt / mL. This was done by adding 0.167 g of the purchased Karstedt's catalyst solution into 10 mL of toluene, and shaking on a Vortex mixer for 24 hours.

Mixtures of hydridomethylsiloxane (MW ~ 2,000 g/mol) and vinyl-terminated poly(dimethylsiloxane) were made with 1:1 molar ratios. This is equivalent to an approximately 15:1 molar ratio of hydridosilanes to terminal vinyl groups. These mixtures were stirred with a spatula by hand to induce the initial dispersal of the particles, and shaken on a Vortex mixer for 24 hours to ensure complete, homogeneous dispersion. An exception to this procedure was made when using the v-PDMS (MW = 62,700 g/mol). The viscosity of this polymer is extremely high,

making homogeneous mixing difficult. For this reason, 150 μL of toluene were added to the mixture for every 1 g of this v-PDMS in order to lower the solution viscosity during mixing.

Nickel particle suspensions were made by adding the desired amount of dry nickel powder to the silicone mixtures. Initial observations found no advantages from modification of these nickel surfaces, and in fact, surfaces with modification by cyclic siloxanes tended to show slightly lower reproducibility. Furthermore, because of the micronic size of these particles, sedimentation was a greater concern than aggregation. For these reasons, surface modification of the nickel powders was not performed for the preparation of samples reported here. After the addition of nickel particles, the mixture was stirred using by hand using a spatula to break up any large aggregates. After this, the suspensions were shaken on a Vortex mixers for 48 hours, in a fashion similar to previously reported techniques.[34,35]

For systems with titania particles, these particles were added to the mixtures after the nickel powder and vigorously stirred. Typically, a tough paste is rapidly formed when 5 vol.% titania particles were added. To avoid this and help the dispersion process, small amounts of toluene were added to lower the viscosity of the system to a point where it showed flow. Titania particles added were modified using 1,3,5,7-tetramethylcyclotetrasiloxane through the vapor phase using conditions discussed in Chapter 2. This surface modification was observed to help facilitate the dispersion of titania particles into the silicone. These suspensions were then shaken on a Vortex mixer for 48 hours, as above.

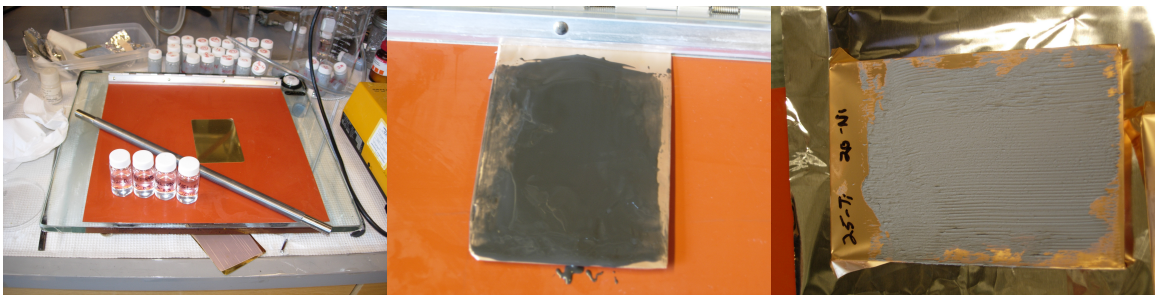

a.) b.) c.)

Figure 4.4. Experimental set-up for the draw down procedure (a.) showing a brass plate, draw down coating rod, and silicone mixtures on a draw down board (b.) a wet film nickel-silicone film after draw down coating and (c.) a cured nickel-titania-silicone film.

Coating of the silicone composites were done using the draw-down coating technique.[16] This is a well known industrial technique used to carefully control coating uniformity and thickness. A draw down steel bar with a 1.02 cm diameter wrapped with a 40 gauge wire was used to uniformly coat the silicone composite over the Xstatic antipad test board. Draw down bars of this size are rated to produce wet films with thicknesses of approximately 102.5 μm. Figure 4.4 shows images of the draw down set-up and both wet and cured films.

Prior to coating of the silicone films, the prepared Karstedt's catalyst solution was added to the silicone-particle mixture in a ratio of 250 μL solution for every 3 g of silicone mixture. The mixture was then stirred by hand using a spatula to prevent sedimentation. Addition of the catalyst initiates the crosslinking process of the vinyl-terminated PDMS and the hydridomethylsiloxanes shown in Figure 1.4a which increases the viscosity of the silicone mixture. During stirring, droplets of the mixture were observed as they slide down the side of a glass scintillation vial. When the consistency was similar to that seen in Daniel-Goldman[18] test, the mixture was spread upon the test board and coated using the draw down bar. The consistency of the droplets showed uniform flow with a smooth interface (i.e. no aggregates were observed). The trail left behind the droplet was also uniform in consistency and opacity. This is easy to determine with nickel, since it is a dark gray color. At consistencies below the proper spreading point, the nickel particles will sediment, creating fluctuations in the color of the trail and transparent silicone can often be observed at the edges of the trail. If the mixture is not coated at the proper time, the silicone will completely crosslink often making a solid material.

After coating by the draw-down technique, these films were allowed to cure at room temperature for four hours and then at 70 °C for 24 hours. Pre-curing at room temperature was found to greatly diminish cracking of the crosslinked film. After this curing process the films were allowed to cool to room temperature prior to characterization of their electrical properties.

4.2.3 Nickel Non-Woven Synthesis

Nickel non-woven materials are made by dissolving 0.12 g $NiCl_2 \cdot 6H_2O$ in 30 mL ethylene glycol. This solution is stirred using a magnetic stir bar until the nickel chloride is

completely dissolved. This solution has a light green color. After stirring for approximately 15 minutes, 1 mL hydrazine hydrate ($N_2H_4 \cdot H_2O$) is added dropwise to the solution mixture. The solution turns a dark purple and is stirred for another 15 minutes. Finally, 1M NaOH is added dropwise to the solution until a pH of 11.5 is reached, and the solution turns a light blue color. This typically equates to ~ 6 mL 1M NaOH. The solution is allowed to stir for another 15 minutes, and is then sealed into a teflon bottle and heated at 60 °C for 4 hours. The resulting nickel non-woven is a black "bird's nest" structure which floats on the liquid surface. Filtration of this solution can be easily performed by magnetically trapping the nickel non-woven and draining the ethylene glycol waste. Mass yield of a dry nickel non-woven material using this procedure is approximately 0.03 g. These nickel non-woven materials can then be broken down into smaller nickel wires by application of an ultrasound horn of a non-woven suspension in water.

4.2.4 Characterization

The electrical properties of nickel-silicone composite films were measured using a two-point probe measurement on a Xstatic Antipad test board over a gap of 63.5 micron using a Keithley 2400 Broad Purpose SourceMeter. Antipad test boards were used to minimize the effects of contact resistance. Current-voltage (I-V) curves were made by measure the current over voltage ranges of 0 to 0.001V, 0 to 0.01V, 0 to 0.1V, 0 to 1.0V, 0 to 10V, and 0 to 100V in that order with three sweeps made per range. After these sweeps are made, if a conductive response was observed, second and third I-V curves are made for the most appropriate voltage range. This Keithley device has an upper current limit of 100 mA, and so no results were obtained for currents above this limit.

Further characterization of these films was performed using a JEOL NeoScope JCM-5000 scanning electron microscope and an Olympus BX60 optical microscope with UMPlanFI objective lenses. Thicknesses of several films were characterized using a Veeco Dektak 150 Surface Profiler profilometer.

4.3 Results and Discussion

4.3.1. Nickel Particles and Wire Synthesis Results

Commercial nickel particles used in making silicone composite films are shown in Figure 4.5. These particles were not coated with gold prior to imaging, as they are conductive materials. Both of these nickel particles show a great deal of polydispersity. The spherical nickel particles (4SP-10) typically range from 0.5 to 10 μm in diameter. Closer inspection of the particle surface shows a great deal of texturing, indicating that the surface of these particles in not completely smooth nor are these particles completely spherical. The nickel flakes shown in Figure 4.5c,d show a corn flake like structure with end-to-end lengths up to 20 μm and thicknesses of approximately 1-2 μm. The faces of these flakes appear to be quite smooth while the edges show a greater deal of roughness. Figure 4.5d also shows the presence of several rough oblong shaped particles, which are not flakes, and exhibit very rough surfaces. No further purification of these commercial particles was performed, and these particles were used as provided.

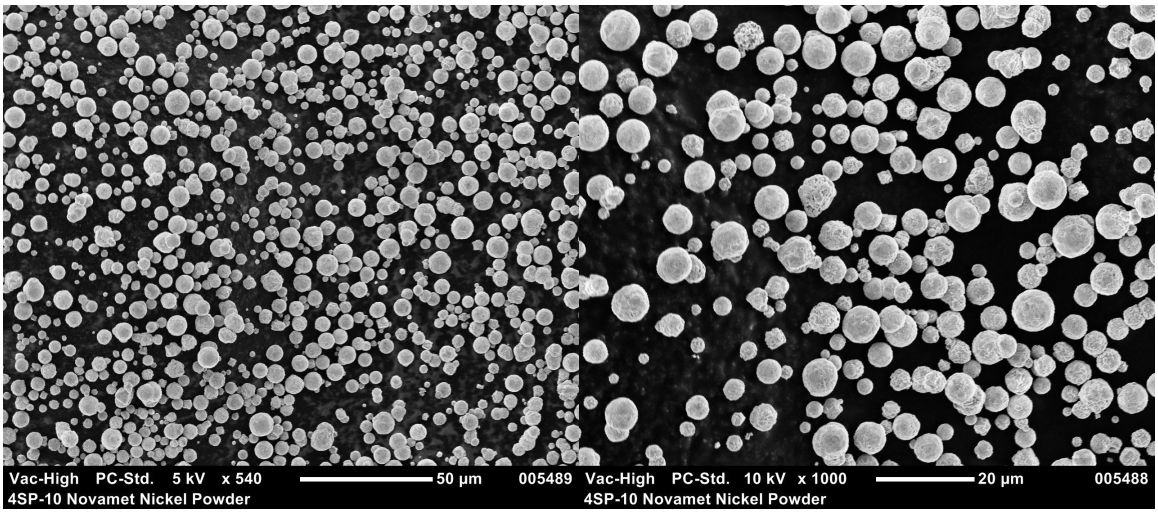

(a.) (b.)

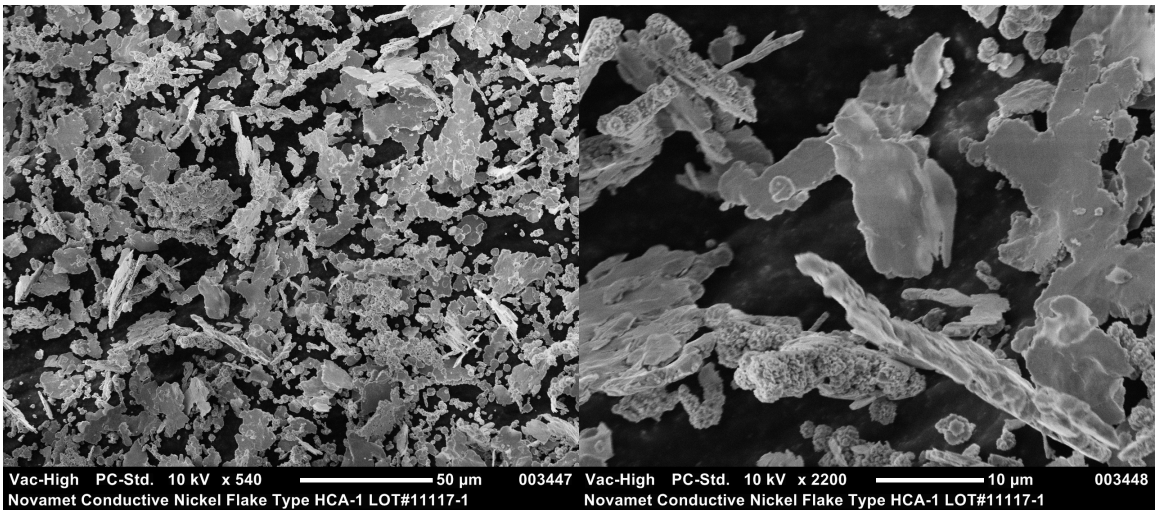

(c.) (d.)

Figure 4.5. Scanning electron microscopy images of commercial nickel particles (a,b) 4SP-10 spherical nickel particles and (c,d) Type HCA-1 conductive nickel flakes.

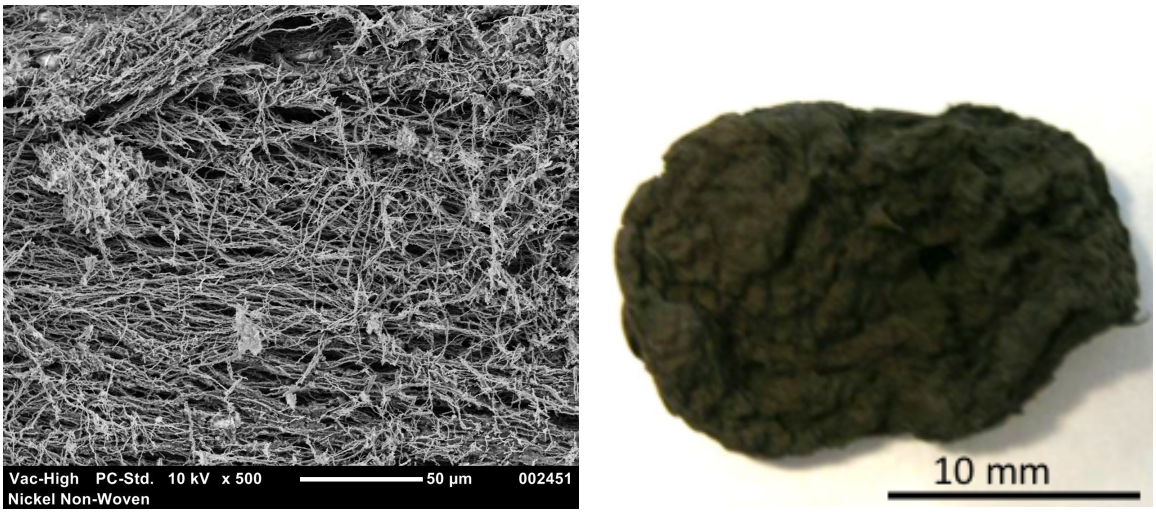

(a.) (b.)

Figure 4.6. Scanning electron microscopy image of a nickel non-woven material (a.) and image of the bulk nickel non-woven material (b.).

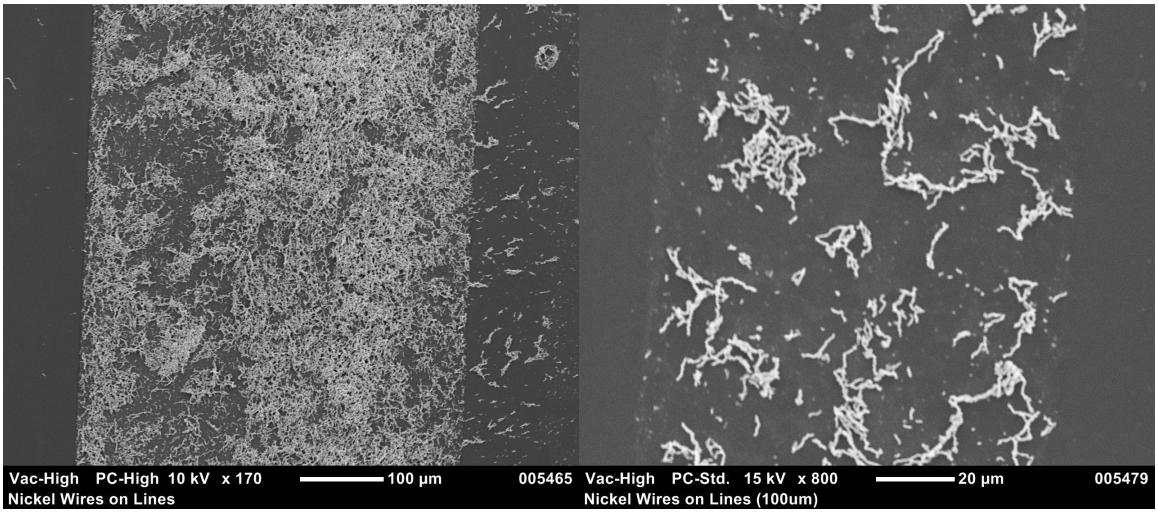

(a.) (b.)

Figure 4.7. Scanning electron microscopy images of nickel wires formed from the disruption and breaking of nickel non-woven materials.

Nickel non-woven materials were prepared as described in Section 4.2.3, and images of the bulk non-woven material can be seen in Figure 4.6. These nickel non-woven materials are continuous networks of nickel wires which form magnetic, electrically conductive and low-density solids. The diameter of the wires within the nickel non-woven are approximately 100-500 nm. Application of a sonic horn to disrupt the non-woven network and break apart the nickel wires was used to produce short nickel wires as shown in Figure 4.7. These nickel wires

are several microns in length while maintaing diameters similar to the non-woven material. Because of the nature of this technique, uniform wire length is not achieved, but wires of different lengths are produced. This results in a mixture of particle wires with different aspect ratios. Regardless, the aspect ratio of these wires is still larger than the spherical particles in Figure 4.5a.

Resistance measurements were performed on loosely packed nickel particles, and the resistivities calculated for these particles are shown in Table 4.1. The resistivities of the different, commercially available nickel particles is approximately the same, while that of the prepared nickel wire is about an order of magnitude lower . This is not attributed to geometric shape of the particles, but rather preparation method, since it is known that the preparation method can have a direct impact on both electrical and magnetic properties. The use of loosely packed nickel particles was performed to give a reasonable upper limit for the conductivity of the composites used in this study. The loosely packed nature also accounts for the difference between these resistivities and that of pure nickel ($7.12 \cdot 10^{-8}$ Ω·m).[36] These nickel particles also have much lower resistivities than both titania[31] and poly(dimethylsiloxane).[5]

Table 4.1. Resistivities of loosely packed nickel particles and literature values for titania and silicones.

Material	4SP-10 Ni	HCA-1 Ni	Ni Wire	P25 TiO2	PDMS
Resistivity (Ω·m)	$1.3\ 10^{-4}$	$1.2\ 10^{-4}$	$1.9 \cdot 10^{-3}$	$7.7 \cdot 10^{5}$	$> 10^{13}$

4.3.2. On the Characterization of the Composite Films

The simplest and most effective method for characterizing these films was visual inspection. It is very easy to visually determine the quality of the films prepared, as seen in Figure 4.8. The films shown in this figure represent three of the most common issues involved in the preparation of silicone films. The left most samples, coated onto brass plates, show an extensive amount of cracking. This is common in samples which are not allowed to pre-cure at room temperature for 4 hours, or use cross-linking ratios other than 1:1 mole. Sample films coated on test boards are shown in the middle of this image and epresent those samples in which

sedimentation and improper dispersion has occurred. This samples shows uneven amounts of nickel throughout the film, as seen by the areas of pure

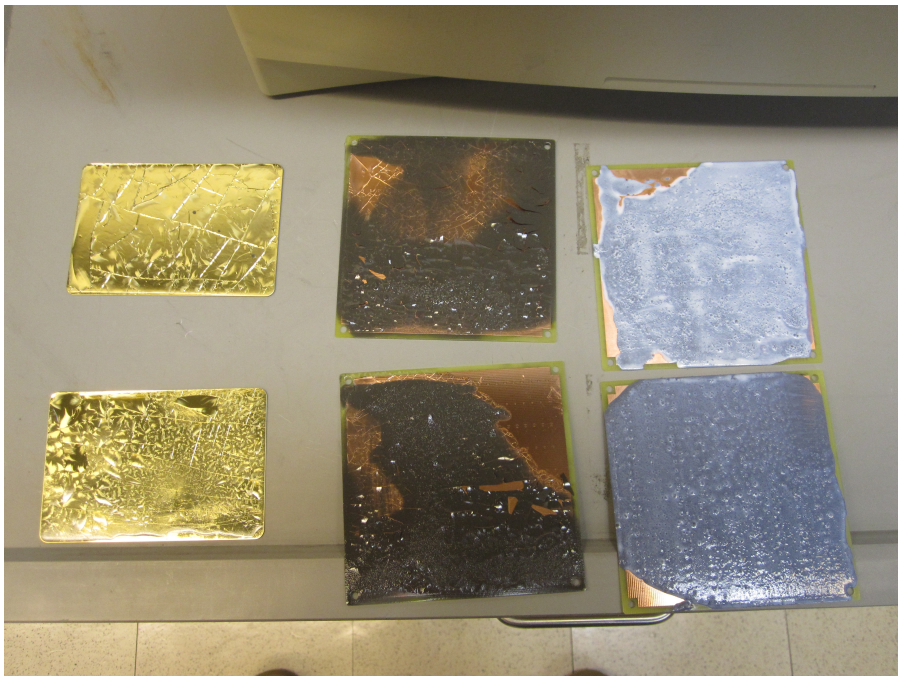

Figure 4.8. Prepared sample films exhibiting poor quality due to cracking (left), sedimentation and poor dispersion (middle), and aggregation (right).

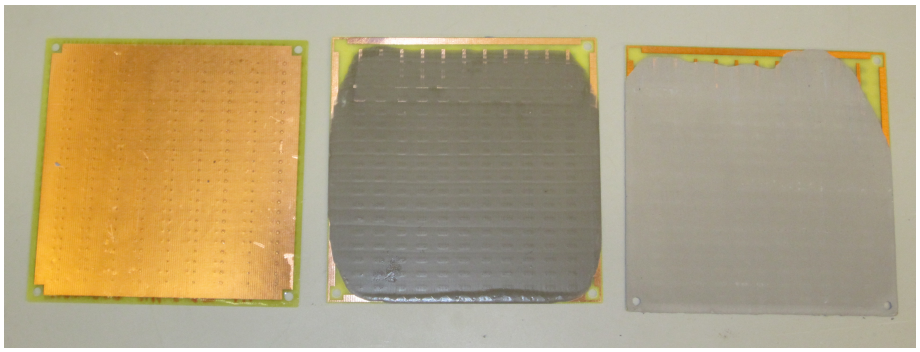

Figure 4.9. Prepared sample films of a pure silicone film (left), 25 vol.% Ni silicone film (middle), and 50 vol.% Ni, 5 vol.% TiO_2 silicone film (right) indicating good coating without the presence of cracking, color density fluctuations, and aggregation.

silicone film. In addition to these issues, these particular samples also show cracking. Finally, the rightmost samples show issues of aggregation. These rightmost samples contain both nickel and titania. The roughness of the film surfaces clearly indicate aggregation. For comparison,

properly prepared surfaces are shown in Figure 4.9. These samples have smooth interfaces, do not show changes in color density, and do not show any cracking. The leftmost film represents the highest particle loading for a film (50% Ni, 5% TiO_2). The slight lip at the bottom of the center film represents where the drawdown coating was stopped, and not any sort of aggregation.

In addition to visual inspection, optical microscopy images were taken to give qualitative representations of the degree of dispersion in the films. Figure 4.10 gives optical micrographs of several films prepared with various particle loading fractions. Silicone films without nickel particles are completely transparent and the bottom of the test board can clearly be seen through the film (Figure 4.10a). Figure 4.10b shows a film prepared just at the percolation threshold. Here, several percolated paths can be seen, but random dispersion seems evident. Increasing the nickel content shows films with a large number of percolated structures. Addition of titania (Figure 4.10e, f) makes the films very opaque, but random dispersion of the particles still seems evident.

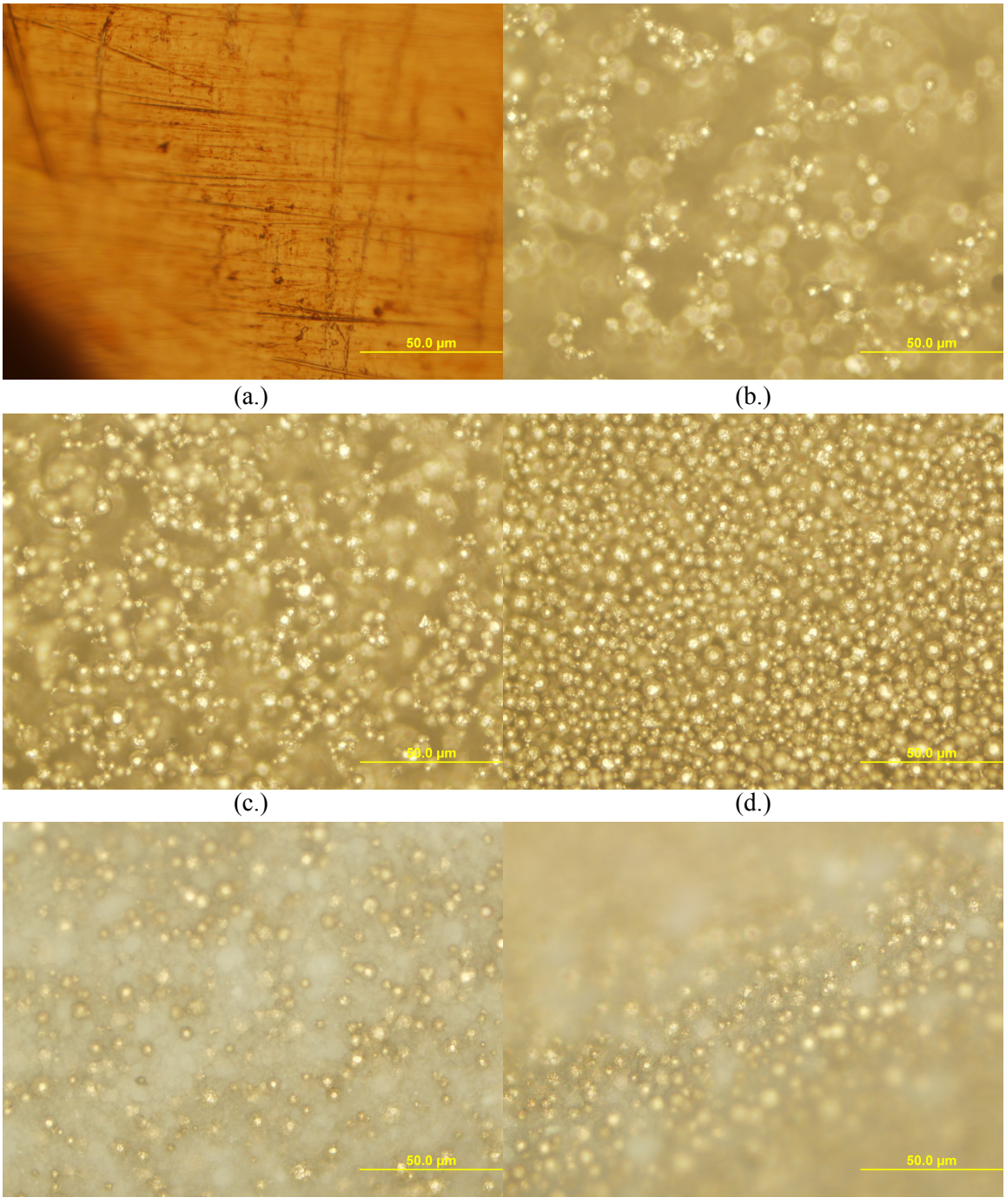

Figure 4.10. Optical micrographs of silicone films with a.) 0 vol.% Ni, b.) 15 vol.% Ni, c.) 25 vol.% Ni, d.) 50 vol.% Ni, e.) 15 vol.% Ni and 5 vol.% TiO_2, and f.) 25 vol.% Ni and 5 vol.% TiO_2.

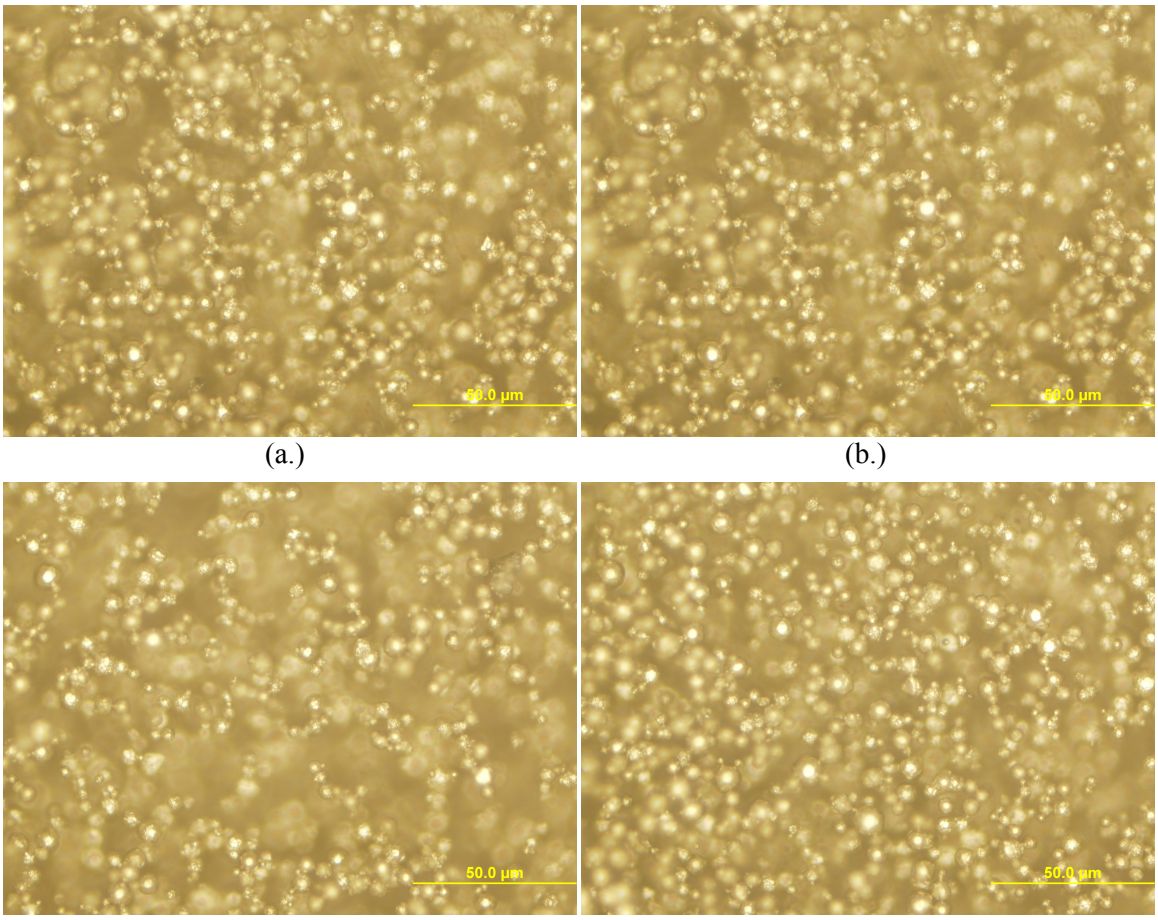

(a.) (b.)

(c.) (d.)

Figure 4.11. Optical micrographs of silicone films with 25 vol.% spherical nickel particles using vinyl-terminated poly(dimethylsiloxane)s with molecular weights of a.) 187 b.) 6,000 c.) 28,000 and d.) 62,700 g/mol.

Figure 4.11 shows films prepared using vinyl-terminated PDMS of different molecular weights filled with 25 vol.% nickel. From the optical micrographs, there does not seem to be any differences in the dispersions of nickel particles in these films, despite the varying viscosities of the vinyl-terminated PDMS. One of the major issues with optical micrographs is their depiction of two-dimensional planes of a three dimensional solid. Therefore, these optical micrographs give only impressions of dispersion in two-dimensions and do not give good impressions of overall dispersion.

Several scanning electron microscopy (SEM) images were also taken of these films. These films were not coated with gold prior to imaging. Figure 4.12 shows some of these images.

Below 25 vol.% Ni, it is difficult to take images of these films due to the high degree of surface charging (Figure 4.12a). Charging becomes less prevalent in films with higher nickel volume percent due to their higher conductivities. Figures 4.12b and 4.12c show nickel particles which show percolation throughout the film. Again, it is difficult to gather three-dimensional information from these images, but they do offer further information on the quality of dispersion.

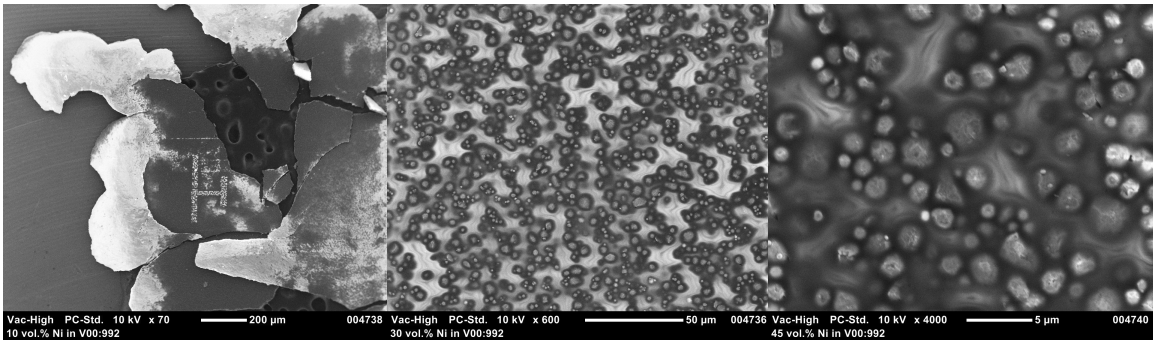

(a.) (b.) (c.)

Figure 4.12. Scanning electron microscope images of silicone films with a.) 10 vol.% Ni, b.) 30 vol.% Ni, and c.) 40 vol.% Ni.

Finally, profilometry was performed on these films to get a general idea of film thickness. This was performed by gently cutting the film with a razor and measuring the thickness between the top of the film and the surface of the test board. Figure 4.13 shows three height profiles for silicone films with various amounts of nickel particles. For the most part, all films measured were approximately 30-40 microns in thickness. There was a dependence on nickel loading volume on thickness of approximately 1 micron per 5 vol.% Ni particles, resulting in ~ 40 micron thicknesses for those samples filled with 50 vol.% Ni.

Figure 4.13. Profilometery displacement profiles for films containing a.) 5 vol.% Ni (29 µm), 20 vol.% Ni (32 µm), and 25 vol.% Ni (33 µm).

4.3.3 Effect of Nickel Particle Loading

Because of the utility of percolation theory in conductive composites, most studies performed on these types of materials are presented in terms of volume percent. For most chemists and materials scientists, the use of volume percent when describing solid materials seems counter-intuitive, since from a practical standpoint all materials used are measured in mass. For this reason, a conversion chart between % vol. and % wt. is shown in Table 4.2. Because of the density of nickel (8.9 g/mL), there is a huge disparity between % vol. and % wt., where materials with large weight fraction do not necessarily have large volume fractions. In addition to this, it should be noted that for each of the nickel particles used in this study, a constant density is assumed.

Table 4.2 Conversion table between nickel volume percent and weight percent.

% vol.	0	5	10	15	20	25	30	35	40	45	50
% wt.	0	32.4	50.5	61.8	69.6	75.3	79.7	83.1	85.9	88.3	90.2

The effect of spherical nickel volume fraction on the conductive response was initially performed using vinyl-terminated PDMS (MW = 187 g/mol) v-PDMS^{187} with hydridomethylsiloxane (MW~2,000) (HMS^{2,000}) in a 1:1 mole ratio so that the mole ratio of the reactive vinyl- and hydridosilane groups was 1:15. This vinyl-terminated PDMS was specifically chosen since it produced the "hardest" silicone film without the formation of cracks. Different mole ratios of 1:0.75 and 1:0.5 of v-PDMS^{187} and HMS^{2,000} were briefly investigated. However, films with these other ratios inevitably led to cracked films. This 1:1 mole ratio film also has the highest crosslink density of the silicone films presented, and should kinetically trap the dispersed particles after crosslinking. This film provides the basis of comparison when determining the effects of particle geometry, crosslinking molecular weight, and titania particles. For that reason, this data is reproduced several times throughout this chapter.

$$R_{app} = \Sigma R_i \approx R_w + R_c + R_{sp} + R_s \qquad \text{(Eq. 4-5)}$$

A few assumptions were made in regards to the two point probe measurements, and should be noted here. Current-voltage (I-V) curves were made, and used to calculate the measured resistance (R_{app}) using Ohm's Law and a linear fit curve, which is suitable to Ohm's Law. However, the measured resistance is not the sample resistance, but rather the sum of all possible sources of resistance in the system (Eq. 4-5). This includes the resistance of the probes (R_w), contact resistance (R_c), constriction resistance (R_{sp}) and the sample resistance (R_s). Of these, the sample resistance, being based on insulating silicones, should be much greater than the other resistances. The probe material is a good conducting metal, and should have negligible resistance. Similarly, the test boards used for this study were designed to minimize contact resistance through the use of copper foil, a good conductor. Of these, the only resistance whose magnitude cannot be speculating on is the constriction resistance which should be a property of the composite material. For this reason, it is considered an inherent part of the sample resistance.

All measurements were taken over the same gap length (r) of 63.5 microns. Therefore, the resistivity can be calculated by multiplying a factor of $2\pi r$ ($\sim 4 \cdot 10^{-4}$ m) using Eq. 4-4 (p. 94). However, for this study, the measured resistance was used for data plots rather than resistivity (the material property) since it more directly reflects the measurements and also scales directly with resistivity. For this reason, the trends observed in the plots and the percolation thresholds calculated are the same as those found in plots of nickel volume fraction and resistivity. Since the change in resistance with respect to nickel volume fraction is several orders of magnitude, plots are given in log scale. Finally, percolation thresholds were calculated by fitting a 4^{th} order polynomial curve and deriving the inflection point of this curve, which is the traditional manner[20] in which percolation thresholds are derived.

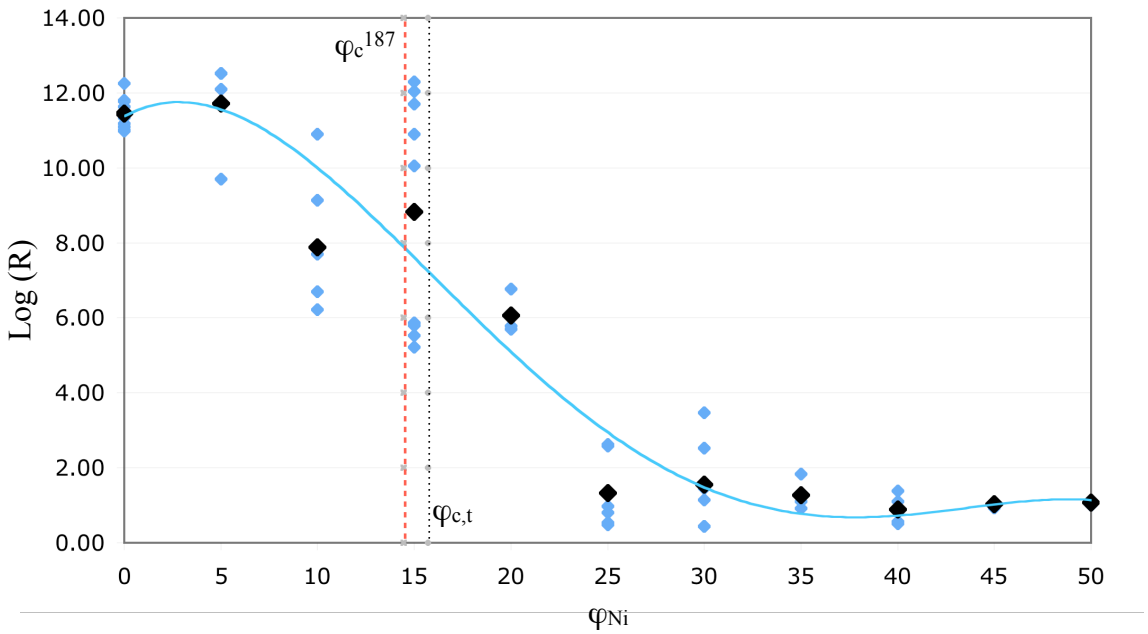

Figure 4.14. Effect of spherical nickel particle volume fraction (φ_{Ni}) on the measured resistance plotted in log scale. The theoretical percolation volume fraction ($\varphi_{c,t}$) of 15.7 and the experimental percolation volume fraction (φ_c^{187}) of 14.44 are plotted as the rightmost vertical line and the leftmost vertical line, respectively. A trend line has been added for convenience.

Figure 4.14 shows the resistance of these silicone composite films as a function of the spherical nickel particle volume fraction. The logarithm of the measured resistance is used to due to the large changes in the measured resistance. A fourth order polynomial was fit to the raw data with a coefficient of determination (R^2) of 0.875. From this polynomial, a percolation threshold for the system using vinyl-terminated PDMS (MW~187), (φ_c^{187}), was determined by taking the second derivative and setting it to zero (determination of an inflection point). The percolation threshold was determined to be 14.44, which is slightly lower than the theoretical value of 15.7. However, given the non-uniformity of the spherical nickel particles, some deviation from theory is probable and expected.

Samples prepared in proximity to the percolation threshold show the highest degree of deviation from the trend, particularly with samples containing 15 vol.% nickel. The percolation threshold defines that a continuous path is observed throughout a sample, but this doesn't preclude the existence of small number of particles forming non-connected chains. For this

reason, there is a finite probability that given a finite area (i.e. the area over which measurement is taken) that a continuous path may be present which does not extend across the width of the entire composite film. Furthermore, the slightest differences in dispersion can produce very different properties in close proximity to this percolation point.

Regardless, there is a drop in resistance several orders in magnitude that occurs above the percolation threshold with increasing nickel volume fraction. The resistance measured of the composite films with nickel volume fractions above 25 vol.% Ni remains fairly constant, but the resistivity of these films remain approximately an order of magnitude higher than that of the dry nickel powder. This is attributed to the effects of the silicone matrix which should add some resistance due to electron tunneling through the silicone at the nickel interface. The trend in Figure 4.12 closely resembles the percolation of homogeneously dispersed particles in a matrix with a deviation of 8% from the theoretical value. This also provides indirect evidence suggesting that these composite films are homogeneous with good dispersion.

4.3.4 "Priming" Effect and Two Layer Systems

An unusual effect is seen in these films even those with high volume fractions of nickel particles which was not mentioned in the previous section. Simply, none of these films show conductive responses until a certain voltage is exceeded, after which the films properties remain constant. Figure 4.15 shows six consecutive current-voltage sweeps of a silicone film containing 50 vol.% nickel. According to Figure 4.14, one would assume these films are quite conductive. However, Figures 4.15a-d show no conductive response for a film of this type. These I-V curves show "negative" current of 0.01 nanoamps. This is effectively zero and the negative response is attributed to the lack of sensitivity of this device at such low currents. However, Figure 4.15e gives the first upward sweep of this curve which shows a sudden change in conductive properties once 38V is reached (100 mA is the maximum measurable current). This "turning on" has been termed[37] the "priming effect". After this priming effect, the electrical properties of these films remains constant. Films of 50 vol.% Ni are quite conductive after this priming effect occurs (Figure 4.15f).

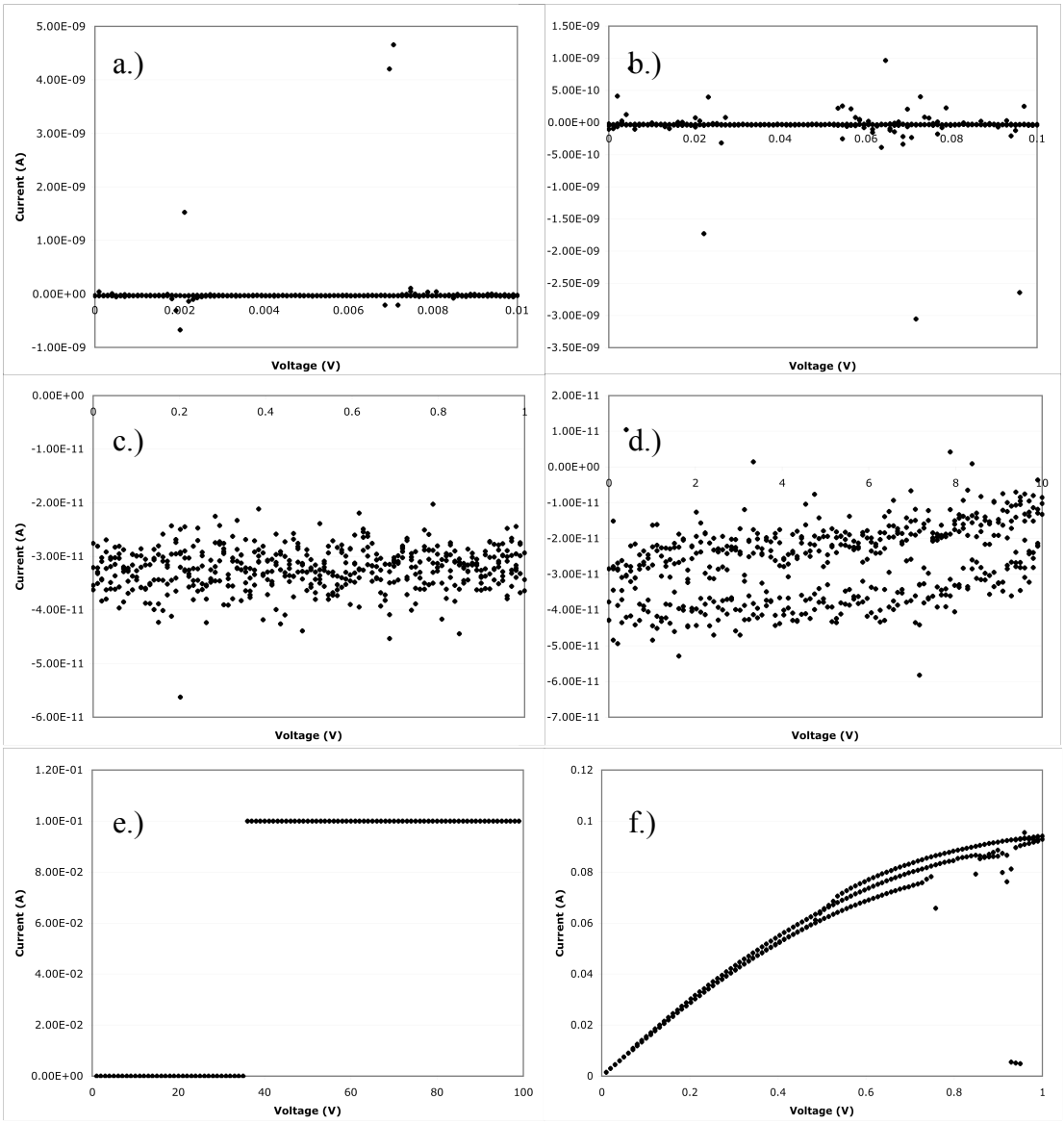

Figure 4.15. Consecutive current-voltage (I-V) curves of a silicone composite film with 50 vol.% spherical nickel particles with three sweeps over voltage ranges of a.) 0 to 0.01 V, b.) 0 to 0.1 V, c.) 0 to 1 V, d.) 0 to 10 V, e.) 0 to 100 V (only the first upward sweep is shown), and f.) 0 to 1 V.

Because of this, all properties of films reported are those after priming at which point the properties are constant. However, it is curious that such an effect should exist at all, especially in films with particularly high nickel volume fractions. This sudden change from non-conductive to its final conductive state suggests some sort of change in the film. Given the "softness" of silicones, it is possible for the particles to be mobile in the film to create more effective

conductive paths in the film. While this theory is not completely dismissed, if this were the case a greater change in films with low nickel particle volume fractions should be observed. Also, it would be expected that the electrical properties of the film after priming should also change as the particles continue to move. However, neither of these effects is observed.

$$Q \propto I^2 \cdot R = R^3/V^2 \qquad \text{(Eq. 4-6)}$$

Still, movement of particles is still a probable occurrence in silicone films. Passing current through a material with a resistance produces heat in a process called Joule heating, also known as Ohmic heating or resistive heating. The heat produced is proportional to the resistance of the material and the current which is passing through the material (Eq. 4-6). Heat produced this way could be softening the silicone matrix and allowing the kinetically trapped particles to become slightly mobile. Silicones have a thermal expansion coefficient (α) ranging from 30-300 ppm/K (Table 1.2). While it is uncertain what the actual role of Joule heating in these films may be, it would explain the mobility of particles in these composites and the priming effect.

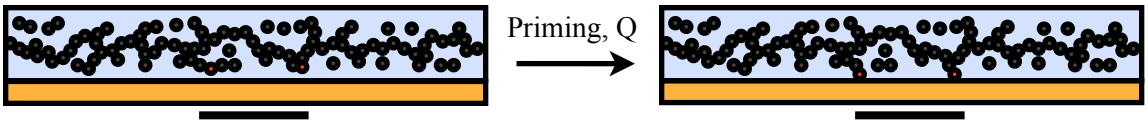

Figure 4.16. Scheme for the proposed mechanism for the priming effect of conductive silicone composite films, in which nickel particles (red) move through a silicone-rich interfacial layer to create a conductive path which connects the two points over the measurement gap (black bar).

However, given that the final properties of these films do not change after priming, and no current is measured passing through the material prior to priming, this effect is believed to be interfacial in nature. Figure 4.16 (drawn to scale) gives a proposed mechanism for the priming of these films. Prior to the priming of these films, there exists a nickel depletion layer at the test board-film interface which is entirely silicone. Since silicone is known for its low surface energy, an interfacial layer of silicone would not be surprising. Because of this depletion layer, even when percolation of the bulk material is apparent, a current cannot pass through this material since the silicone is a good insulator and will not allow current to pass into the bulk of the

material. With application of an increasing voltage, the interface begins to locally heat, allowing for a nickel particle to move through this depletion layer. At a certain point, the nickel particle comes into contact with the probe and creates a direct path for the current to move through the bulk of the material.

The concept of an interfacial particle depletion layer is not without precedence. A great deal of theoretical work has been performed in describing the density of particles in a composite at hard wall interfaces.[38-41] In each of these cases, a low particle density depletion layer is predicted with a thickness on the order of magnitude of the radius of the hard sphere. Entropic effects are given as the origin of this depletion layer, as the confinement of a particle at a hard wall-liquid interface is not entropically favorable, and work is required to increase move particles to the hard wall interface. No further work was done in this study to validate the arguments proposed by other authors, but the experimental observations noted here seem consistent with these previous reports.

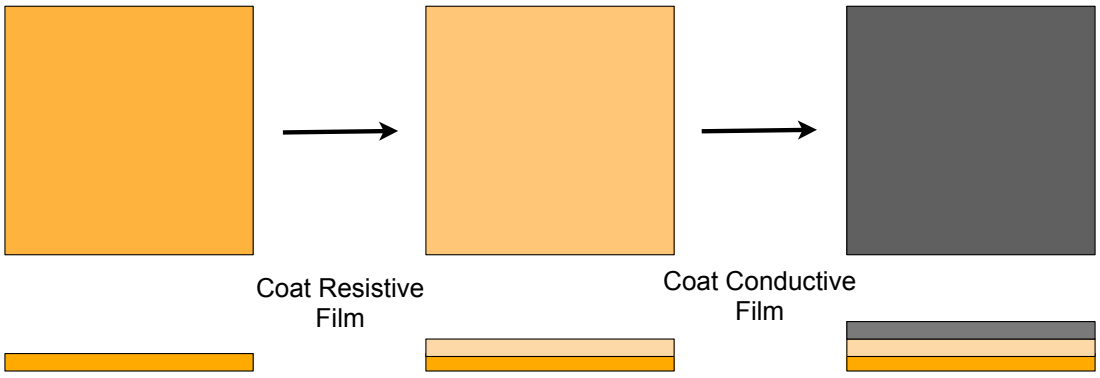

Figure 4.17. Scheme of stacked silicone layer (two-layer) systems.

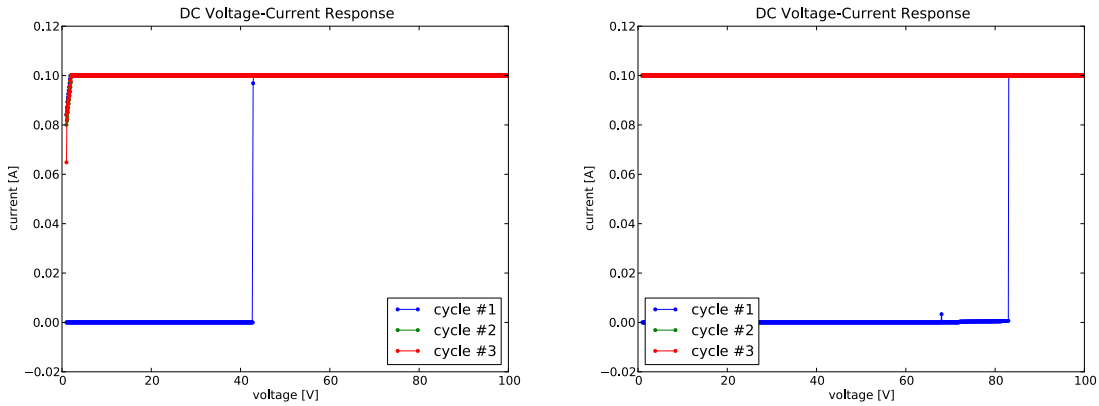

Figure 4.18. Current-voltage curves for a two layer systems of a.) a silicone film containing 25 vol.% spherical nickel particles coated over a 19.6 μm thick pure silicone film, and b.) a silicone film containing 25 vol.% spherical nickel particles coated over a 27 μm thick silicone film containing 5 vol.% titania.

To investigate this priming process, two layer systems were developed in which a conductive film is coated over a non-conductive film. Figure 4.17 gives a depiction of this process. Current-voltage curves (not shown) indicated no conductive response even after the application of 100 V. The thickness of these films was measured by profilometry to be approximately 20 microns in thickness, which is slightly larger than the particle sizes. Samples of this kind exhibited the same priming effect as single layer systems. Figure 4.18 gives current-voltage curves for two such systems. These results indicate that the nickel particles must move through the silicone layer in order to establish contact with test board surface. It is not believed that the silicone is conducting, since the voltages used in this study are well below the reported breakdown voltage of PDMS. While this offers an explanation for the drastic change in properties that is observed in these systems upon the application of high voltages, no direct evidence for a depletion layer was established. Nor was the effect of heating these films to high temperatures investigated.

4.3.5. Effect of Nickel Particle Geometry.

The effect of nickel geometry was investigated by comparing the results of spherical surfaces with those using both nickel flakes and nickel wires. Figure 4.19 shows the electrical

responses of these samples. Similar to the films containing spherical particles, fourth order polynomials were fit to the data for samples with flakes and wires with coefficients of determination of 0.94 and 0.99, respectively. From these, percolation thresholds for films prepared using vinyl-terminated PDMS (MW~187) with nickel flakes ($\varphi_{c,flakes}^{187}$) and wires ($\varphi_{c,wire}^{187}$) were determined to be 1.59 and 4.24, respectively.

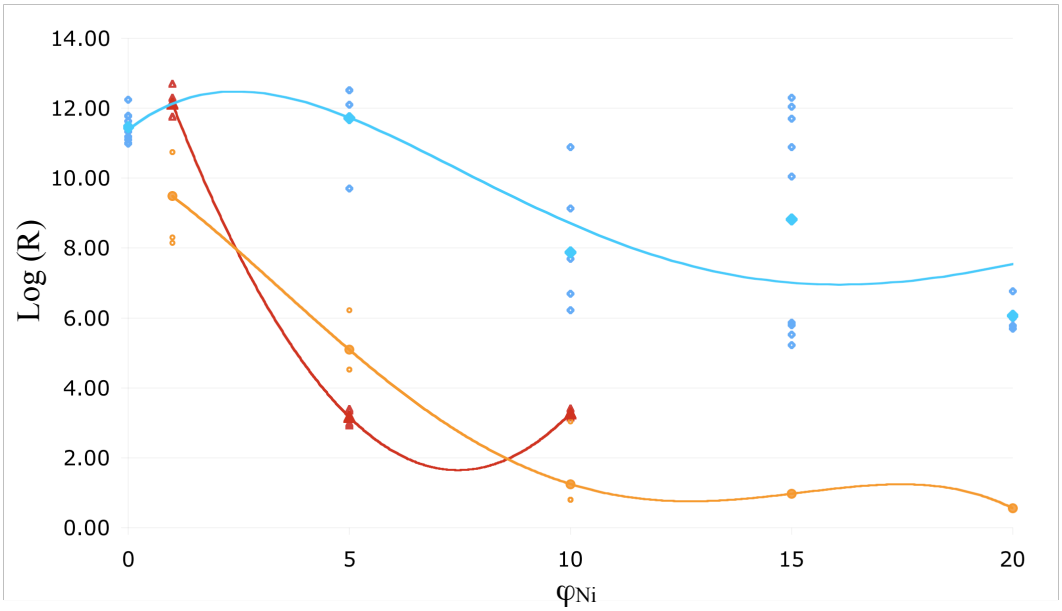

Figure 4.19. Effect of nickel particle geometry on the electrical resistance of a silicone composite film using spherical nickel particles (diamonds), nickel flakes (circles), and nickel wires (triangles) in which the solid shapes are average values of individual samples (open shapes). Trend lines have been added for convenience.

As expected, increasing the aspect ratio of the nickel particle greatly decreases the percolation of these samples. These results are in good agreement with previous reports using particles with different aspect ratios.[26] Simply, particles with higher aspect ratios have a higher probability of forming contacts in a given material, thereby decreasing the percolation threshold. This drop in percolation threshold with increasing aspect ratio is believed to be solely an effect of the geometry of the particle and not affected by how well other geometries conduct electricity.

4.3.6 Effect of Crosslinking Molecular Weight

Silicone films were made using vinyl-terminated PDMS with different molecular weights to affect the crosslink density of the prepared film. Percolation theory is not affected by the matrix material, and films with different material properties should exhibit the same electrical properties as those presented early in this chapter. Figure 4.20 shows the electrical resistance of silicone films with different nickel volume fractions.

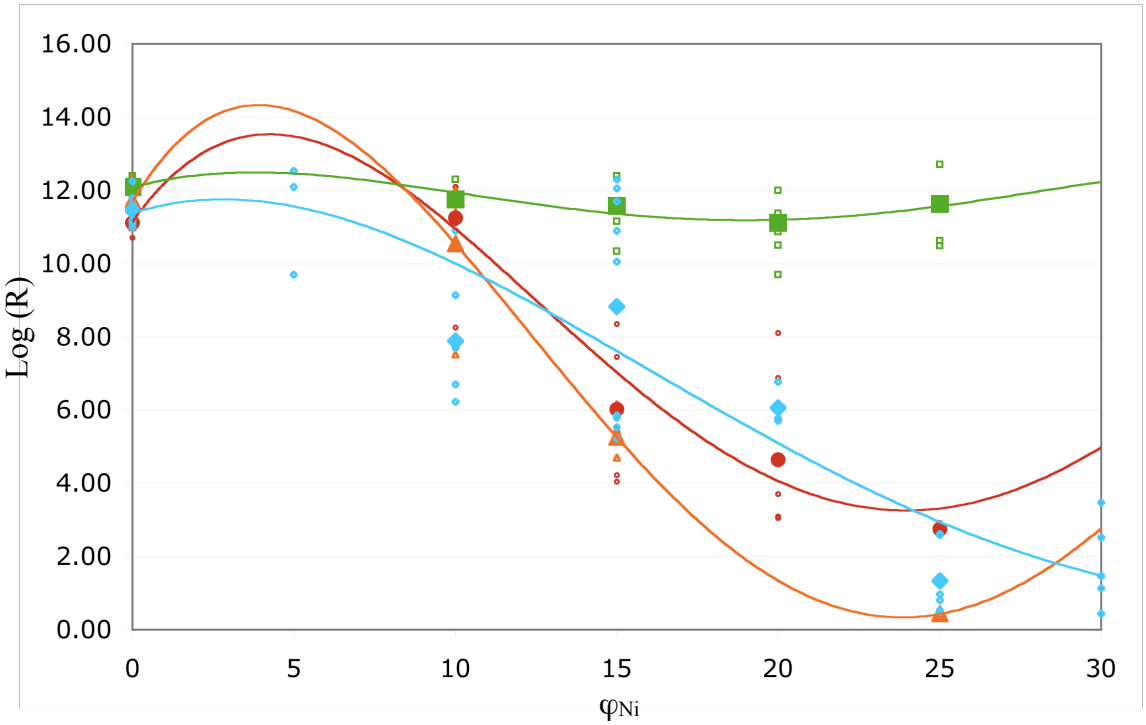

Figure 4.20. Effect of vinyl-terminated poly(dimethylsiloxane) molecular weight on electrical resistance a silicone composite film containing spherical nickel particles where the molecular weight is 187 (diamonds), 6,000 (triangles), 28,000 (circles), and 62,700 (squares) g / mol. Closed objects are averages of individual samples. Trend lines have been added for convenience.

Table 4.3. Nickel volume fraction percolation thresholds and log (Resistance) for nickel volume fractions of 50 for silicone films using different molecular weights of vinyl-terminated PDMS.

MW (g/mol)	187	6,000	28,000	62,700
η (cSt.)	0.7	100	1,000	10,000
φ_c	14.44	12.13	12.06	$30 < \varphi_c < 50$
Log (R), φ_{50}	1.07	1.51	0.45	0.65

The films presented in Figure 4.20 were prepared using 1:1 mole ratios of hydridomethylsiloxanes and vinyl-terminated PDMS of different molecular weights. Qualitatively speaking, increasing the molecular weight increases the "softness" of the film. This is due to a decrease in the crosslink density and increase in average crosslink molecular weight. Coefficients of determination for the fitted fourth order polynomials were 0.875, 0.84, 0.95, and 0.94 in order of increasing molecular weight. With the exception of those samples prepared using the v-PDMS with a 62,700 g/mol molecular weight, there appears to be only a slight change in the calculated percolation threshold. If any trend is to be claimed, there is a slight decrease in percolation threshold, though it does not appear to be significant. Table 4.3 gives calculated percolation thresholds and resistances for a nickel volume fraction of 50, which is not shown in Figure 4.20.

The deviation from the expected results for samples prepared using v-PDMS (MW = 62,700 g/mol) is attributed to the high viscosity of this silicone fluid and the greater difficulty in dispersion. If a homogeneous dispersion was not initially formed, these samples should not follow traditional percolation theory. This may also be an effect of the nickel depletion layer. For the high viscosity PDMS, it may be more difficult for a nickel particle to cross this depletion layer to make contact with the test board surface.

4.3.7 Effect of Titania Nanoparticles

The effects of adding titania nanoparticles into nickel-silicone composite films was investigated. It was initially believed that these three-component composites would offer a way to carefully control the electrical properties of a film, or to make voltage-switchable coatings. However, it was found that anatase titania has a fairly high resistance, and acts more as an insulator in these systems than a semi-conductor. Figure 4.21 gives the resistance of nickel-silicone composite films with different volume fractions of titania added to them. From this data, it appears that the addition of titania particles greatly increases the resistance a the composite film. Log scale resistances for composites films with 50 vol.% spherical nickel particles are 1.07, 3.65, 2.60 for titania volume fractions of 0, 0.01, and 0.05, respectively. The difference in

resistance between films prepared with volume fraction of 0.01 and 0.05 is attributed to the difficulty in preparing homogeneous binary dispersions with such high particle volume fractions, and these samples were not completely homogeneous. While the log scale resistances decrease slightly at 50 vol.% nickel, they are still much higher than those films without titania particles.

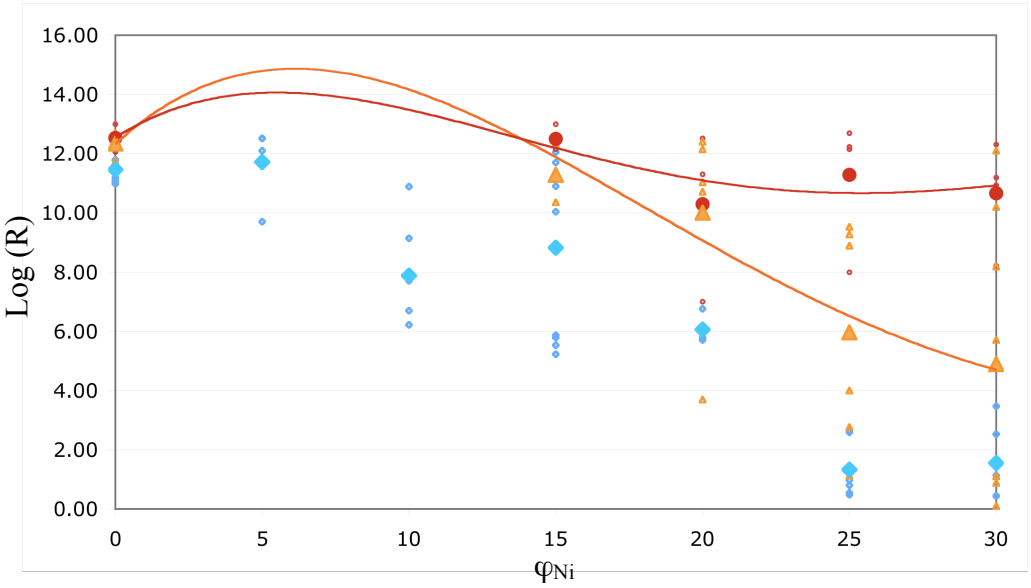

Figure 4.21. Effect of titania volume fraction on electrical resistance of nickel-silicone composite film containing spherical nickel particles where the titania volume fraction is 0 (diamonds), 0.01(circles), and 0.05 (triangles). Closed objects are averages of individual samples. Trend lines have been added for convenience.

It is common to attempt to imagine these films as nickel particles in a titania/silicone matrix, and it was with that outlook that these films were originally prepared. However, this view is not entirely accurate since it does not fully express the nature of the system. Percolation of systems with binary mixtures of two different filler materials has seen very little work due to the system complexity. Binary mixtures of particles in suspensions may undergo unexpected phenomena such as coaggregation.[12] It has been proposed by others that small particles prevent percolation by inserting themselves between the larger particles in what is known as the "hard-core, soft skin" model.[42] For this reason, it is difficult to determine the quality and homogeneity of dispersion for such systems. Furthermore, the addition of nanoparticles into these mixtures

greatly increases the viscosity of the silicone composite making it more difficult to create homogeneous dispersions and even coatings. Regardless, it appears that even a small volume fraction of titania can have a profound impact on the properties of these films and prevent electrical conductance.

4.4 Conclusions

Silicone-nickel composite films follow traditional percolation phenomena found in most conductive composite systems. A shift in electrical properties of these films from non-conductive to a constant electrical response after application of high voltages may be caused by a nickel depletion layer which exists at the film-test board interface, and is overcome by the movement of the nickel particles upon local heating of at the interface. The use of nickel particles with higher aspect ratios was found to decrease the percolation threshold. Increase of vinyl-terminated PDMS in the preparation of these films was found to have little effect on the electrical properties of the prepared film but does make dispersion of the particles much more difficult. Finally, the addition of titania nanoparticles decreases the conductive response typically seen for samples with nickel volume fraction above the percolation threshold and may indicate more complex material interactions than the binary systems.

4.5 References

1. Chatterjee, A.K., Industrial Ceramics, 2011, 31, 1-13.
2. Farrokhpay, S., Adv. Coll. Interf. Sci., 2009, 151, 24-32.
3. Bian, P., McCarthy, T.J., Langmuir, 2010, 26, 6145-6148.
4. Holm, C., Weis, J.J., Current Opinion Coll. Interf. Sci., 2005, 10, 133-140.
5. Rochow, E.G., Introduction to the Chemistry of the Silicones. J. Wiley & Sons, Chapman & Hall: New York, London, 1946.
6. Zhou, W.Y., Qi, S.H., Tu, C.C., Zhao, H.Z., Wang, C.F., Kou, J.L., J. Appl. Polym. Sci., 2007, 104, 1312-1318.
7. Sau, K.P., Khastgir, D., Chaki, T.K., Die Angewandte Makromol. Chemie, 1998, 258, 11-17.

8. Ausanio, G., Barone, A.C., Campana, C., Iannotti, V., Sensors and Actuators A, 2006, 127, 56-62.

9. Kim, J.A., Lee, S.H., Park, H., Kim, J.H., Park, T.H., Nanotechnology, 2010, 21, 165102.

10. Schaer, E., Guizani, S., Choplin, L., Chemical Engineering Science, 2006, 61, 5664.

11. Zhou, J., Ralston, J., Sedev, R., Beattie, D.A., J. Coll. Interf. Sci., 2009, 331, 251-262.

12. Smith, W.E., Zukoski, C.F., J. Colloid Interf. Sci., 2006, 304, 359-369.

13. Thomas, D.N., Judd, S.J., Fawcett, N., Wat. Res., 1999, 33, 1579-1592.

14. Gregory, J., Advances in Coll. Interf. Sci., 2009, 147-148, 1

15. Sudduth, R.D., Pigment & Resin Tech., 2008, 37, 375-388.

16. Koleske, J.V., ed., Paint and Coating Testing Manual: 14th edition of the Gardner-Sward Handbook, American Society for Testing and Materials, Ann Arbor, 1995.

17. Daniel, F.K., Goldman, P., Industrial and Engineering Chemistry, Analytical Edition, 1946, 18, 26.

18. Genovese, D.B., Adv. Coll. Interf. Sci., 2012, 171, 1-16.

19. Ruschau, G.R., Yoshikawa, S., Newnham, R.E., J. Appl. Phys., 1992, 72, 953-959.

20. Kirkpatr, S., Reviews of Modern Physics, 1973, 45, 574-588.

21. Bunde, A., Dieterich, W., J. Electroceramics, 2000, 5, 81-92.

22. Nan, C.-W., Shen, Y., Ma, J., Annu. Rev. Mater. Res., 2010, 40, 131-151.

23. Zallen, R., The Physics of Amorphous Solids, John Wiley & Sons, New York, 1983.

24. Machavariani, V.Sh., J. Phys.: Condens. Matter, 2001, 13, 6797-6812.

25. Cai, W-Z., Tu, S-T., Gong J-M., J. Composite Mater., 2006, 40, 2131-2142.

26. Yi, J.Y., Choi, G.M., J. Electroceramics, 1999, 3, 361-369.

27. Schroder, D.K., Semiconductor Material and Device Characterization, John Wiley & Sons, New York, 1990.

28. Hofmann, Ph., Wells, J.W., J. Phys.: Condens. Matter, 2009, 21, 013003.

29. Mark, J.E., ed., Polymer Data Handbook, Oxford University Press: New York; 1999.

30. Essen, L., Froome, K.D., Proc. Phys. Soc. B., 1951, 64, 862-875

31. Salah, N.H., Bouhelassa, M., Bekkouche, S., Boultif, A., Desalination, 2004, 166, 347-354.

32. Gray, D.S., Tien, J., Chen, C.S., Adv. Mater., 2004, 16, 393.

33. Zhang, J., Feng, S.Y., Ma, Q.Y., J. Appl. Polym. Sci., 2003, 89, 1548-1554.

34. Doi, M., Kawaguchi, M., Kato, T., Colloids and Surfaces A: Physiochem. Eng. Aspects, 2002, 211, 223-231.

35. Sun, Y., Gu, A., Liang, G., Yuan, L., J. Appl. Polym. Sci., 2011, 121, 2018.

36. Lide, D.R., ed., CRC Handbook of Chemistry and Physics, 75th ed., CRC Press, Inc., Ann Arbor, 1994.

37. Personal correspondence with Robert Fleming, Shocking Technologies, San Jose, CA.

38. Balberg, I., Binenbaum, N., Physical Review B, 1987, 35, 8749-8752.

39. Buzzacchi, M., Pagonabarraga, I., Wilding, N.B., J. Chem. Phys., 2004, 121, 11362-11373.

40. Siderius, D.W., Corti, D.S., Physical Review E, 2005, 71, 031641.

41. Siderius, D.W., Corti, D.S., Physical Review E, 2007, 75, 011108.

42. Siderius, D.W., Corti, D.S., Physical Review E, 2011, 83, 031126

43. Balberg, I., Binenbaum, N., Physical Review B, 1987, 35, 8749-8752.

CHAPTER 5

DEWETTING FROM SUPERHYDROPHOBIC SURFACES: MICROCAPILLARY BRIDGE RUPTURE AND ITS APPLICATIONS

5.1 Introduction

5.1.1 Background

Many of the basic concepts regarding wetting phenomena and contact angle hysteresis were discussed in the introduction of this dissertation (Chapter 1). Briefly, the study of wetting was initiated by Thomas Young in 1804[1] and has since grown to study all variety of surfaces. One of the most popular areas of this field deals with superhydrophobic surfaces. There has been a great deal of confusion with regards to the classification of these surfaces,[2] but the most useful characterization and classification of a surface is its advancing (θ_A) and receding (θ_R) contact angles. These two contact angles represent a finite range of contact angles which can formed upon a given surface. The difference between these two contact angles is known as hysteresis. A great deal of confusion has arisen due to contact angle hysteresis, particularly due to the work of Wenzel[3] in 1936 and Cassie and Baxter[4] in 1944, and this confusion has been previously addressed,[2,5] and will not be further discussed here.

The advancing and receding contact angles define the specific conformations necessary for a sessile droplet to move across a surface. When a sessile water droplet moves on a solid surface, the drop must either advance or recede at every point on the three phase solid/liquid/vapor contact line.[6] For this droplet to move, a force must be applied to either the drop or the surface, and this force is typically a gravitational field (Figure 5.1a). A droplet at rest on a surface is in the shape of a section of a sphere. When the surface is tilted (a gravitation field is applied), the droplet must contort its shape from a sphere to a section of a tapered ellipsoid. When the surface is tilted enough for motion (sufficient force is applied) the drop generally slides with a constant, reproducible shape, with a receding contact angle formed at the uphill-most point on the

three phase contact line and an advancing contact angle formed at the downhill-most point on the three phase contact.

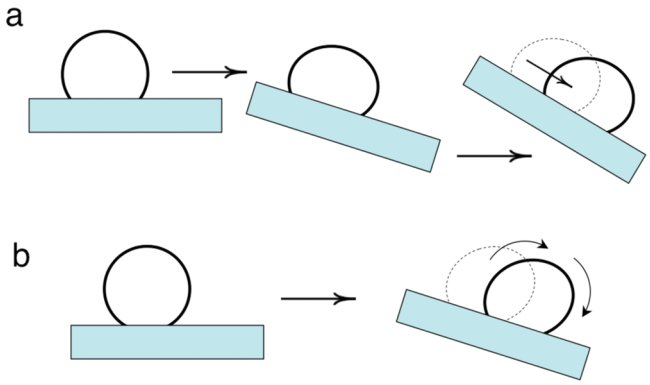

Figure 5.1. Two-dimensional representations of a drop a.) sliding and b.) rolling on a surface.[7]

Two-dimensional representations, such as Figure 5.1, do not capture the entire process of this motion, and there is a variety of contact angles ranging from a little lower than the advancing contact angle to a little more than the receding contact angle which form along the droplet perimeter.[8,9] Despite this complexity, the events which occur at the downhill-most point and the uphill-most point are nearly identical to those which occur during advancing and receding contact angle measurements (Figure 1.6), respectively. For this reason, both advancing and receding contact angles can be measured on a surface which does not need to be tilted.

Topography can have a profound effect on the measured contact angles.[10,11] Molecular topography, or lack of topography, can be used to control and eliminate contact angle hysteresis[10-12]. On surface with physical features, such as posts, the surface can distort and destabilize the contact line, producing contact angles which can exceed 150. Production of these exceptionally high contact angles was inspired by the lotus leaf,[13] and represents the behavior which is now commonly called "superhydrophobicity".[14-16] The mechanism for motion on a superhydrophobic surface is different than that of smooth surfaces. Whereas droplets typically slide across a smooth surface (Figure 1a), they roll on a superhydrophobic surface (Figure 1b).

For traditional superhydrophobic surfaces which contain some kind of regularly ordered posts, the advancing contact line does not advance, but rather propels the droplet forward by

creating new contact lines as the liquid-vapor interface of the droplet descends on the next topographic feature in a concerted fashion. In simpler terms, as the droplet "leans" forward, the surface of the droplet comes into contact with the next post (or "falls down" on it). Because the macroscopic advancing contact angle is so high, one can view this as the droplet interface coming almost directly down onto an adjacent post and spontaneously wetting the top of the post surface. The post surface is spontaneously wet since the contact angle of the macroscopic drop is typically much higher than the microscopic contact angles for the post surface, and already in a conformational state to advance across the top of the post.

The receding contact line events are different than the advancing contact line events. This difference in events is normal, and mechanisms for advancing and receding are typically not the opposites of each other. For the contact line to recede across a structured surface, disjoining events must occur between the liquid and the tops of the post surface in concerted events. Again, the macroscopic conformation (θ_R) is much higher than the microscopic contact angle of a post surface. Therefore, the receding contact line slides only slightly across the microscopic post and the droplet must simply detach itself from the post surface during the receding process.

While it is stated here that a sliding mechanism is typical for smooth surfaces, and a rolling mechanism is typical for a superhydrophobic surface, these two mechanisms represent the extremes of droplet motion and in reality a mixture of the two processes is probably more normal for most prepared surfaces.[8,9] These events at the receding and advancing contact line can also be concerted, synchronous, or sequential, and the events at the receding contact line do not depend on the events at the advancing contact line, but for the entirety of the droplet to move, both events must occur.

Because advancing and receding contact angles are conformations of kinetic movement, these values indicate the degree to which a droplet must distort in order to move. Contact angle hysteresis and its causes were considered in detail ~70 years ago[17] and were equated to the force required for drop motion ~50 years ago.[18,19] Without hysteresis ($\theta_A = \theta_R$), the droplet does not have to contort its shape from a section of a sphere to move or during movement, and no force is

required to move the drop. Many surface of this kind have been prepared,[11,12,20] and the causes for hysteresis on smooth surfaces has been previously discussed in detail.[8,9,21,22]

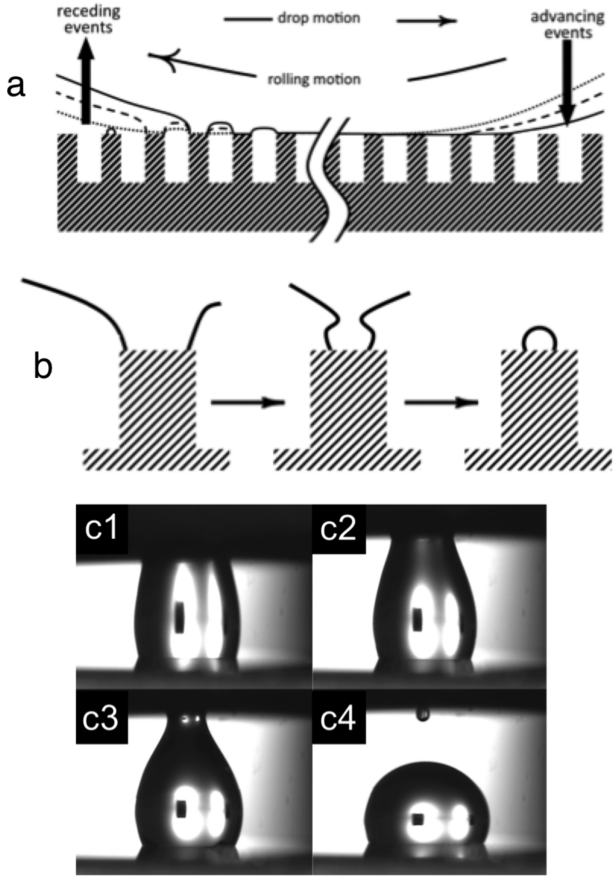

Figure 5.2. (a.) Depiction of a drop exhibiting high advancing and receding contact angles and rolling on a surface containing posts. (b.) Capillary bridge rupturing from a post surface during a receding event at the contact line. (c.) Selected frames from a movie of a capillary bridge rupturing as two smooth hydrophobic surfaces are separated.[12,23]

Despite the great deal of study already performed on both smooth and superhydrophobic surfaces to understand the mechanisms for advancing and receding contact lines, it was not until more careful analysis of selected frames from a movie of a capillary bridge rupture (Figure 5.2c) that a more careful consideration of the depinning mechanism of liquids from superhydrophobic surfaces was deemed necessary. Figure 5.2a depicts a droplet rolling across a superhydrophobic surface containing posts. Since the receding contact angles very high, from the vantage point of the post top, the liquid appears to be removed in an almost tensile manner during droplet

detachment (Figure 5.2b). If this is the case, the liquid must undergo a capillary bridge failure. In capillary bridge failures, a droplet is left behind upon disruption of the bridge.

A droplet left behind after capillary bridge rupture can be seen in Figure 5.2c, in which two hydrophobic surfaces are brought into contact and then separated. Image c4 shows this tiny droplet clearly on the upper surface. For this reason, it is believed that small μL-sized water droplets are continuously left behind during the recession process of a water droplet across a superhydrophobic post surface due to the disjoining of liquid from these posts. However, no water droplets have ever been viewed on post surfaces of these kinds. This is attributed to the known rapid evaporation of microliter-sized water droplets.[24]

Recently, Reyssat and Quéré[25] and Mognetti and Yoemans[26] have referred to "pinning events" as the cause of hysteresis and described possible shapes of menisci that may form at receding contact lines, and resemble early capillary bridge formation. Also, several reports have been made which may indicate the existence of these droplets.[27-31] In 1950, Bikerman[27] described "ribbons" that were stretched and finally ruptured. Fort,[28] in 2002, predicted that any experiments designed to observe water "left behind" would fail. Li, Ma, and Lan[31] observed a "dark stripe" in a high speed video recording and attributed this to a "liquid layer being left behind on the microposts" due to the "pinch-off of liquid threads." This would be consistent with a microcapillary bridge rupture.

It would seem that to experimentally verify the existence of droplets left behind, the use of a non-volatile, high surface tension liquid would need to be used to replicate this mechanism without the evaporative problems associated with water. Ionic liquids have found many applications over the last decade.[32-35] Ionic liquids have been used as high surface tension liquids which exhibit no vapor pressure.[33,34] Ionic liquids have also been used as imaging fluids for submicrometer-scale chemical patterns on smooth surfaces.[35] For these reasons, ionic liquids seem especially suited as probe fluids for high-vacuum analytical techniques.

Although not experimentally addressed in this work, post surface geometry should greatly affect the disjoining mechanism of liquids and have profound effects on the receding contact

angle. The effects of curvature and topography on contact line pinning has been discussed in some detail[23,36]. Figure 5.3 gives two post surfaces with identical Cassie area fractions and Wenzel roughness ratios, but the sign of curvature is the opposite of the other. For discussion, the post surfaces are a material that exhibit a receding contact angle of $\theta_R = 90°$. A tensile force pulls the liquid from each of the post surfaces. For the pillar with positive curvature (left), this tensile action forces the receding contact line to an angle less than the microscopic receding contact angle of 90°. This geometry can be seen to "help" the depinning process, and surfaces of this type would be expected to have higher receding contact angles. On the other had, a tensile force on pillars with negative curvature will attempt to force the contact line to a contact angle higher than 90°, and cause greater adherence to the pillar top. Surfaces with this geometry should exhibit lower receding contact angles. Furthermore, a droplet left on a pillar with negative curvature will most likely have a larger volume than one on a pillar with positive curvature.

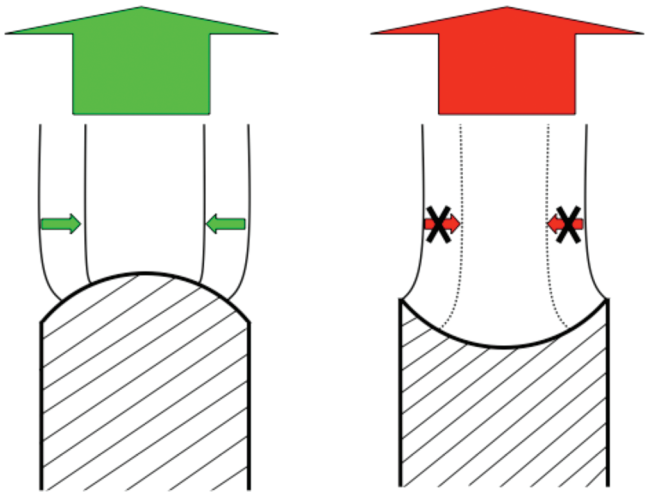

Figure 5.3. Capillary bridges on posts made of a material that exhibits a receding contact angle of 90°. Tensile force (upward) on the capillary bridge attached to the post with positive curvature (left) forces the contact angle to a lower value and the contact line to recede. An upward tensile force on the post with negative curvature (right) forces the contact angle to a higher value.

Finally, there are two general prejudices typically associated with contact angle hysteresis. The first is that hysteresis is an attribute of a "bad" surface. There are no "bad" surfaces, and each is special in its own way. In reality, hysteresis is a normal aspect of all

surfaces and should be exhibited by all but a select few specially prepared surfaces. The second general prejudice is that hysteresis exists purely as a philosophical argument without any proper applications. This is simply not true. Contact line hysteresis and the receding contact line depinning of liquids from solid surfaces do have useful applications, and this is discussed later in this chapter.

5.1.2 Objectives

The objectives of this work were to use ionic liquids to investigate the mechanism of liquids dewetting a regularly ordered, pillared surface. Ionic liquids are particularly useful in high vacuum analytical techniques, such as scanning electron microscopy, due to their lack of vapor pressure. In addition to this, ionic liquids with high surface tensions are commercially available. It was also the objective of this work to demonstrate the utility of this dewetting processes for the fabrication of uniform arrays of crystals.

5.2 Experimental Section

5.2.1 Materials

Regularly ordered, pillared surfaces with staggered rhombus posts with major and minor axes of 6 microns and 3 microns, respectively, and 40 micron height were prepared in a square array using photolithography from a previously reported manner.[37] Tridecafluoro-1,1,2,2-hydrooctyldimethylchlorosilane was purchased from Gelest, Inc. Dimethylbis(β-hydroxyethyl)ammonium methanesulfonate (N+S-) was received from Evonik. Sodium chloride, magnesium chloride, sucrose, and ethanol were purchased from Fisher Chemical. Poly(ethylene glycol) (Mn ~ 300 g/mol) was purchased from Aldrich.

5.2.2 Procedure

The post surfaces were hydrophobized through the vapor phase using tridecafluoro-1,1,2,2-hydrooctyldimethylchlorosilane for 72 hours at 70 °C. After this surface modification, the samples were rinsed using toluene, acetone, and water (in that order) and dried under nitrogen.

Contact angles were measured on these surfaces using water, and then dried under nitrogen. Afterward, contact angles were measured using the ionic liquid, (N^+S^-), rinsed thoroughly with water, and dried under nitrogen. Ionic liquids are miscible in water, and this should remove any residual ionic liquid after contact angles were measured.

For a majority of the samples, the surfaces were then dipped into the ionic liquid or other solution and removed at rate of approximately 1 cm/s such that the surface was perpendicular to the liquid-vapor interface. For a few samples, a droplet of the ionic liquid was placed on the surface and allowed to roll across it. All samples were then analyzed using scanning electron microscopy.

5.2.3 Characterization

Advancing and receding contact angles (θ_A / θ_R) of water and dimethylbis(β-hydroxyethyl)ammonium methanesulfonate were taken using a Ramé-Hart telescopic goniometer in the manner described in Chapter 1. Scanning electron microscopy was performed on these surfaces using a JEOL NeoScope JCM-5000 scanning electron microscope.

5.3 Results and Discussion

5.3.1 Dewetting Mechanism of Ionic Liquids from Superhydrophobic Surfaces

The structure of dimethylbis(β-hydroxyethyl)ammonium methanesulfonate (N^+S^-) is shown in Figure 5.4a. This ionic liquid has a previously reported[36] surface tension of 66.4 dyn/ cm, and exhibits no volatile components, making it especially suited for scanning electron microscopy. Surfaces with staggered rhombus posts (Figure 5.4b) treated with a fluorinated silane exhibited contact angles of θ_A / θ_R = 164° / 152° using this ionic liquid, and contact angles of θ_A / θ_R = 169° / 156° using water.

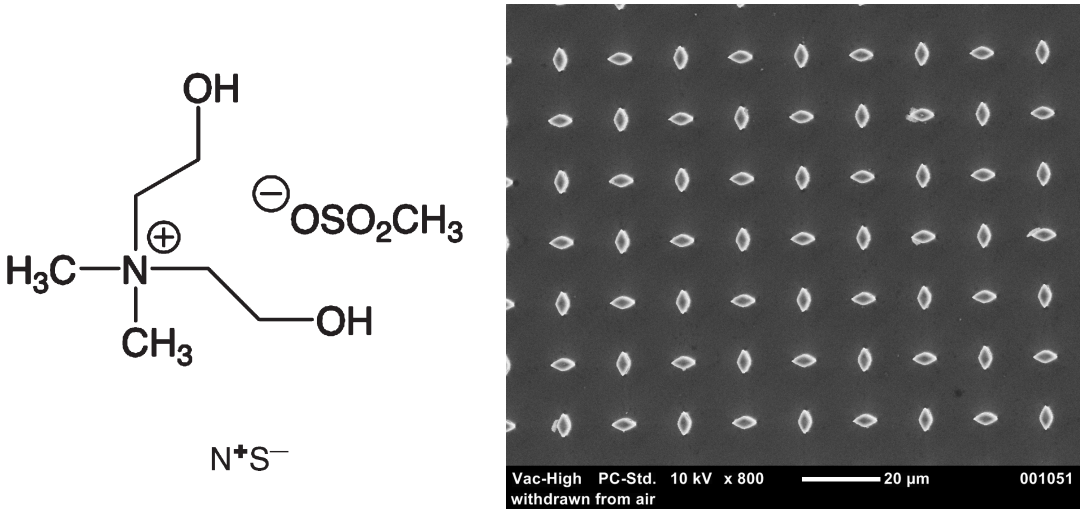

(a.) (b.)

Figure 5.4. a.) Structure of dimethylbis(β-hydroxyethyl)ammonium methanesulfonate (N^+S^-) ionic liquid. b.) scanning electron microscopy image of a staggered rhombus post surface.

Figure 5.5 shows images of a staggered rhombus surface withdrawn from the ionic liquid at a rate of approximately 1 cm/s. Unless otherwise noted, all samples reported in this chapter were withdrawn from liquids in such a way that the top of the images shown was removed from the liquid prior to the bottom (i.e. the top of the images left the liquid first). From the images, a single droplet appears on the top of every single post. These droplets are femtoliters in volume and nearly all sit within the center of the post. The presence of these droplets gives strong evidence for the mechanism of microcapillary failure as the dewetting process from superhydrophobic surfaces. This mechanism is implicated as the "cause" of hysteresis in these types of surfaces. Figure 5.6 shows images of surfaces withdrawn from a solution of N^+S^- in water in a 1:3 volume ratio. The ionic liquid droplets remaining on the post surfaces is significantly smaller than those using pure ionic liquid, and these droplets are approximately 25% of the volume of the droplets seen in Figure 5.5. This suggests the rapid evaporation of water from the droplet, leaving a smaller drop of ionic liquid.

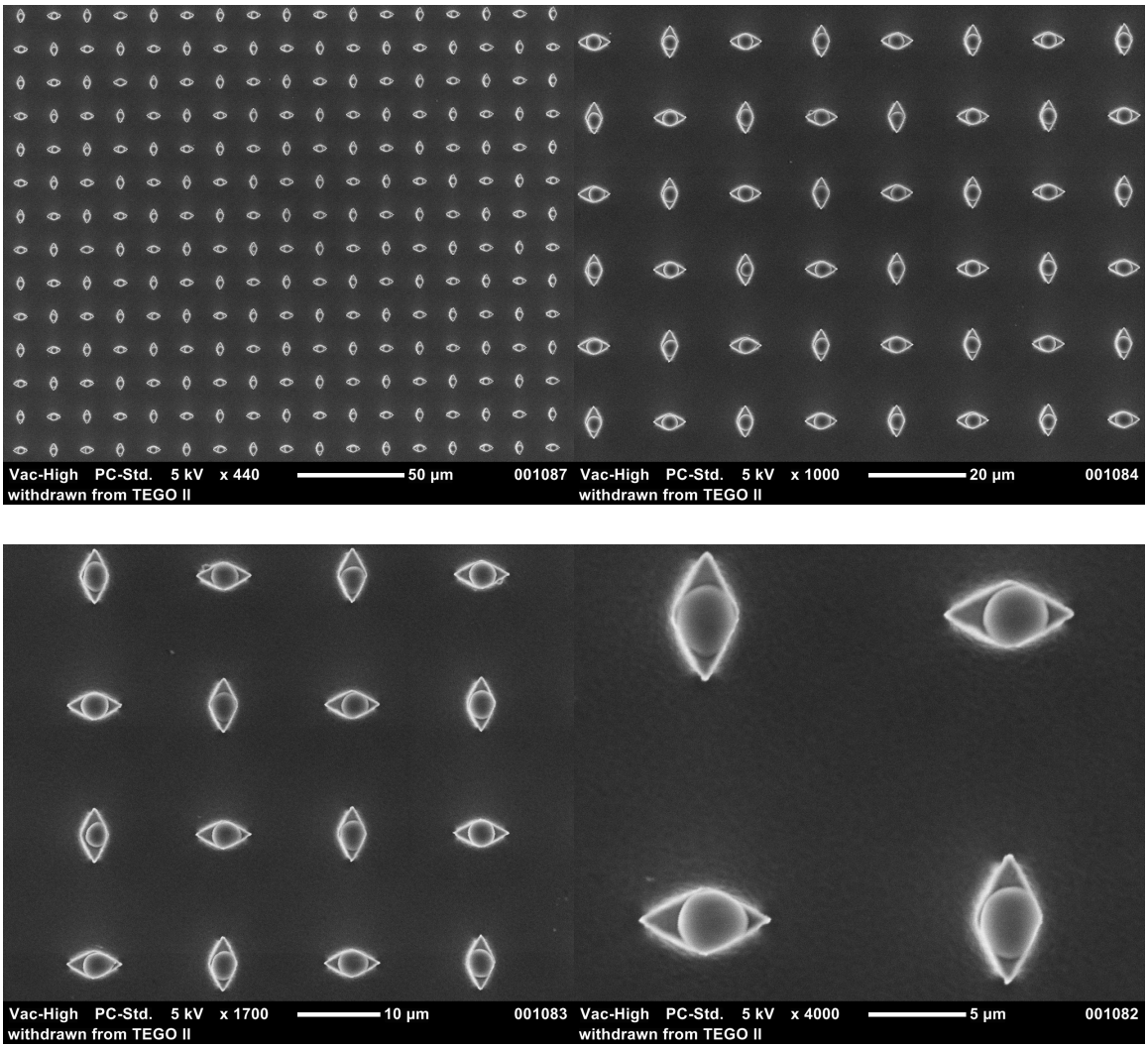

Figure 5.5. Scanning electron microscope images of a staggered rhombus post surface withdrawn from ionic liquid at a rate of ~ 1 cm/s.

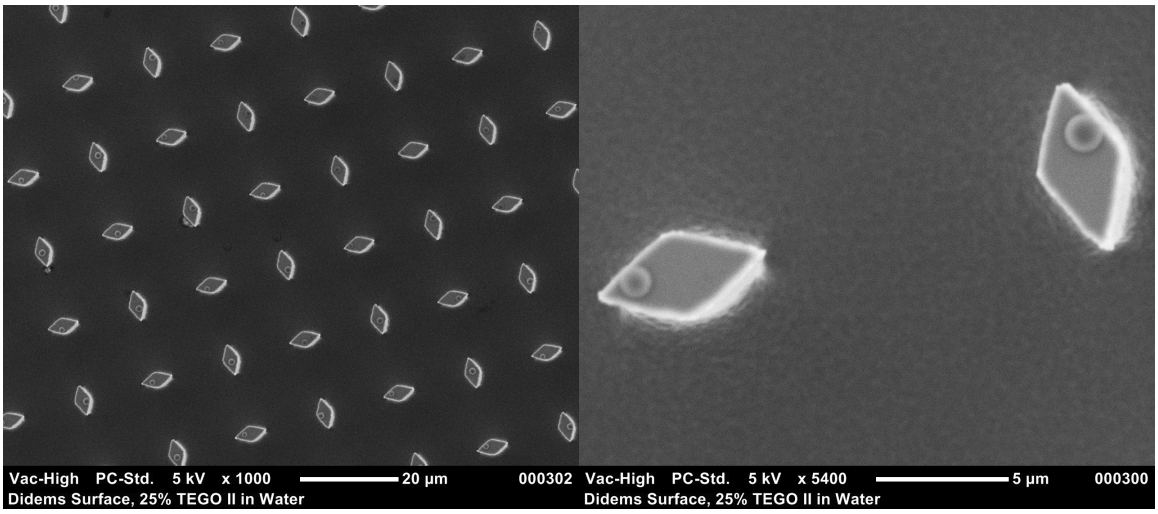

Figure 5.6. Scanning electron microscopy images of a staggered rhombus post after withdrawal from a 3:1 volume mixture of water and ionic liquid.

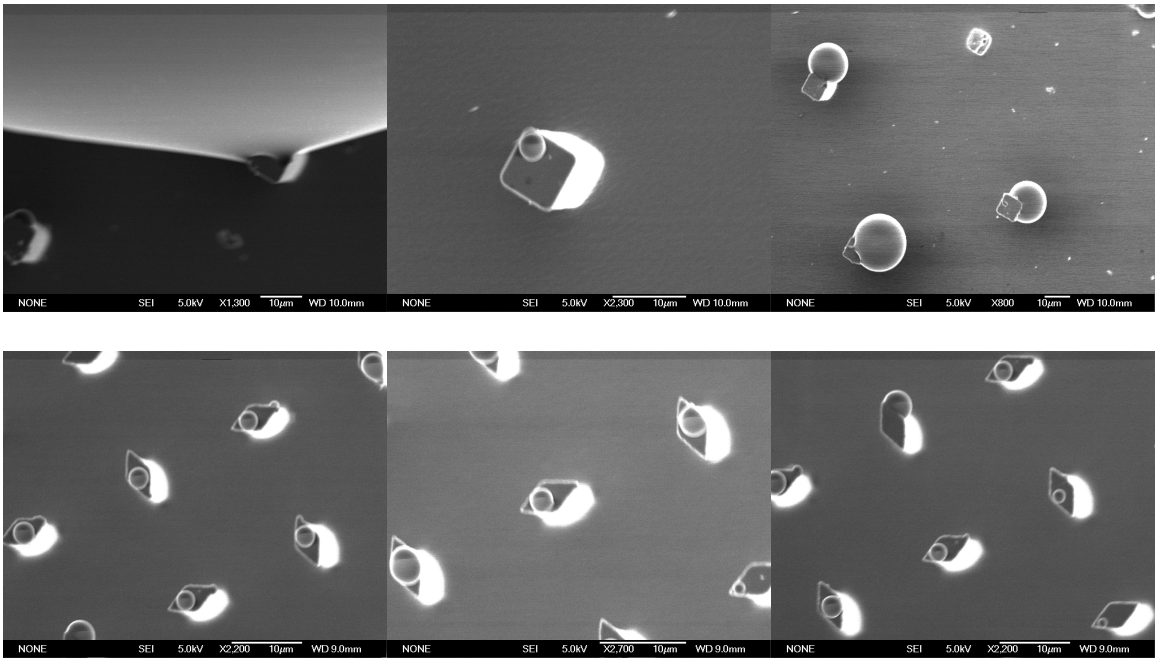

Figure 5.7. Scanning electron images of post surfaces after the rolling of an ionic liquid.

Figure 5.7 shows scanning electron images of two different post surfaces after a droplet of ionic liquid has rolled across the surface. Unlike dipping of these surfaces, the receding events around the parameter of the droplet do not occur in a uniform manner. For this reason, there is a non-uniformity in the size of the droplet left behind. Furthermore, the angle over which the

contact line recedes over these post surfaces may be significant, and this offers an explanation for the orientation and "hanging" of the droplets in the upper images. The upper left image shows a square post half submerged in the ionic liquid droplet after it has been rolled over. This image shows some distortion in the smooth liquid interface, and may be a prelude to capillary bridge formation.

The effect of orientation of removal was investigated using post grid surfaces, shown in Figure 5.8. This grid surface can be viewed as a surface containing square holes in it. These samples were removed with 0°, 45°, and 90° relative orientations. From the images, droplets formed on the ridges between the intersections and not at the intersections. A simple surface area argument suggests that a capillary bridge at an intersection (X-shaped cross section) would move spontaneously from the intersection to a ridge to decrease the liquid-vapor surface area. The presence of smaller droplets may also suggest some regular defect along the ridge which is acting as a pinning site. The droplets on these surfaces and those with regularly ordered posts give good indication for the microcapillary bridge rupture which occurs. Formation of the droplets occurs at pinning sites and accounts for the hysteresis of these surfaces.

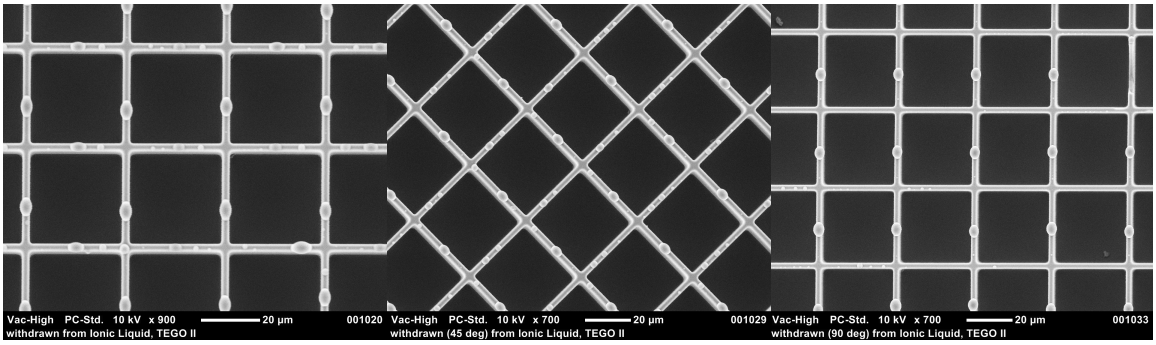

(a.) (b.) (c.)

Figure 5.8. Images of a grid post surface after removal from ionic liquid at a.) 0°, b.) 45°, and c.) 90° relative to an arbitrary (0°) direction.

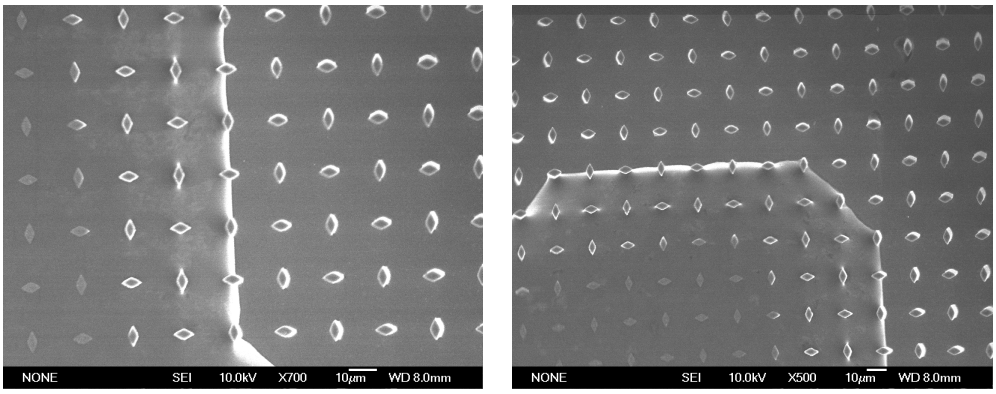

Figure 5.9. Images of a staggered rhombus post after withdrawn from a 1:1 volume ratio mixture of ethanol and ionic liquid.

A few surfaces were dipped into ethanol-ionic liquid mixtures (Figure 5.9) with less favorable results. These ethanol-ionic liquid mixtures do not offer any insight into the microcapillary bridge rupture, since the addition of ethanol lowers the surface tension of the mixture significantly enough to allows the mixture to wet between the posts. Rather, these images are presented purely to illustrate the contortion of the contact line which these regularly ordered posts can produce.

The formation of droplets on superhydrophobic surface with posts has been performed countless times by many researchers, although almost always unknowingly. However, liquid droplets have not been observed due to rapid evaporation. Ionic liquids overcome this problem due to their non-volatility, and can also be used as probe fluids. The droplets seen in the images presented here suggest that the mechanism for microcapillary bridge rupture is reasonable and probable.

5.3.2 Dip-Coating Deposition of Uniform Salt Crystals

Ionic liquids are salts that happen to be liquids around room temperature. For this reason, mixtures of ionic liquids with water are essentially salt solutions, and the size of a ionic liquid droplet left behind on the surface was directly proportional to the concentration of the solution used. With this in mind, it should also be possible to form solid salt crystals of uniform size in arrays. Figure 5.10 shows supported crystals of sodium chloride on staggered rhombus posts.

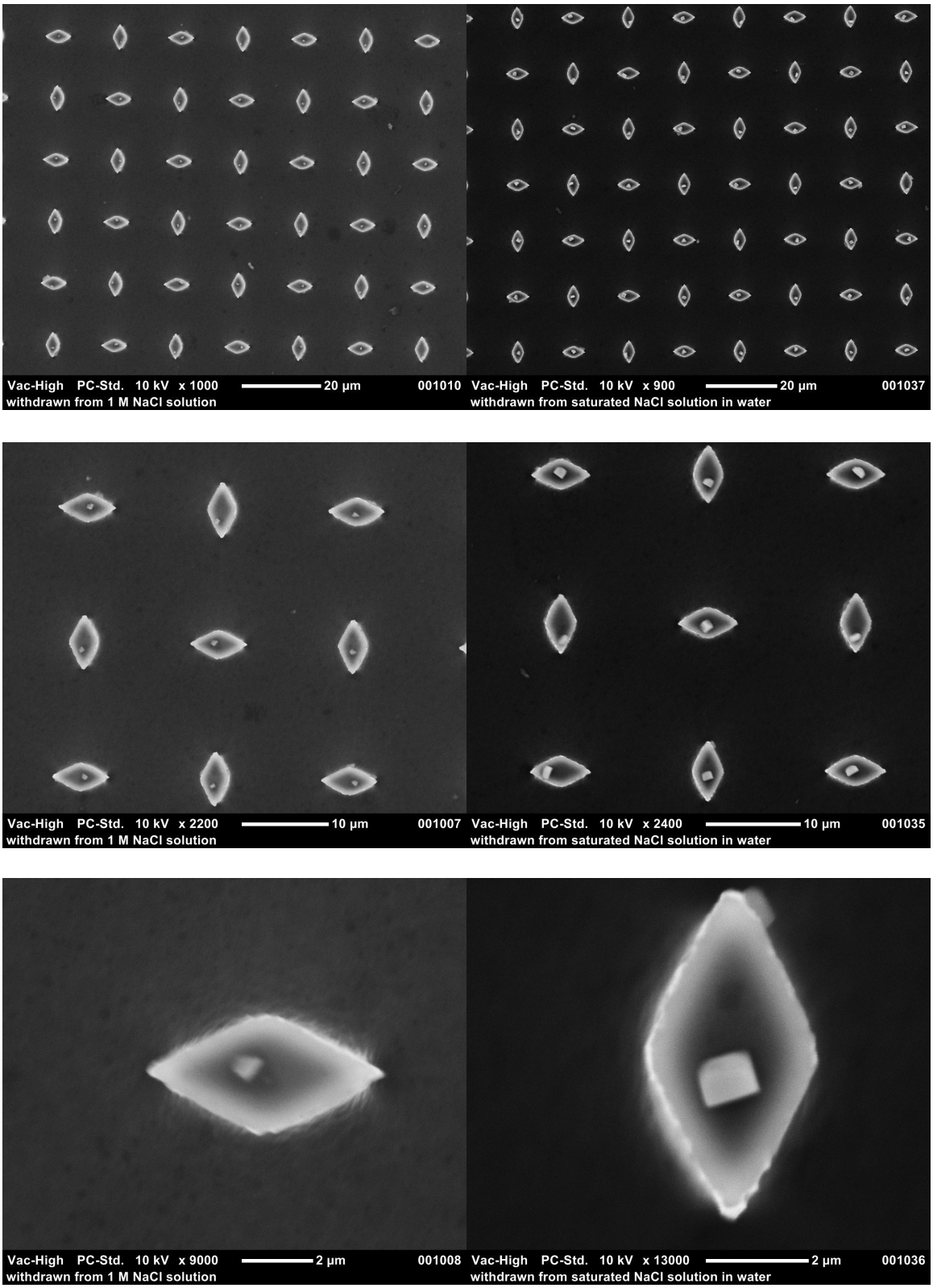

Figure 5.10. Sodium chloride crystals supported on the posts after withdrawal from a 1M (left column) and 4.3M (right column) aqueous solution.

Similar to the images of ionic liquids on these posts, there exists a sodium chloride crystal on each post surface, and the size of the crystal formed is affected by the concentration of the solution used. Image analysis was performed to give simple estimates of the size of the sodium chloride crystal and the contact diameter and volume of the droplet from which it came. For salt crystals formed using 1M NaCl concentrations, an average cube length of 0.5 μm was used. Assuming a cubic crystal shape, the mass of each individual salt crystal was calculated to be 0.3 picograms, a droplet contact diameter of ~2.8 μm and a droplet size of ~ 7 femtoliters was also estimated. For the salt crystals formed using a 4.3M NaCl concentration, a crystal mass of 2.3 picograms, a droplet contact diameter of ~3.2 μm, and a droplet volume of ~ 10 femtoliters were calculated. These contact diameter values are consistent with the dimensions of the post surface.

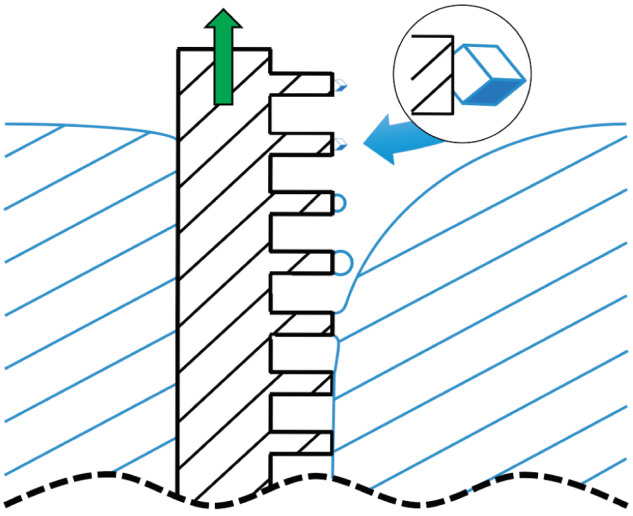

Figure 5.11. Dip-Coating Crystallization.[38]

This procedure was a simple dipping process by hand and no humidity control was performed to carefully control the crystallization. However, this technique was able to form uniform crystals of sodium chloride in an ordered array. This application has been named "dip-coating crystallization" (Figure 5.11) and utilizes the dewetting mechanism of liquids from superhydrophobic surfaces. Salt solution droplets of uniform size can be placed on the top of these posts due to the microcapillary bridge rupture which occurs during this process. Since

small droplets of water evaporate rapidly, these crystals can be quickly formed. Admittedly, sodium chloride is not the most interesting crystal material, and better quality crystals could most likely be prepared by controlling the humidity and rate of removal from solutions.

Figure 5.12 shows magnesium chloride and sucrose deposited on post surfaces. As with the other images shown, these materials were deposited on each post of the surface. However, unlike sodium chloride, they do not show good crystallization. This is attributed to the lack of control over humidity and crystallization process during these experiments. However, this does give good evidence that any water soluble material (so long as the surface tension of the solution remains large) can be deposited in this manner.

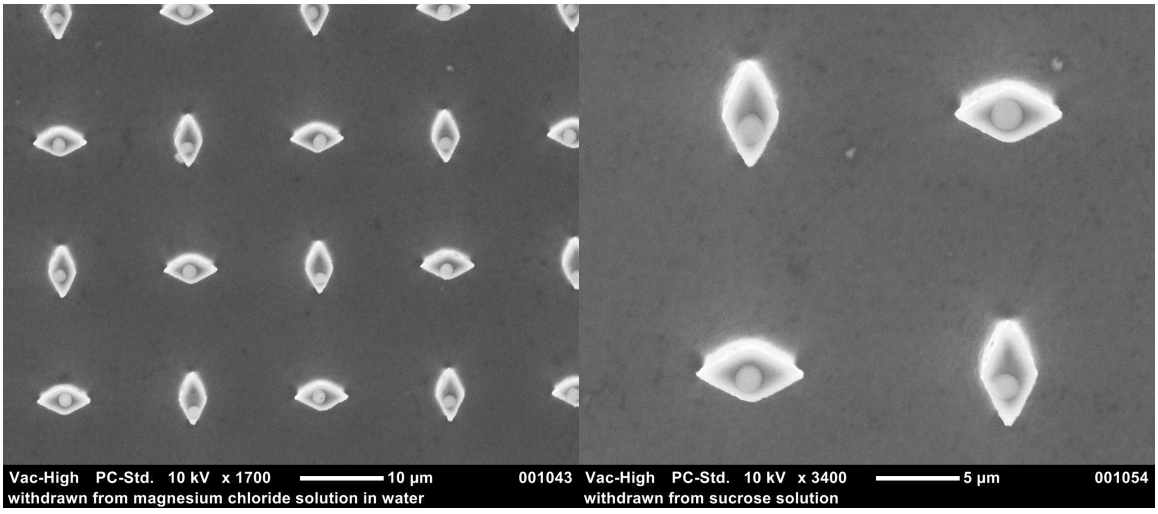

Figure 5.12. Scanning electron microscopy images of magnesium chloride (left) and sucrose (right) supported on a pillared surface

Other researchers have found use of this technique for the controlled deposition of materials. Subsequent to this work, Su *et al.*[39] reproduced these results using a variety of different post geometries. They note that sodium chloride always forms a cubic crystal despite the post geometry. This gives evidence that liquids will leave behind droplets on all pinning sites, and is not specific to any one geometry. Renaud *et al.*[40] provided direct evidence for the formation of capillary bridges from specially prepared post surfaces by using a UV-curable Norland optical adhesive (NOA) to kinetically trap these capillary bridges (Figure 5.13).

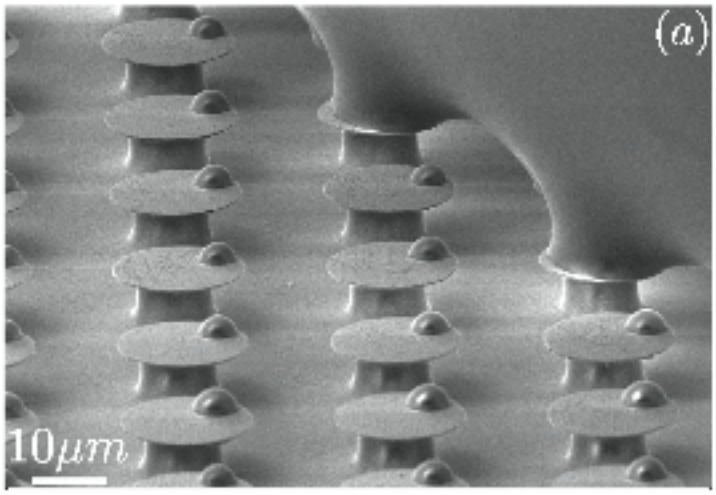

Figure 5.13. Capillary bridges of cured Norland optical adhesive at the receding contact line.[40]

5.3.3 Comments on Dewetting from Smooth Surfaces

Preliminary results show that contact line pinning from smooth, chemically patterned surfaces can be used in the same manner as superhydrophobic surface to selectively deposit materials. While very little work was done on these kinds of surfaces, Figure 5.14 shows ionic liquid droplets and sodium chloride crystals on hydrophilic spots in a hydrophobic plane after dipping the surface into ionic liquid and a 4.3M sodium chloride solution, respectively.

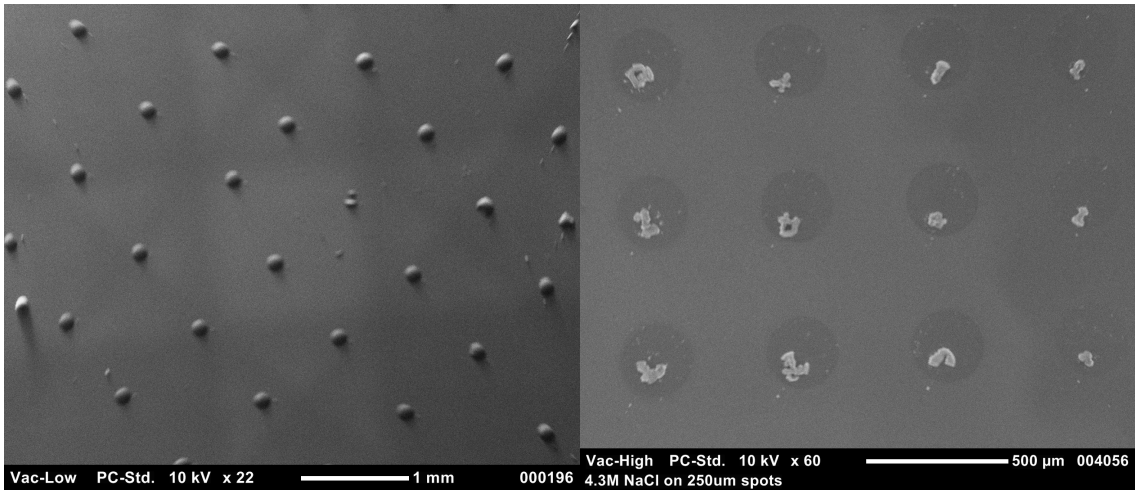

Figure 5.14. Ionic liquids (left) and sodium chloride crystals (right) left on hydrophilic spots in a hydrophobic plane after recession of a contact line by removal from a liquid.

These images are shown to highlight the advantages and uses of contact line pinning for the controlled deposition of materials and to show that there is still an active field of study. It is not suggested that the deposition of these materials is caused by tensile capillary bridge rupture, and no work was performed to understand the mechanics of this deposition process. It is probable that these droplets are formed through sessile capillary bridge failure, similar to the failure of hanging droplets previously reported.[41]

5.4 Conclusions

Contact angle hysteresis of superhydrophobic pillared surfaces is attributed to microcapillary bridge formation. The dewetting process by which a contact line recedes is attributed to capillary bridge failure. Ionic liquids were used to observe evidence of the microcapillary bridge failure by the formation of deposited droplets on the surfaces. Ionic liquids were found to be good probe fluids for high-vacuum analytical techniques. Furthermore, this dewetting process was used for the controlled formation and deposition of sodium chloride crystals. The applicability of this process for the deposition of other materials was briefly investigated, and it is suggested that careful control of crystallization parameters can produce well-ordered, uniform crystals through a simple dip-coating technique.

5.5 References

1. Young, T., Philos. Trans. R. Soc. London, 1805, 95, 65.
2. Gao, L., McCarthy, T.J., Langmuir, 2008, 24, 9183.
3. Wenzel, R.N., Ind. Eng. Chem., 1936, 28, 988.
4. Cassie, A.B.D., Baxter, S., Trans. Faraday Soc., 1944, 40, 546.
5. Gao, L., McCarthy, T.J., Langmuir, 2009, 25, 7249.
6. Gao, L., McCarthy T.J., Langmuir, 2009, 25, 14105.
7. Krumpfer, J.W., McCarthy, T.J., Langmuir, 2011, 27, 2166.
8. Gao, L., McCarthy, T.J., Langmuir, 2006, 22, 2966.
9. Gao, L., McCarthy, T.J., Langmuir, 2006, 22, 6234.

10. Fadeev, A.Y., McCarthy, T.J., Langmuir, 1999, 15, 3759.

11. Chen, W., Fadeev, A.Y., Hsieh, M.C., Oner, D., Youngblood, J., McCarthy, T.J., Langmuir, 1999, 15, 3395.

12. Krumpfer, J.W., McCarthy, T.J., Faraday Discuss., 2010, 146, 103.

13. Feng, L., Li, S.H., Li, Y.S., Li, H.J., Zhang, L.J., Zhai, J., Song, Y.L., Liu, B.Q., Jiang, L., Zhu, D.B., Adv. Mater., 2002, 14, 1857.

14. Roach, P., Shirtcliffe, N.J., Newton, M.I., Soft Matter, 2008, 4, 224.

15. Marmur, A., Langmuir, 2004, 20, 3517.

16. Gao, L., McCarthy, T.J., 2006, 22, 5998.

17. MacDougall, G., Ockrent, C., Proc. R. Soc. London, 1943, 180A, 151.

18. Furmidge, C.G., J. Colloid Sci., 1962, 17, 309.

19. Kawasaki, K., J. Colloid Sci., 1960, 15, 402.

20. Fadeev, A.Y., McCarthy, T.J., Langmuir, 2000, 16, 7268.

21. Gao, L., McCarthy, T.J., Langmuir, 2007, 23, 3762.

22. Gao, L., McCarthy, T.J., Langmuir, 2009, 25, 7249.

23. Gao, L., McCarthy, T.J., Langmuir, 2008, 24, 9183.

24. Briones, A.M., Ervin, J.S., Putman, S.A., Langmuir, 2010, 26, 13272.

25. Reyssat, M., Quéré, D., J. Phys. Chem. B, 2009, 113, 3906.

26. Mognetti, B.M., Yeomans, J.M., Langmuir, 2010, 26, 18162.

27. Bikerman, J.J., J. Colloid Sci., 1950, 5, 349.

28. Roura, P., Fort, J., Langmuir, 2002, 18, 566.

29. Patankar, N.A., Langmuir, 2003, 19, 1249

30. Chibowski, E., Adv. Colloid Interface Sci., 2003, 103, 149.

31. Li, X., Ma, X., Lan, Z., Langmuir, 2010, 26, 4831.

32. Vancov, T., Alston, A.S., Brown, T., McIntosh, S., Renewable Energy, 2012, 45, 1.

33. Gao, L., McCarthy, T.J., Langmuir, 2007, 23, 10445.

34. Batchelor, T., Cunder, J., Fadeev, A.Y., J. Colloid Interface Sci., 2009, 330, 415.

35. Hozumi, A., Bian, P., McCarthy, T.J., J. Am. Chem. Soc., 2010, 132, 5602.

36. Gao, L., McCarthy, T.J., J. Am. Chem. Soc., 2007, 129, 3804.

37. Öner, D., McCarthy, T.J., Langmuir, 2000, 16, 7777.

38. Krumpfer, J.W., McCarthy, T.J., J. Am. Chem. Soc., 2011, 133, 5764.

39. Su, B., Wang, S., Ma, J., Song, Y., Jiang, L., Adv. Funct. Mater., 2011, 21, 3297.

40. Renaud, D., Phillippe, B., Maxime, H. Boukherroub, R., Thomy, V., Senez, V., Small, 2012, 8, 1229.

41. Cheng, D., McCarthy, T.J., Langmuir, 2011, 27, 3693.

BIBILIOGRAPHY

Adamson, A.W., Gast, A.P., *Physical Chemistry of Surfaces*. J. Wiley & Sons: New York, **1997**.

Allen, N.S., Edge, M., Sandoval, G., Verran, J., Stratton, J., Maltby, J., *Photochemistry and Photobiology*, **2005**, *81*, 279-290.

Aranguren, M.I., Mora, E., Macosko, C.W., J. Coll. Interf. Sci., 1997, 195, 329-337.

Arkles, B., Larson, G., eds., Silicon Compounds: Silanes and Silicones Catalogue, 2nd ed., Gelest, Inc., Morrisville, 2008.

Arkles, B., Youlin, P., Kim, Y.M., Eisenbraun, E., Miller, C., Kaloyeros, A.E., *J. Adhesion Sci. Tech.*, **2011**, *26*, 41-54.

Ausanio, G., Barone, A.C., Campana, C., Iannotti, V., Sensors and Actuators A, 2006, 127, 56-62.

Bageli, N., N., Bryk, M.T., Ukr. Khim. Zh., 1981, 47, 409.

Balberg, I., Binenbaum, N., Physical Review B, 1987, 35, 8749-8752.

Ballance, D.S., Camilletti, R.C., Gentle, T.E., U.S. Patent 5,145,723, Sept. 8, 1992.

Bartell, F.E., Whitney, C.E., *J. Phys. Chem.*, **1932**, *36*, 3115.

Batchelor, T., Cunder, J., Fadeev, A.Y., J. Colloid Interface Sci., 2009, 330, 415.

Bernardini, C., Stoyanov, S.D., Stuart, M.A.C., Arnaudov, L.N., Leermakers, F.A.M., *Langmuir,* **2011**, *27*, 2501-2508.

Berzelius, J.J., *Ann. Phys. Chem.*, **1824**, *1*, 169.

Bian, P., McCarthy, T.J., Langmuir, 2010, 26, 6145-6148.

Bikerman, J.J., J. Colloid Sci., 1950, 5, 349.

Bokobza, L., J. Applied Polym. Sci., 2004, 93, 2095-2104.

Briones, A.M., Ervin, J.S., Putman, S.A., Langmuir, 2010, 26, 13272.

Brook, M.A., Grande, J.B., Ganachaund, F., *Adv. Polym. Sci.*, **2011**, *235*, 161-183.

Brzoska, J.B., Azouz, I.B., Rondelez, F., Langmuir, 1994, 10, 4367.

Bunde, A., Dieterich, W., J. Electroceramics, 2000, 5, 81-92.

Buzzacchi, M., Pagonabarraga, I., Wilding, N.B., *J. Chem. Phys.*, **2004**, *121*, 11362-11373.

Cai, W-Z., Tu, S-T., Gong J-M., J. Composite Mater., 2006, 40, 2131-2142.

Cao, C., Fadeev, A.Y., McCarthy, T.J., Langmuir, 2001, 17, 757.

Carp, O., Huismann, C.L., Reller, A., *Progress in Solid State Chemistry*, **2004**, *32*, 33-177.

Cassie, A.B.D., Baxter, S., *Trans. Faraday Soc.*, **1944**, *40*, 546.

Chatterjee, A.K., Industrial Ceramics, 2011, 31, 1-13.

Chen, W., Fadeev, A.Y., Hsieh, M.C., Öner, D., Youngblood, J., McCarthy, T.J., Langmuir, 1999, 15, 3395-3399.

Cheng, D.F., McCarthy, T.J., *Langmuir*, **2011**, *27*, 3693-3697.

Cheng, D., Urata, C., Masheder, B., Hozumi, A., *J. Am. Chem. Soc.*, **2012**, *134*, 10191-10199.

Chibowski, E., Adv. Colloid Interface Sci., 2003, 103, 149.

Clarson, S.J., Semlyen, J.A., *Siloxane Polymers*. Prentice Hill: Englewood Cliffs; **1993**.

Cohen-Addad, J. P., de Gennes, P. G., C. R. Acad. Sci. Paris, Ser. II, 1994, 319, 25–30.

Daniel, F.K., Goldman, P., Industrial and Engineering Chemistry, Analytical Edition, 1946, 18, 26.

DeGroot, Jr., J.V., Macosko, C.W., J. Coll. Interf. Sci., 1999, 217, 86-93.

Diebold, U., *Surf. Sci. Rep.*, **2003**, *48*, 53-229.

Dlubek, G., De, U., Pionetck, J., Arutyunov, N.Y., Edelmann, M., Krause-Rehberg, R., *Macromol. Chem. Phys.*, **2005**, *206*, 827-840.

Doi, M., Kawaguchi, M., Kato, T., Colloids and Surfaces A: Physiochem. Eng. Aspects, 2002, 211, 223-231.

Dufour, F., Cassaignon, S., Durupthy, O., Colbeau-Justin, C., Chaneac, C., *Euro. J. Inorganic Chem.*, **2012**, *16*, 2707-2715.

Essen, L., Froome, K.D., Proc. Phys. Soc. B., 1951, 64, 862-875

Fadeev, A.Y., McCarthy, T.J., *J. Am. Chem. Soc.*, **1999**, *121*, 12184-12185.

Fadeev, A.Y., McCarthy, T.J., *Langmuir*, **1999**, *15*, 3759-3766.

Fadeev, A.Y., McCarthy, T.J., Langmuir, 1999, 15, 7238.

Fadeev, A.Y., McCarthy, T.J., Langmuir, 2000, 16, 7268.

Fadeev, A.Y., Kazakevich, Y.V., Langmuir, 2002, 18, 2665-2672.

Farrokhpay, S., Adv. Coll. Interf. Sci., 2009, 151, 24-32.

Feng, L., Li, S.H., Li, Y.S., Li, H.J., Zhang, L.J., Zhai, J., Song, Y.L., Liu, B.Q., Jiang, L., Zhu, D.B., Adv. Mater., 2002, 14, 1857.

Finholt, A. E.; Bond, A. C.; Wilzbach, K. E.; Schlesinger, H. I., *J. Am. Chem. Soc.,* **1947**, *69*, 2692.

Fox, H.W., Taylor, P.W., Zisman, W.A., Indust. Engin. Chem., 1947, 39, 1401-1409.

Furmidge, C.G., J. Colloid Sci., 1962, 17, 309.

Gamble, L. Hugenschmidt, M.B., Campbell, C.T., Jurgens, T.A., Rogers Jr., J.W., *J. Am. Chem. Soc.*, **1993**, *115*, 12096-12105.

Gao, L., McCarthy, T.J., Langmuir, 2006, 22, 2966.

Gao, L., McCarthy, T.J., Langmuir, 2006, 22, 6234.

Gao, L., McCarthy, T.J., Langmuir, 2006, 22, 5998.

Gao, L., McCarthy, T.J., J. Am. Chem. Soc., 2007, 129, 3804.

Gao, L., McCarthy, T.J., Langmuir, 2007, 23, 3762.

Gao, L., McCarthy, T.J., Langmuir, 2007, 23, 10445-10447.

Gao, L., McCarthy, T.J., Langmuir, 2008, 24, 9183.

Gao, L., McCarthy, T.J., Langmuir, 2009, 25, 7249.

Gao, L., McCarthy T.J., Langmuir, 2009, 25, 14105.

Gao, W.; Dickinson, L.; Grozinger, C.; Morin, F.G.; Reven, L. *Langmuir*, **1996**, *12*, 6429.

Gentile, T.E., U.S. Patent 5,165,955, Nov. 24, 1992.

Genovese, D.B., Adv. Coll. Interf. Sci., 2012, 171, 1-16.

Graiver, D., Farminer, K.W., Narayan, R., *J. Polym. Environ.*, **2003**, *11*, 129-136.

Gray, D.S., Tien, J., Chen, C.S., Adv. Mater., 2004, 16, 393.

Gregory, J., Advances in Coll. Interf. Sci., 2009, 147-148, 1.

Gretton, M.J., Kamino, B.A., Brook, M.A., Bender, T.P., *Macromol.*, **2012**, *45*, 723-728.

Gupta, P., Ulman, A., Fanfan, S., Korniakov, A., Loos, K., J. Am. Chem. Soc., 2005, 127, 4.

Helmy, R., Fadeev, A.Y., *Langmuir*, **2002**, *18*, 8924-8928.

Henderson, M.A., *Surf. Sci. Rep.*, **2002,** *46,* 1.

Hertl, W., Hair, M.L., J. Phys. Chem., 1971, 75, 2181.

Hiemstra, T., Van Riemsdijk, W.H., J. Colloid and Interf. Sci., 2006, 301, 1.

Hofmann, Ph., Wells, J.W., J. Phys.: Condens. Matter, 2009, 21, 013003.

Hofmann, S., Depth Profiling in AES, XPS, *Practical Surface Analysis*, Wiley Press, New York, **1996**.

Holm, C., Weis, J.J., Current Opinion Coll. Interf. Sci., 2005, 10, 133-140.

Hozumi, A., Bian, P., McCarthy, T.J., J. Am. Chem. Soc., 2010, 132, 5602.

Hu, Y., Hadziomerspahic, A., Wang, Y., Macromolecules, 2010, 43, 8233-8238.

Hunter, M.J., Gordon, M.S., Barry, A.J., Hyde, J.F., Heidenreich, R.D., Ind. Eng. Chem., 1947, 39, 1389.

Hyde, J.F., J. Am. Chem. Soc., 1953, 75, 2166-2167.

Ladenburg, A., *Ann*., **1972**, *164*, 300.

Lai, S.K., Batra, A., Cohen, C., Polymer, 2005, 46, 4204.

Liebhafsky, H.A., *Silicones Under the Monogram*. J. Wiley & Sons: New York, **1978**.

Lide, D.R., ed., CRC Handbook of Chemistry and Physics, 75th ed., CRC Press, Inc., Ann Arbor, 1994.

Kantor, S.W., J. Am. Chem. Soc., 1953, 75, 2712-2714.

Kantor, S.W., Grubb, W.T., Ostoff, R.C., *J. Am. Chem. Soc.*, **1954**, *76*, 5191.

Kasprzyk-Hordern, B., Advances Coll. Interf. Sci., 2004, 110, 19-48.

Kawasaki, K., J. Colloid Sci., 1960, 15, 402.

Kim, J.A., Lee, S.H., Park, H., Kim, J.H., Park, T.H., Nanotechnology, 2010, 21, 165102.

Kipping, F.S., Lloyd, L.L., *J. Chem. Soc.*, **1901**, *79*, 449-459.

Kipping, F.S., *Proc. R. Soc. (London)*, **1937**, *159*, (A589), 0139-0148.

Kirkpatr, S., Reviews of Modern Physics, 1973, 45, 574-588.

Kirstein, K., Reichmann, K., Preis, W., Mitsche, S., *J. European Ceramic Soc.*, **2011**, *31*, 2339-2349.

Kole, S., Srivasta, S.K., Tripathy, D.K., Showmick, A.K., J. Appl. Polym. Sci., 2003, 54, 1329.

Koleske, J.V., ed., Paint and Coating Testing Manual: 14th edition of the Gardner-Sward Handbook, American Society for Testing and Materials, Ann Arbor, 1995.

Kosmulski, M., *Chemical Properties of Material Surfaces*, Cambridge University Press, Cambridge, **1994**.

Krumpfer, J.W., Fadeev, A.Y., Langmuir, 2006, 22, 8271-8272.

Krumpfer, J.W., McCarthy, T.J., *Faraday Discuss*., **2010**, *146*, 103-111.

Krumpfer, J.W., McCarthy, T.J., J. Am. Chem. Soc., 2011, 133, 5764.

Krumpfer, J.W., McCarthy, T.J., Langmuir, 2011, 27, 2166-2169.

Krumpfer, J.W., McCarthy, T.J., *Langmuir*, **2011**, *27*, 11514-11519.

Leger, L., Hervet, H., Deruelle, M., Adsorption on Silica Surfaces, Marcel Dekker, New York, 2000.

Li, X., Ma, X., Lan, Z., Langmuir, 2010, 26, 4831.

Liu, Y., Liu, Ch., Zhang, Z., *Chem. Engin. J.*, **2008**, *138*, 596-601.

Liu, Y., Wang, L., Krumpfer, J.W., Watkins, J.J., McCarthy, T.J., J. Am. Chem. Soc., 2012, submitted.

Losche, M., Schmitt, J., Decher, G., Bouwman, W.G., Kjaer, K., Macromolecules, 1998, 5, 1074.

MacDougall, G., Ockrent, C., Proc. R. Soc. London, 1943, 180A, 151.

Machavariani, V.Sh., J. Phys.: Condens. Matter, 2001, 13, 6797-6812.

Marinova, K.G., Christova, D., Tcholakova, S., Efremov, E., Denkov, N.D., Langmuir, 2005, 21, 11729.

Mark, J.E., *Acc. Chem. Res.*, **2004**, *37*, 946.

Mark, J.E., ed., *Polymer Data Handbook*, Oxford University Press: New York; **1999**.

Marmur, A., Langmuir, 2004, 20, 3517.

Marmur, A., Bittoun, E., *Langmuir*, **2009**, *25*, 1277.

Marsden, J., U.S. Patent 2,445,794, July 27, **1948**.

Martra, G., *Applied Catalysis A: General*, **2000**, *200***,** 275-285**.**

Maus, L., Walker, W.C., Zettlemoyer, A.C., *Industrial and Chemical Engineering*, **1955**, *47*, 696.

McCarthy, T.J., Fadeev, A.Y., U.S. Patent 6,331,329 B1, Dec. 18, 2001.

McCarthy, T.J., Fadeev, A.Y., U.S. Patent 6,673,459 B2, Jan. 6, 2004.

McElwee, J., Helmy, R., Fadeev, A.Y., *J. Coll. Interf. Sci.*, **2005**, *285*, 551-556.

McGregor, R.R., Silicones and Their Uses, McGraw-Hill, New York, 1954.

Mendez, A., Bosch, E., Roses, M., Neue, U.D., J. Chromatography A, 2003, 986, 33-44.

Mognetti, B.M., Yeomans, J.M., Langmuir, 2010, 26, 18162.

Morris, G.E., Skinner, W.A., Self, P.G., Marth, R., St.C., *Colloids Surfaces A: Physiochem. Eng. Aspects*, **1999**, *155*, 27-41.

Morterra, C., Magnacca, G., Catalysis Today, 1996, 27, 497-532.

Mukaihata, N., Matsui, H., Kawahara, T., Fukui, H., Tada, H., *J. Phys. Chem. C.*, **2008**, *112*, 8702-8707.

Nan, C.-W., Shen, Y., Ma, J., Annu. Rev. Mater. Res., 2010, 40, 131-151.

Nawrocki, J., Chem. Anal. (Warsaw), 1995, 40, 183-193.

Odian, G. G., *Principles of Polymerization. 4th ed.*; Wiley: Hoboken, N.J., **2004**.

Öner, D., McCarthy, T.J., *Langmuir*, **2000**, *16*, 7777-7782.

Osaheni, J.A., Truby, K.E., Silvi, N., Macromol. Symp., 2001, 169, 216-268.

Patankar, N.A., Langmuir, 2003, 19, 1249

Paul, D.R., Mark, J.E., *Progress in Polymer Science*, **2010**, *35*, 893-901.

Pauling, L., *J. Am. Chem. Soc.*, **1932**, *54*, 3570-3582.

Pauling, L., *American Mineralogist*, **1980**, *65*, 321-323.

Pease, D.C., *J. Phys. Chem.*, **1945**, *49*, 107.

Pettibone, J.M.; Cwiertny, D.M.; Scherer, M.; Grassian, V.H. *Langmuir*, **2008**, *24*, 6659.

Plueddemann, E.P., Silane Coupling Agents, Plenum Press, New York, 1982.

Post, H.W., *Silicones and Other Organosilicon Compounds*. Reinhold: New York, **1949**.

Poznyak, S.K., Kokorin, A.I., Kulak, A.I., *J. Electroanal. Chem.*, **1998**, *442*, 99-105.

Renaud, D., Phillippe, B., Maxime, H. Boukherroub, R., Thomy, V., Senez, V., Small, 2012, 8, 1229.

Reyssat, M., Quéré, D., J. Phys. Chem. B, 2009, 113, 3906.

Roach, P., Shirtcliffe, N.J., Newton, M.I., Soft Matter, 2008, 4, 224.

Rochow, E.G., *J. Am. Chem. Soc.*, **1945**, *67*, 1772.

Rochow, E.G., *Introduction to the Chemistry of the Silicones*. J. Wiley & Sons, Chapman & Hall: New York, London, **1946**.

Rochow, E.G., *Silicon and Silicones*. Spring-Verlag: Berlin; New York, **1987**.

Roura, P., Fort, J., Langmuir, 2002, 18, 566.

Ruschau, G.R., Yoshikawa, S., Newnham, R.E., J. Appl. Phys., 1992, 72, 953-959.

Sainte-Claire Deville, H.E., *Compt. rend. acad. sci.*, **1854**, *39*, 321.

Salah, N.H., Bouhelassa, M., Bekkouche, S., Boultif, A., Desalination, 2004, 166, 347-354.

Sau, K.P., Khastgir, D., Chaki, T.K., Die Angewandte Makromol. Chemie, 1998, 258, 11-17.

Schaer, E., Guizani, S., Choplin, L., Chemical Engineering Science, 2006, 61, 5664.

Schaer, E., Gagnard, C., Choplin, L., Canpont, D., *Powder Technology*, **2006**, *168*, 156.

Schmidt, D.L., Cobern, C.E., DeKoven, B.M., Potter, G.E., Meyers, G.F., Fischer, D.A., Nature, 1994, 368, 39.

Schroder, D.K., Semiconductor Material and Device Characterization, John Wiley & Sons, New York, 1990.

Selimovic, S., Maynard, S. M., Hu, Y. J., Rheol., 2007, 51, 325–340.

Şerbescu, A., Saalwächter, K., Polymer, 2010, 50, 5434-5442.

Seyferth, D., *Organometallics*, **2001**, *20*, 4978-4992.

Shafi, K.V.P.M., Ulman, A., Yan, X, Yang, N., Himmelhaus, M., Grunze, M., *Langmuir*, **2001**, *17*, 1726-1730.

Siderius, D.W., Corti, D.S., *Physical Review E*, **2005**, *71*, 031641.

Siderius, D.W., Corti, D.S., *Physical Review E*, **2007**, *75*, 011108.

Siderius, D.W., Corti, D.S., *Physical Review E*, **2011**, *83*, 031126.

Smith, W.E., Zukoski, C.F., *J. Colloid Interf. Sci.*, **2006**, *304*, 359-369.

Smith, J.S., Borodin, O., Smith, G.D., Kober, E.M., J. Polym. Sci. B: Polym. Phys., 2007, 45, 1599-1615.

Soares, R.F., Leite, C.A.P., Botter, Jr., W., Galembeck, F., J. Applied Polym. Sci., 1996, 60, 2001-2006.

Stein, J., Lewis, L. N., Gao, Y., Scott, R. A., *J. Am. Chem. Soc*., **1999**, *121*, 3693- 3703.

Stock, A., Somieski, C., *Ber. Dtsch. Chem. Ges.*, **1919**, *52*, 695-724.

Su, B., Wang, S., Ma, J., Song, Y., Jiang, L., Adv. Funct. Mater., 2011, 21, 3297.

Sudduth, R.D., Pigment & Resin Tech., 2008, 37, 375-388.

Sun, Y., Gu, A., Liang, G., Yuan, L., J. Appl. Polym. Sci., 2011, 121, 2018.

Tada, H., *Langmuir*, **1995**, *11*, 3281-3284.

Tamura, H., Mita, K., Tanaka, A., Ito, M., J. Colloid and Interf. Sci., 2001, 243, 202.

Thomas, D.N., Judd, S.J., Fawcett, N., Wat. Res., 1999, 33, 1579-1592.

Thomson, T., *Annals of Philosophy*, **1814,** *3,* 450-454.

Tripp, C., P., Combes, J.R., Langmuir, 1998, 14, 7348.

Tsantilis, S., Pratsinis, S.E., *Aerosol Science*, **2004**, *35*, 405-420.

Vancov, T., Alston, A.S., Brown, T., McIntosh, S., Renewable Energy, 2012, 45, 1.

Veraprath, S., Lehmann, R.G., J. Env. Polym. Degrad., 1997, 5, 17-31.

Vichi, F.M., Galembeck, F., J. Adhesion Sci. Technol., 1999, 13, 973-982.

Wang, C., Ying, J.Y., *Chem. Mater.*, **1999**, *11*, 3113-3120.

Warrick, E.L., *Forty Years of Firsts*. McGraw-Hill: New York, **1990**.

Wasserman, S.R., Tao, Y.-T., Whitesides, W.G., Langmuir, 1989, 5, 1074.

Wenzel, R.N., *Ind. Eng. Chem.*, **1936**, *28*, 988.

Xu, S., Lehmann, R.G., Miller, J.R., Chanra, G., Environ. Sci. Technol., 1998, 32, 1199.

Yi, J.Y., Choi, G.M., J. Electroceramics, 1999, 3, 361-369.

Young, T., *Philos. Trans. R. Soc. London*, **1805**, *95*, 65.

Zallen, R., The Physics of Amorphous Solids, John Wiley & Sons, New York, 1983.

Zhang, J., Feng, S.Y., Ma, Q.Y., J. Appl. Polym. Sci., 2003, 89, 1548-1554.

Zheng, P., McCarthy, T.J., *Langmuir*, **2010**, *26*, 18585-18590.

Zheng, P., McCarthy, T.J., *Langmuir*, **2011**, *27*, 7976-7979.

Zheng, P. McCarthy, T.J., *J. Am. Chem. Soc.*, **2012**, *134*, 2024-2027.

Zhou, J., Ralston, J., Sedev, R., Beattie, D.A., J. Coll. Interf. Sci., 2009, 331, 251-262.

Zhou, W.Y., Qi, S.H., Tu, C.C., Zhao, H.Z., Wang, C.F., Kou, J.L., J. Appl. Polym. Sci., 2007, 104, 1312-1318.